

AN ABSTRACT OF THE THESIS OF

Theresa Kathryn Daniels for the degree of Master of Science in Civil Engineering
presented on July 6, 2004.

Title: Reliability Based Bridge Assessment Using Modified Compression Field Theory
and Oregon Specific Truck Loading

Abstract approved: **Redacted for privacy**

David V. Rosowsky

Assessment of an existing bridge is needed when the structure exhibits signs of distress. Assessment practices require refinement in the calculation of loading and resistance while maintaining an acceptable level of risk, to minimize costs associated with repair, replacement and weight restrictions. Previous risk-based assessments evaluated the strength cases for shear and moment individually and used the live load model in the American Association of State and Highway Transportation Officials (AASHTO) specification. The methodology for assessment presented here is for use by the State of Oregon, which has over 500 cast-in-place reinforced concrete deck-girder (RCDG) bridges exhibiting distress in the form of diagonal tension cracks. It integrates full-scale testing for capacity, which found that the girder capacity requires assessment of shear and moment simultaneously, with field data and an Oregon specific truck loading.

A live load model (load spectrum) is developed for Oregon using the available weigh-in-motion (WIM) data for truck traffic on Oregon State highways. Field data are used to

estimate live load distribution factors. Results (including a statistical characterization) from full-scale laboratory testing of RCDGs revealed the section capacity is reasonably predicted using modified compression field theory (MCFT) accounting for shear and moment interaction. Potentially critical sections in a girder are defined and load effect (shear and moment) and capacity are calculated at each section. The statistical characterization for MCFT is considered for the section capacity and is compared to the load effect (shear and moment), which is considered to be deterministic. A second-moment reliability index (β) is calculated and used to determine the critical section in a girder. Using the annual load effects produced by WIM data, a low cycle fatigue (LCF) evaluation is made for the critical section to address the issue of yielding in the stirrups.

The assessment methodology can be applied to other structural members (i.e., bent caps, and columns) using appropriate capacity models as recommended by future research efforts. Once applied to the bridge system, use of both the safety assessment and LCF evaluation will enable engineers to rationally establish load restrictions based on an owner selected target reliability index developed for the State's bridge inventory, prioritize bridges (or segments of a bridge) for repair, and evaluate how repeated events that cause yielding in the stirrups may reduce the life of a bridge.

©Copyright by Theresa Kathryn Daniels
July 6, 2004
All Rights Reserved

Reliability Based Bridge Assessment Using Modified Compression Field Theory and
Oregon Specific Truck Loading

by
Theresa Kathryn Daniels

A THESIS

submitted to

Oregon State University

in partial fulfillment of
the requirements for the
degree of

Master of Science

Presented July 6, 2004
Commencement June 2005

Master of Science thesis of Theresa Kathryn Daniels presented on July 6, 2004.

APPROVED:

Redacted for privacy

Major Professor, representing Civil Engineering

Redacted for privacy

Head of the Department of Civil, Construction and Environmental Engineering

Redacted for privacy

Dean of the Graduate School

I understand that my thesis will become part of the permanent collection of Oregon State University libraries. My signature below authorizes release of my thesis to any reader upon request.

Redacted for privacy

Theresa Kathryn Daniels, Author

ACKNOWLEDGEMENTS

I would like to acknowledge the following people:

- Dr. Christopher Higgins for giving me this opportunity;
- Dr. David Rosowsky for opening my eyes to the world of probability and reliability in structural engineering;
- Dr. Thomas Miller and Dr. Solomon Yim for their counsel during the duration of the project;
- My fiancée, Scott McAuliffe, for supporting me throughout this endeavor;
- Melissa Robelo and Ae-young Lee for their support and laughter;
- David Fifer for supplying me with the raw weigh-in-motion data;
- And the Oregon Department of Transportation for funding this research.

TABLE OF CONTENTS

	<u>Page</u>
OVERVIEW	1
INTRODUCTION.....	2
BACKGROUND.....	3
OBJECTIVES	7
ANALYSIS METHODS.....	8
Types of Data Available	8
Using the Data	10
Permit Data.....	10
REALTIME Data	14
Raw WIM Data.....	15
RESULTS	17
Truck Spectrum Characteristics.....	17
Live Load Effect.....	27
Representative Rating Vehicle Live Load Effects.....	30
APPLICATION.....	34
Bridge Description.....	34
Identify Potential Critical Sections	37
Calculate Loading	37
Dead Load	38
Live Load.....	38
Service Level Performance	42
Calculate Capacity	45
Safety Assessment – One time Overloads	50

TABLE OF CONTENTS (Continued)

	<u>Page</u>
Calculate the Reliability Index	52
Compare the Reliability Index.....	55
Low-Cycle Fatigue	56
CONCLUSIONS.....	60
RECOMMENDATIONS AND FUTURE WORK.....	63
Load Data.....	63
Application.....	64
REFERENCES.....	65
APPENDICES.....	68
APPENDIX A – TRUCK LOADING	69
APPENDIX B – HAUNCH/TAPER STUDY	86
APPENDIX C – RATING VEHICLES.....	95
APPENDIX D – McKENZIE RIVER BRIDGE	130

LIST OF FIGURES

<u>Figure</u>	<u>Page</u>
R1 – Flowchart for extracting truck and bridge response statistics.....	9
R2 – Permits issued by Oregon Motor Carrier in 2002 (105,781 Total).....	11
R3 – Single Trip Permits issued by Oregon Motor Carrier in 2002 (28,091 Total).....	12
R4 – Woodburn POE GVW distribution December 18, 2002 (1,868 Trucks).....	15
R5 – GVW histograms for all trucks captured by Wilbur WIM.	19
R6 – Accumulated WIM collection in 2003.	20
R7 – Comparison of WIM stations on Interstate 5.....	20
R8 – Axle weight histograms for all trucks captured by Wilbur WIM.....	21
R9 – Steer axle weight histograms for all trucks captured by Wilbur WIM.	22
R10 – Histograms of vehicle type for all trucks captured by Wilbur WIM.	23
R11 – Histograms of axle number per vehicle for all trucks captured by Wilbur WIM.	24
R12 – Histograms of steer to rear axle length for all trucks captured by Wilbur WIM.	25
R13 – Histogram of Permit Table classification for all trucks captured by Wilbur WIM. .	26
R14 – Comparison of WIM vehicle permit classifications.	27
R15 – Load effect history of Rating Vehicle 8 on three (50 ft) - span continuous bridge. .	29
R16 – Maximum load effects for 1 year of Wilbur WIM permit vehicles (14,510) on a four (50ft) – span continuous bridge.	32
R17 – Maximum load effects for 1 year of Wilbur WIM permit vehicles (14,510) on a three (120 ft) – span continuous bridge.	32
R18 – Maximum load effects for 1 year of Wilbur WIM vehicles (14,510) on a two (25 ft) – span continuous bridge.	33

LIST OF FIGURES (Continued)

<u>Figure</u>	<u>Page</u>
R19 – Flowchart for safety assessment and low cycle fatigue evaluation.	35
R20 – McKenzie River bridge deck cross-section.	36
R21 – Profile view of McKenzie River bridge with cross-section locations (feet).....	36
R22 – Existing cracks on the McKenzie River bridge exterior girder in span 1 near support B. The first diaphragm framing is 12.5 ft from support B centerline.	36
R23 – Modal shear produced at 42 ft in span 1 of three (50 ft) - span continuous bridge. .	41
R24 – Service level performance histogram for diagonal cracking for the McKenzie River bridge at 42 ft. in span 1 (AASHTO-LRFD).	44
R25 – Service level performance histogram for diagonal cracking for the McKenzie River bridge at 42 ft. in span 1 (Field data).....	44
R26 – Laboratory results plotted on Normal probability paper.	46
R27 – Cross-section for McKenzie River Bridge at 42 ft in span 1 (<i>RESPONS 2000TM</i>)...	49
R28 – Disconnect of AASHTO-MCFT compared to R2K at points of inflection.	49
R29 – Illustration of how the reliabiltiy index is calculated.	51
R30 – Safety assessment for exterior girder of McKenzie River bridge (08175N) using ODOT Rating Vehicles.	53
R31 – Safety assessment for the exterior girder for the cross-section at 42 ft. in span 1. Live load distribution and impact factors from AASHTO-LRFD are applied.	54
R32 – Safety assessment for the exterior girder for the cross-section at 42 ft. in span 1. Live load distribution and impact factors from field data.	55
R33 – Low cycle fatigue evaluation for exterior girder of McKenzie R. bridge at 42 ft. in span 1 (AASHTO-LRFD).	58
R34 – Low cycle fatigue evaluation for exterior girder of McKenzie R. bridge at 42 ft. in span 1 (field data)..	58

LIST OF FIGURES (Continued)

<u>Figure</u>	<u>Page</u>
R35 – Annual cycles with load effects greater than the amplified yield points.....	59

LIST OF TABLES

<u>Table</u>	<u>Page</u>
R1 – Rating Vehicles with representative load effects for permit categories.	31
R2 – Distribution and impact factors for McKenzie River Bridge exterior girder.....	39
R3 – Shear prediction statistics from laboratory testing [Higgins et al., 2004b].	46

LIST OF APPENDIX FIGURES

<u>Figure</u>	<u>Page</u>
A1 – Legal weight table [Oregon Motor Carrier].	72
A2 – Extended legal weight table [Oregon Motor Carrier].....	73
A3 – Permit Table 3 [Oregon Motor Carrier].	74
A4 – Permit Table 4 [Oregon Motor Carrier].	76
A5 – Permit Table 5 [Oregon Motor Carrier].	78
A6 – Location of WIM stations in Oregon.	80
A7 – Example of an overweight permit.	80
A8 – Example of REALTIME data.....	81
A9 – Example of raw WIM data.	82
A10 – Classifications used for WIM collection in Oregon [Oregon Motor Carrier].	83
A11 – Data collected at weigh station visits.	84
A12 – Maximum shear produced at 5 ft. away from support B of the McKenzie River bridge plotted on Lognormal probability paper.....	85
B1 – Percent change in shear for tapered sections of a three (50 ft)-span continuous bridge.....	90
B2 – Percent change in moment for tapered sections of a three (50 ft)-span continuous bridge.....	91
B3 – Percent change in shear for haunched sections of a three (50 ft)-span continuous bridge.....	92
B4 – Percent change in moment for haunched sections of a three (50 ft)-span continuous bridge.....	93
C1 – Rating Vehicle 1	96
C2 – Rating Vehicle 2.....	96
C3 – Rating Vehicle 3.....	96

LIST OF APPENDIX FIGURES (Continued)

<u>Figure</u>	<u>Page</u>
C4 – Rating Vehicle 4	96
C5 – Rating Vehicle 5	97
C6 – Rating Vehicle 6	97
C7 – Rating Vehicle 7	97
C8 – Rating Vehicle 8	97
C9 – Rating Vehicle 9	98
C10 – Rating Vehicle 10	98
C11 – Rating Vehicle 11	98
C12 – Maximum shear and moment load effects produced by one year of Wilbur WIM vehicles classified as Permit Tables 3, 4 and 5 and the eleven rating vehicles for a single (11 ft) span simply-supported bridge evaluated at 7 ft from left support in span one.	101
C13 – Maximum shear and moment load effects produced by one year of Wilbur WIM vehicles classified as Permit Tables 3, 4 and 5 and the eleven rating vehicles for a single (64 ft) span simply-supported bridge evaluated at 60 ft from left support in span one.	102
C14 – Summary of the maximum shear vs corresponding moment and the maximum moment vs corresponding shear for two-span continuous bridges with 70 ft, 50 ft, and 25 ft spans all evaluated 4 ft from the first continuous support in span one.....	103
C15 – Maximum shear vs corresponding moment and the maximum moment vs corresponding shear load effects produced by one year of Wilbur WIM vehicles classified as Permit Tables 3, 4 and 5 and the eleven rating vehicles for two (70 ft) -span continuous bridge evaluated at 66 ft from left support in span one.	104
C16 – Maximum shear vs corresponding moment and the maximum moment vs corresponding shear load effects produced by one year of Wilbur WIM vehicles classified as Permit Tables 3, 4 and 5 and the eleven rating vehicles for two (50 ft) -span continuous bridge evaluated at 46 ft from left support in span one.	105

LIST OF APPENDIX FIGURES (Continued)

<u>Figure</u>	<u>Page</u>
C17 – Maximum shear vs corresponding moment and the maximum moment vs corresponding shear load effects produced by one year of Wilbur WIM vehicles classified as Permit Tables 3, 4 and 5 and the eleven rating vehicles for two (25 ft) -span continuous bridge evaluated at 21 ft from left support in span one.....	106
C18 – Maximum shear vs corresponding moment and the maximum moment vs corresponding shear load effects produced by one year of Wilbur WIM vehicles classified as Permit Tables 3, 4 and 5 and the eleven rating vehicles for two (25 ft) -span continuous bridge evaluated at 21 ft from left support in span one.....	107
C19 – Summary of the maximum shear vs corresponding moment and the maximum moment vs corresponding shear for three-span continuous bridges with 120 ft and 50 ft spans both evaluated 4 ft from the first continuous support in span one.	108
C20 – Maximum shear vs corresponding moment and the maximum moment vs corresponding shear load effects produced by one year of Wilbur WIM vehicles classified as Permit Tables 3, 4 and 5 and the eleven rating vehicles for three (120 ft) -span continuous bridge evaluated at 116 ft from left support in span one.	109
C21 – Maximum shear vs corresponding moment and the maximum moment vs corresponding shear load effects produced by one year of Wilbur WIM vehicles classified as Permit Tables 3, 4 and 5 and the eleven rating vehicles for three (120 ft) -span continuous bridge evaluated at 4 ft from left support in span two.....	110
C22 – Maximum shear vs corresponding moment and the maximum moment vs corresponding shear load effects produced by one year of Wilbur WIM vehicles classified as Permit Tables 3, 4 and 5 and the eleven rating vehicles for three (120 ft) -span continuous bridge evaluated at 116 ft from left support in span two.	111
C23 – Maximum shear vs corresponding moment and the maximum moment vs corresponding shear load effects produced by one year of Wilbur WIM vehicles classified as Permit Tables 3, 4 and 5 and the eleven rating vehicles for three (120 ft) -span continuous bridge evaluated at 4 ft from left support in span three...	112
C24 – Maximum shear vs corresponding moment and the maximum moment vs corresponding shear load effects produced by one year of Wilbur WIM vehicles classified as Permit Tables 3, 4 and 5 and the eleven rating vehicles for three (50 ft) -span continuous bridge evaluated at 46 ft from left support in span one.....	113

LIST OF APPENDIX FIGURES (Continued)

<u>Figure</u>	<u>Page</u>
C25 – Maximum shear vs corresponding moment and the maximum moment vs corresponding shear load effects produced by one year of Wilbur WIM vehicles classified as Permit Tables 3, 4 and 5 and the eleven rating vehicles for three (50 ft) -span continuous bridge evaluated at 4 ft from left support in span two.....	114
C26 – Maximum shear vs corresponding moment and the maximum moment vs corresponding shear load effects produced by one year of Wilbur WIM vehicles classified as Permit Tables 3, 4 and 5 and the eleven rating vehicles for three (50 ft) -span continuous bridge evaluated at 46 ft from left support in span two.....	115
C27 – Maximum shear vs corresponding moment and the maximum moment vs corresponding shear load effects produced by one year of Wilbur WIM vehicles classified as Permit Tables 3, 4 and 5 and the eleven rating vehicles for three (50 ft) -span continuous bridge evaluated at 4 ft from left support in span three.....	116
C28 – Summary of the maximum shear vs corresponding moment and the maximum moment vs corresponding shear for four-span continuous bridges with 70 ft and 50 ft spans both evaluated 4 ft from the first continuous support in span one.	117
C29 – Maximum shear vs corresponding moment and the maximum moment vs corresponding shear load effects produced by one year of Wilbur WIM vehicles classified as Permit Tables 3, 4 and 5 and the eleven rating vehicles for four (70 ft) -span continuous bridge evaluated at 66 ft from left support in span one.....	118
C30 – Maximum shear vs corresponding moment and the maximum moment vs corresponding shear load effects produced by one year of Wilbur WIM vehicles classified as Permit Tables 3, 4 and 5 and the eleven rating vehicles for four (70 ft) -span continuous bridge evaluated at 4 ft from left support in span two.....	119
C31 – Maximum shear vs corresponding moment and the maximum moment vs corresponding shear load effects produced by one year of Wilbur WIM vehicles classified as Permit Tables 3, 4 and 5 and the eleven rating vehicles for four (70 ft) -span continuous bridge evaluated at 66 ft from left support in span two.....	120
C32 – Maximum shear vs corresponding moment and the maximum moment vs corresponding shear load effects produced by one year of Wilbur WIM vehicles classified as Permit Tables 3, 4 and 5 and the eleven rating vehicles for four (70 ft) -span continuous bridge evaluated at 4 ft from left support in span three.....	121
C33 – Maximum shear vs corresponding moment and the maximum moment vs corresponding shear load effects produced by one year of Wilbur WIM vehicles classified as Permit Tables 3, 4 and 5 and the eleven rating vehicles for four (70 ft) -span continuous bridge evaluated at 66 ft from left support in span three...	122

LIST OF APPENDIX FIGURES (Continued)

<u>Figure</u>	<u>Page</u>
C34 – Maximum shear vs corresponding moment and the maximum moment vs corresponding shear load effects produced by one year of Wilbur WIM vehicles classified as Permit Tables 3, 4 and 5 and the eleven rating vehicles for four (70 ft) -span continuous bridge evaluated at 4 ft from left support in span four	123
C35 – Maximum shear vs corresponding moment and the maximum moment vs corresponding shear load effects produced by one year of Wilbur WIM vehicles classified as Permit Tables 3, 4 and 5 and the eleven rating vehicles for four (50 ft) -span continuous bridge evaluated at 46 ft from left support in span one.....	124
C36 – Maximum shear vs corresponding moment and the maximum moment vs corresponding shear load effects produced by one year of Wilbur WIM vehicles classified as Permit Tables 3, 4 and 5 and the eleven rating vehicles for four (50 ft) -span continuous bridge evaluated at 4 ft from left support in span two.....	125
C37 – Maximum shear vs corresponding moment and the maximum moment vs corresponding shear load effects produced by one year of Wilbur WIM vehicles classified as Permit Tables 3, 4 and 5 and the eleven rating vehicles for four (50 ft) -span continuous bridge evaluated at 46 ft from left support in span two.....	126
C38 – Maximum shear vs corresponding moment and the maximum moment vs corresponding shear load effects produced by one year of Wilbur WIM vehicles classified as Permit Tables 3, 4 and 5 and the eleven rating vehicles for four (50 ft) -span continuous bridge evaluated at 4 ft from left support in span three.....	127
C39 – Maximum shear vs corresponding moment and the maximum moment vs corresponding shear load effects produced by one year of Wilbur WIM vehicles classified as Permit Tables 3, 4 and 5 and the eleven rating vehicles for four (50 ft) -span continuous bridge evaluated at 46 ft from left support in span three...	128
C40 – Maximum shear vs corresponding moment and the maximum moment vs corresponding shear load effects produced by one year of Wilbur WIM vehicles classified as Permit Tables 3, 4 and 5 and the eleven rating vehicles for four (50 ft) -span continuous bridge evaluated at 4 ft from left support in span four.	129
D1 – McKenzie River Bridge detailed drawing.....	131
D2 – McKenzie R. Bridge; Span 1 at 4 ft. (<i>RESPONSE 2000TM</i>).....	132
D3 – McKenzie R. Bridge; Span 1 at 8 ft. (<i>RESPONSE 2000TM</i>).....	132
D4 – McKenzie R. Bridge; Span 1 at 12.5 ft. (<i>RESPONSE 2000TM</i>).....	133

LIST OF APPENDIX FIGURES (Continued)

<u>Figure</u>	<u>Page</u>
D5 – McKenzie R. Bridge; Span 1 at 25 ft. (<i>RESPONSE 2000TM</i>).....	133
D6 – McKenzie R. Bridge; Span 1 at 37.5 ft. (<i>RESPONSE 2000TM</i>).....	134
D7 – McKenzie R. Bridge; Span 1 at 42 ft. (<i>RESPONSE 2000TM</i>).....	134
D8 – McKenzie R. Bridge; Span 1 at 46 ft. (<i>RESPONSE 2000TM</i>).....	135
D9 – McKenzie R. Bridge; Span 2 at 4 ft. (<i>RESPONSE 2000TM</i>).....	135
D10 – McKenzie R. Bridge; Span 2 at 8 ft. (<i>RESPONSE 2000TM</i>).....	136
D11 – McKenzie R. Bridge; Span 2 at 12.5 ft. (<i>RESPONSE 2000TM</i>).....	136
D12 – McKenzie R. Bridge; Span 2 at 25 ft. (<i>RESPONSE 2000TM</i>).....	137

LIST OF APPENDIX TABLES

<u>Table</u>	<u>Page</u>
B1 – Summary of percent change at key points dependent on loading and haunch or taper ratios.	89
C1 – ODOT Rating Vehicles in table form.	99
C2 – Wilbur WIM vehicles classified as Permit Table 5 in 2003.	100

RELIABILITY BASED BRIDGE ASSESSMENT USING MODIFIED COMPRESSION FIELD THEORY AND OREGON SPECIFIC TRUCK LOADING

OVERVIEW

Assessment of an existing bridge is needed when the structure exhibits signs of distress or the structure usage changes. Assessment practices require refinement in the calculation of loading and resistance, while maintaining an acceptable level of safety, to minimize costs associated with repair, replacements, and weight restrictions. The following details an investigation of the vehicle loading found in Oregon using available collected data for truck traffic within the State. The load effects produced by these vehicles are calculated for various bridge indeterminacies and span lengths. The service level loading is evaluated to explain diagonal cracking displayed by many of Oregon's 1950's vintage reinforced concrete deck girder bridges. A methodology is developed for safety assessment of a bridge girder relative to the load demand. An example is illustrated using the methodology and incorporates laboratory testing and field data. The end result is a rational basis for determining weight restrictions and prioritizations for replacement or repair.

INTRODUCTION

The Oregon Department of Transportation (ODOT) has identified over 500 cast-in-place reinforced concrete deck-girder (RCDG) bridges with diagonal cracks. Of these cracked bridges, 220 are along the I-5 and I-84 corridors and were built between 1947 and 1962. The cracked bridges have warranted weight restrictions (which in turn cause large detours) in addition to significant costs for inspections, replacements, and emergency repairs. ODOT routinely collects data on truck traffic traveling on State highways. In other parts of the world this type of data has been widely used for bridge assessment purposes. This study demonstrates implementation of an assessment methodology which integrates truck data, field data, and analysis methods, that can be used by bridge engineers to aid in making load rating, posting, repair, and replacement decisions.

BACKGROUND

The bridges considered in this study were built in the period between 1947 and 1962, prior to the introduction of load and resistance factor design. In the 1970's and 1980's, the application of probability theory to quantify the risk (relative safety) associated with design practices in structural engineering was introduced. This new approach recognized that absolute reliability is unattainable in the presence of uncertainty and variability in the loading and resistance. Reliability-based design insures that the probability of unfavorable performance is economically acceptably small [Ellingwood *et al.*, 1980]. Earlier safety factors used as part of a working-stress design philosophy were phased out as they could not provide a consistent safety margin throughout a design or system.

Capacity (R) and load (S) are characterized as random variables by probability distributions. Variables comprising the capacity include material properties, section geometry, and specified strengths, to name a few. Statistics for the random variables in the capacity of conventionally reinforced concrete, for both shear and moment, and considering various members and components, were developed by Ellingwood *et al.* [1980]. Statistical parameters for a bridge live load model were developed by Nowak and Hong [1991] from truck surveys and by simulation. Assuming both the capacity and loading distributions are Normal, then the reliability problem reduces to the simple R - S form:

$$p_f = P[R < S] = P[R - S < 0] = P[M < 0] \quad [R1]$$

$$p_f = \Phi\left(\frac{\mu_S - \mu_R}{\sqrt{\sigma_S^2 + \sigma_R^2}}\right) = \Phi\left(\frac{0 - \mu_M}{\sigma_M}\right) \quad [R2]$$

where, $M=R-S$ is the safety margin (or limit state function), μ and σ are the mean and standard deviation (first and second order statistics) of the respective random variables, and $\Phi(\cdot)$ = the standard normal cumulative distribution function. The term p_f represents the probability that a limit state will be met or exceeded during the design life. The reliability index, β , is simply the number of standard deviations from the mean of the safety margin to the failure criteria ($M=0$) and is related to the probability of failure, p_f , through the following equation:

$$p_f = \Phi(-\beta) \quad [R3]$$

A value of $\beta = 3.5$ corresponds to a probability of exceedence of 2 in 10,000, while $\beta = 2.5$ corresponds to 62 in 10,000. However, since probability laws cannot be determined exactly, p_f is referred to as a “notional” probability, indicating that it should be interpreted in a comparative sense rather than in a relative frequency sense [Ellingwood *et al.*, 1980]. Even so, β is a useful comparative measure of reliability and can be used to evaluate relative safety of various designs as long as the first and second order statistics are handled consistently [Ellingwood *et al.*, 1980].

Provisions in the current AASHTO-LRFD Bridge Design Specification [2003] are calibrated for a target reliability index of 3.5. This index was derived for a severe traffic-loading case (including the presence of 5000 Annual Daily Truck Traffic) in the LRFD design criteria. Following this approach, it is natural that the current state-of-the-art method for load rating bridges also uses load and resistance factors. The AASHTO Manual for Condition Evaluation and Load and Resistance Factor Rating (LRFR) of

Highway Bridges [2003] adopts a reduced target reliability index of 2.5. This index was calibrated to past AASHTO operating level load ratings and reflects the reduced exposure period, consideration of site realities, and the economic considerations of rating vs. design.

Examples of risk-based approaches to bridge safety assessment are shown in work by Stewart *et al.*, [2002] and Akgul and Frangopol [2003]. The example bridges used by Stewart *et al.*, [2002] were simply supported and the limit state examined was for the situation when flexure at mid-span exceeded the structural resistance. The AASHTO live load model was used. Akgul and Frangopol [2003] showed how initial operational bridge rating factors compared to initial system reliability indices. For the comparison, the capacity was calculated using the AASHTO Standard Specification 16th Edition [1996] and the loading distribution also used the AASHTO live load model.

A reliability-based safety assessment follows, but with two distinctions from previous work. In earlier work, as in the AASHTO Standard Specification 16th Edition for capacity, moment and shear were each treated separately so each could be resolved into a simple *R-S* problem. However, the method to calculate capacity has changed to Modified Compression Field Theory (MCFT) both in AASHTO-LRFD [2003] and AASHTO-LRFR [2003]. This research creates an *R-S* problem while accounting for the simultaneous moment-shear interaction in strength (capacity) prediction. In addition, an Oregon-specific load spectrum will be developed and applied. The State of Oregon has collected weigh-in-motion data and permit data for vehicles on the state highway system. Over 14,000 vehicles that exceeded legal limits were captured by one WIM station in one year alone compared to 10,000 surveyed trucks in the major study used that has influenced the load

model found in today's AASHTO specification. The current specification is based on surveys performed in the Detroit area by Agarwal and Wolkowicz [1976] and covered about 10,000 heavy vehicles (only trucks that appeared to be heavily loaded were measured and included in the data base). In addition, the load effects were calculated for simple spans ranging from 30-200 ft. in length [Nowak and Hong, 1991]. In this study they are calculated for multiple bridge indeterminacies and span lengths representative of bridges contained in a database of Oregon bridges [Higgins *et al.*, 2004a]. Therefore, in the following reliability assessment of 1950's vintage conventionally reinforced concrete deck girder bridges, MCFT is used to predict capacity and the load demand used in the analysis will be Oregon-specific. Note that instead of treating load as a random quantity using a statistical distribution (which is the goal for future work) it is treated as a discrete value in this reliability analysis using MCFT. The key to the study is that the statistical first and second moments will be handled consistently between all bridge sections examined and β will be treated in a truly relative sense.

The information collected for the load and resistance has potential use for risk ranking as a bridge management tool. Risk ranking allows the comparison of bridges by evaluating bridges with a conditional probability (developed by Stewart and Val [1999]) that reflects relative frequency of overloads, years in service, inspection information, and consequence of failure (where the consequence of failure is similar for all bridges considered so risk-ranking is appropriate) [Stewart *et al.*, 2002]. Thus, risk ranking is an area for possible application of the load spectrum developed herein.

OBJECTIVES

Load spectrum is defined in this study as the frequency and range of different vehicles described by their gross vehicle weight, length, number of axles, axle weights and axle spacings, as well as the frequency and range of load effects produced by these vehicles on various bridge span lengths and indeterminacies. The objectives of this study are:

- To make use of available truck data to characterize an Oregon-specific load spectrum.
- To transform the load spectrum into load effect (shear and moment). This represents the load side of the “load \leq resistance” equation.
- To determine if load effects produced by the rating vehicles used by the ODOT Bridge Group envelope load effects produced by collected vehicle data for a variety of bridge spans and indeterminacies.
- To evaluate the likelihood of operating loads exceeding the cracking shear in high moment regions.

The next two objectives evaluate the capacity of RCDG bridge girders with respect to the load demand.

- Develop a method for safety assessment to evaluate one-time overloads at various sections along a bridge girder.
- Propose a method for addressing low-cycle fatigue on cracked RCDG bridge girders.

These last two objectives comprise the methodology that will aid bridge engineers in making load rating and posting decisions for RCDG bridges.

ANALYSIS METHODS

The flow chart in Figure R1 illustrates the process being used to create the load spectrum, service level performance histogram, and the figures to compare load effects with the resistance/strength of the bridges. The bold boxes indicate the six objectives for this study. The chart is organized to illustrate the calculations of load on the left and resistance on the right. The method integrates load data, bridge data, field data and laboratory data. Dotted lines encircle items that are input and output. An item with a dashed line indicates an area for possible future development. Items with a shadow box indicate that additional data may continually be added as they are collected for further refinement.

Types of Data Available

There are two sources of truck data regularly collected by ODOT: permit data and weigh-in-motion data. Permit data are the collection of permits issued for vehicles that exceed legal limits, whether due to height, length, or weight. These permits are individual forms filled out for each truck. The data are kept for 39 months. Weigh-in-motion (WIM) is the process of collecting vehicle information such as length, speed, axle weights, and gross vehicle weight (GVW) while the vehicle is moving. There is a +/- 2-3% error rate as a result of the fluctuation of weight distribution due to the truck being in motion [Fifer, 2002]. This is most evident for trucks hauling liquids, livestock, and for log trucks without middle supports. In Oregon, the current WIM system is set up near weigh stations, but could be located anywhere additional information on trucks may be desired. WIM data are further divided into two types, REALTIME and raw.

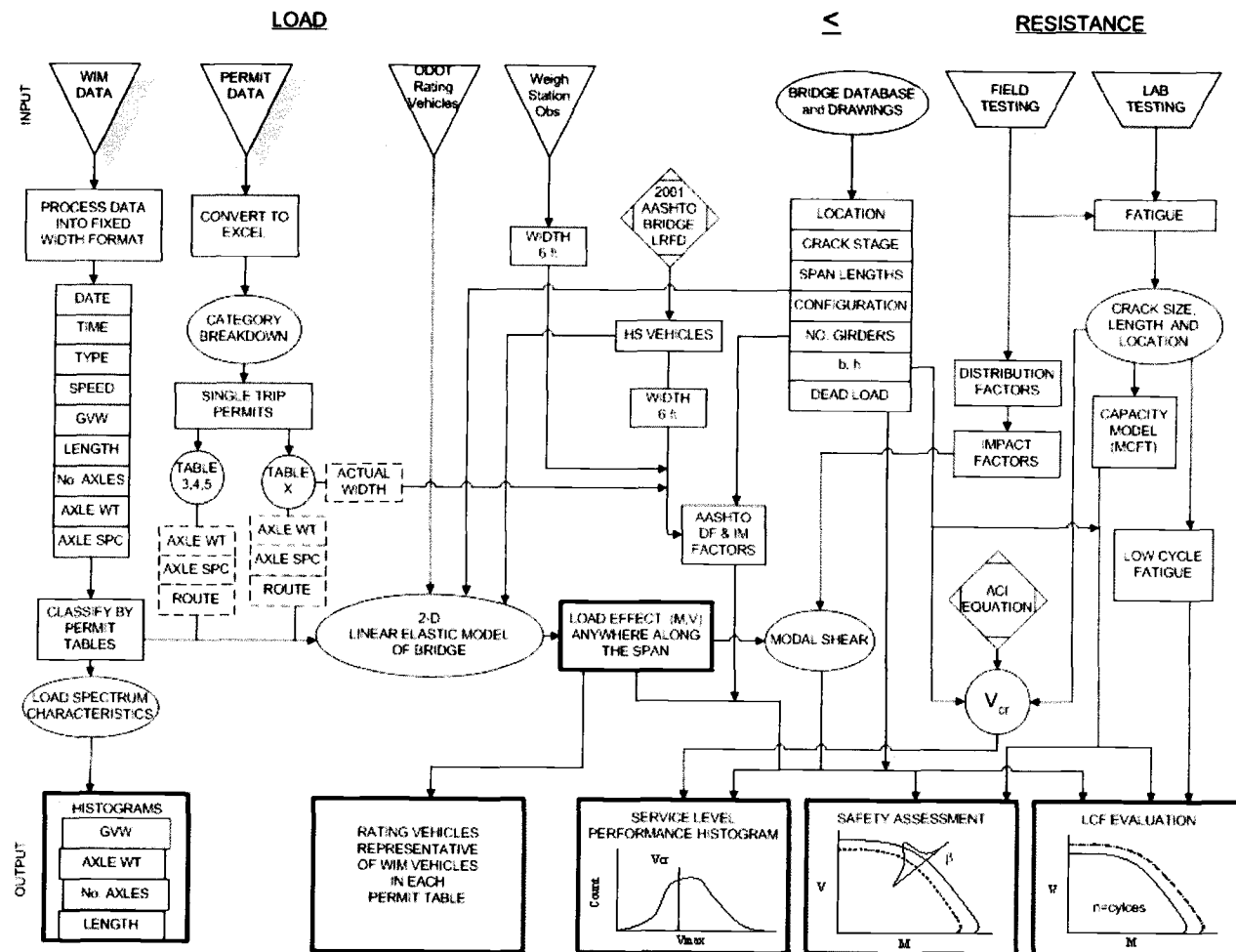


Fig. R1 – Flowchart for extracting truck and bridge response statistics.

REALTIME data combine both the raw data and static data recorded at the weigh station. REALTIME is the result of the GreenLight Program that allows trucks with transponders and within their registered limit to bypass weigh stations instead of having to stop. When a truck goes into a weigh station and is weighed, the static readings over-write the WIM data for that vehicle. The data lines for all trucks receiving either a green light or a static reading are then kept in an EXCEL friendly format as a record of enforcement. REALTIME data are only collected during operating hours of the weigh station.

Raw data, on the other hand, are purely WIM measurements. The record is collected for the entire day, every day and contains all vehicles (including cars, RVs, motorcycles, etc.), but can be filtered to show only vehicles classified, for example, as Type 5 or above. In other words, the record can be narrowed to contain only truck data as it has for this study. It is stored in a text file and saved for 100 days.

Using the Data

Permit Data

Before using the permit data, some familiarity with the vocabulary and permit system is required. A collection of the key terms is contained in Appendix A along with the Permit Tables 1, 2, 3, 4, and 5. To use the data it must be converted from individual forms into an EXCEL friendly format. An example permit is contained in Appendix A.

Figure R2 shows the category breakdown of all the permits issued in 2002. Permits are either Continuous Trip (CTP) or Single Trip (STP). The first three segments are Continuous Trip permits. These permits are issued on a yearly basis. The truck driver

receives a map showing roads not to be used and is expected to comply. Table 1 permits allow vehicles that have legal weights, but exceed the height or length limits or fall into Exception 1 or 2 (described in Appendix A). Table 2 permits are trucks that have legal axles, but are longer, so the GVW is allowed to exceed the 80,000 lb legal limit but must be less than 105,500 lbs. The first part of Permit Table 3, up to 98,000 lbs, is continuous-trip heavy-hauls. These vehicles are allowed more weight on a shorter wheelbase. Permit Table 3 trucks are allowed 43,000 lb tandem axles whereas Permit Tables 1 and 2 only allow 34,000 lb tandems.

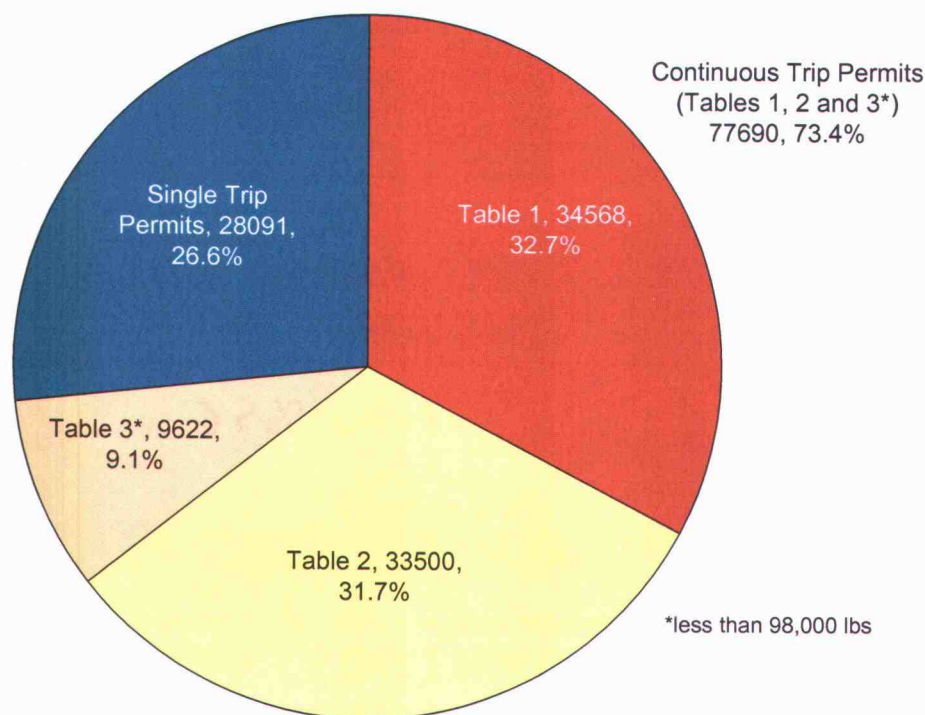


Fig. R2 – Permits issued by Oregon Motor Carrier in 2002 (105,781 Total).

Single Trip permits, on the other hand, are issued on a per trip basis. The truck has between 3 and 7 days to make the trip before the permit expires, and the route to be used is

stated explicitly on the permit. The Single Trip permit category can be broken down again as shown in Figure R3. Since these vehicles can make only one trip with the permit, one-way or round-trip, these numbers are better indicators of how many trucks of this type are on the road. These permits tend to be related to the construction, logging and power industries to name a few. From the monthly breakdown it is evident that more of these permits are issued during Oregon's drier months, which coincides with the construction season and thus the increased need to transport large construction equipment. Over half of the single trip permits are for Permit Table 5 which allows vehicles to have the most weight on the shortest wheel base. It also allows triple axles of 65,000 lbs.

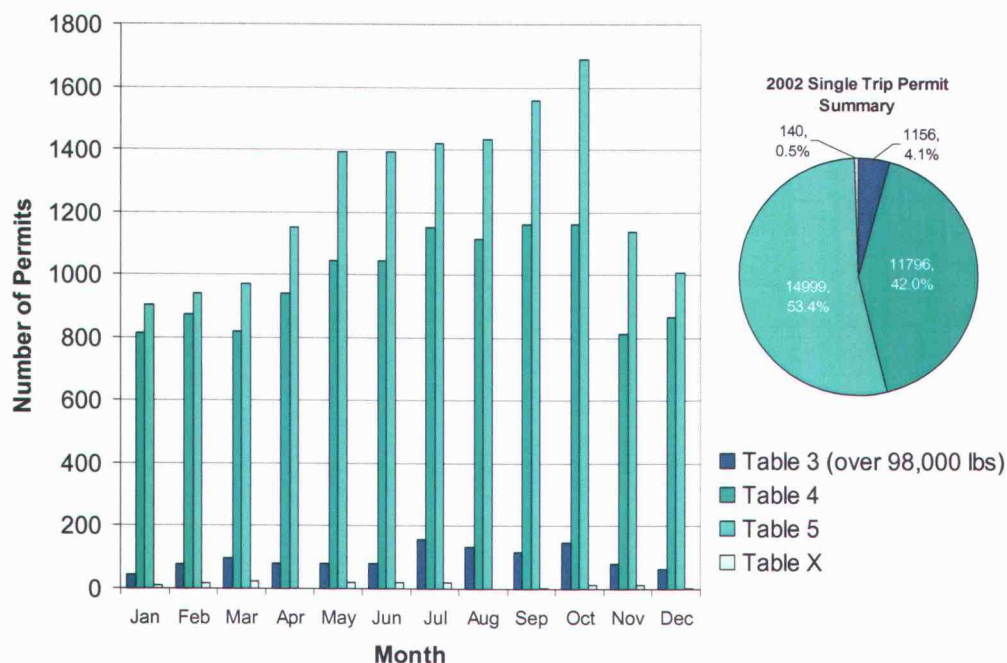


Fig. R3 – Single Trip Permits issued by Oregon Motor Carrier in 2002 (28,091 Total).

Permits are also issued for trucks that fall outside of Permit Table 5. These trucks will be referred to as Permit Table X. For a truck like this, the axle weights and spacings must be known at time of application, and the configuration approved by the ODOT Bridge Group. The route is explicitly stated. Many times specific directions are also given for speed and time of travel as well as for flaggers and escort vehicles.

The permit data as currently collected do not provide enough information (excluding Table X) to accurately depict a vehicle for use in the load model. The information about axle grouping is given by the permit table, the load length, and the number of axles. It will be shown in the Rating Vehicle Representation section that there is not a clear boundary between the load effects produced by vehicles that are classified in the various permit tables. A program was written to convert the limited information provided in the permit data into individual axle weights and spacings. A group of WIM vehicles that appeared fully loaded was selected for the program testing. The load effects produced by the program had poor correlation to the load effects produced by the actual WIM data. Therefore, the permit data could not be used to reliably estimate load effects for these trucks. The permit data, however, are important because trucks with STPs take shorter trips and therefore, are not as likely to be captured at WIM stations. Since WIM stations are not located in close proximity to most bridges in the system, there is reason to believe that permit vehicles could cross bridges and not be included in the WIM data. The importance of these infrequent large loads will become apparent when considering low-cycle fatigue.

REALTIME Data

REALTIME data are easier to use since they are already in an EXCEL friendly format. An example of this data is shown in Appendix A. The Woodburn weigh stations on I-5 for the day of 12-18-02 will be used in an example since these stations have the most activity of any in the State. The distribution of GVW for trucks at the Woodburn Port-of Entry (POE) is shown in Figure R4 graphed on normal probability paper. If the GVWs were distributed normally, then the points would line up in a straight diagonal line. Since the points do not line up, it is quite clear that either the distribution is not normal and/or the GVW distribution is multimodal. When the plot becomes more horizontal it indicates that a large number of trucks is near that GVW. This occurs at 20,000 lbs, 35,000 lbs, 80,000 lbs, and again near 105,500 lbs. These last two are the GVW limits of Permit Table 1 and Table 2, indicating, as expected, that many trucks operate near the table limits.

Bridge response is a function of load effect, and the load effect from each truck will be dependent on many factors. These factors are GVW, length, width, number of axles, individual axle weight, and axle spacings of the truck, as well as the geometry of each particular bridge [Moses and Ghosn, 1985]. Since REALTIME data contain GVW, number of axles and axle group weights, but do not include length and are collected only during the hours of operation of the weigh station, they do not provide all the required information needed for creating the load spectrum.

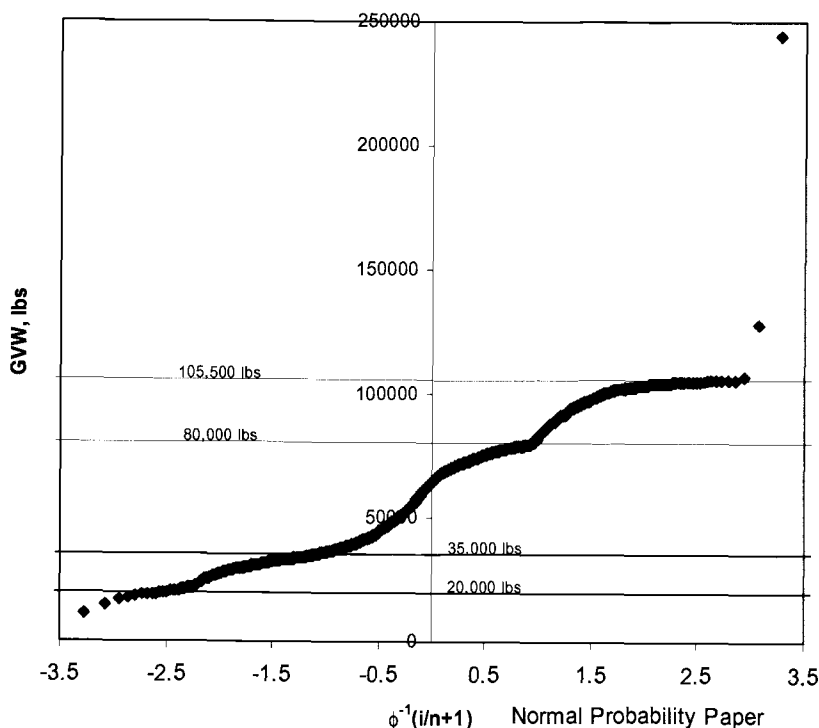


Fig. R4 – Woodburn POE GVW distribution December 18, 2002 (1,868 Trucks).

Raw WIM Data

The text format of raw WIM data required considerable post-processing to be useful in this study. The data must undergo a format transformation, but this can be done only after all spurious data have been removed (currently a labor intensive process). From this data all the information needed about each truck, except for the width, can be extracted either directly or indirectly. An example of the raw WIM data is shown in Appendix A as well as the classifications used in Oregon's WIM study for the vehicle type number. The items extracted directly are the truck type, GVW, speed, time, front to rear axle length, and the individual axle weights. Indirectly, from the pictogram included in the data, the number of

axles can be counted, and the relative spacing of each axle proportioned to the front to rear axle length to obtain estimates of individual axle spacings.

The format transformation was performed using a FORTRAN program written specifically for this purpose. The resulting file lists the time, type, speed, GVW, length, number of axles, axle weights, and axle spacings for each truck, and can be used in EXCEL for data regression and analysis. The data were then classified into the various permit tables with the aide of another FORTRAN program written for this purpose. The classification program does not take into account any of the exceptions allowed for each permit table. For example, a vehicle that is normally classified as Permit Table 1 using Exception 1 will be classified as Permit Table 3 by the program. (Exception 1 allows two consecutive tandems up to 34,000 lbs each if the axle spacing is at least 30 ft. Permit Table 1 without the exceptions would require 39 ft.) The WIM data are classified by the program for use in the Representative Rating Vehicle section.

RESULTS

Truck Spectrum Characteristics

Currently, one year of data (January 30, 2003 – 2004) from the Wilbur WIM collector 7 miles north of Roseburg on I-5 have been analyzed. Figures R5 to R10 show the characteristics of the truck traffic.

The GVW for all WIM trucks captured at Wilbur during the first collection period of 97 days (238,463 trucks) is shown in Figure R5 in both arithmetic and logarithmic scale. GVW is plotted in 1 ton increments. The number of trucks is plotted logarithmically to make it easier to see the large but infrequent GVW values. The GVW peaks are near 10,000 lbs, 32,000 lbs, 70,000 lbs, and 98,000 lbs. These last three peaks correspond to the category limits represented by the horizontal portions of the normal linearized cumulative distribution function (CDF) of GVW using REALTIME data (Figure R4).

The accumulation of WIM data for extended periods of time refines the tail distribution for large GVWs as illustrated by Figure R6. The vehicle counts are normalized to the number of vehicles in each respective collection period. It is evident that in a short time period the general shape and modes are defined. It also shows that as more data are added to the load spectrum, the upper tail becomes more clearly defined.

A comparison of GVW is made between three WIM collection sites on Interstate 5 in Figure R7. Woodburn POE is southbound, while Wilbur and Booth Ranch are southbound and northbound, respectively, at the same location. The normalized GVW histograms

indicate that the vehicle pattern is consistent for the three stations. Note that the largest amount of data is shown for Wilbur, while Woodburn POE only contains one month and Booth Ranch has just two weeks. The normalized data indicate the proportion of GVWs captured at each site. The histogram for Woodburn POE in Figure R7 indicates that a larger proportion of vehicles with large GVWs is observed at the Woodburn POE site compared to Wilbur or Booth Ranch.

For the first collection time period at Wilbur (97 days), the histogram for axle weights in 1 ton increments for 1,268,978 axles is shown in Figure R8 in both arithmetic and logarithmic scale. The two peaks are at 10,000 and 14,000 lbs. A legal tandem axle is 34,000 lbs, and this may explain why the second individual axle weight peak is about half that value. When only the weight of the steer (front) axle is plotted, it shows that the most common weight is 10,000 lbs as shown in Figure R9, and presumably drives the first peak in Figure R8.

Vehicle type and number of axles are also collected in WIM data. Type 11 is a 5-axle semi-truck. The histograms for vehicle type and number of axles clearly show that the dominant vehicle is a 5-axle semi-truck as illustrated in Figures R10 and R11. It is also observed that in the 97 day collection period at Wilbur, as well as for the entire year, there were no vehicles with more than eleven axles.

The last item collected by WIM is the truck length measured from the steer axle to the rear axle. The histogram for the truck front to rear axle length suggests that the modal truck is 55-60 ft. long as shown in Figure R12.

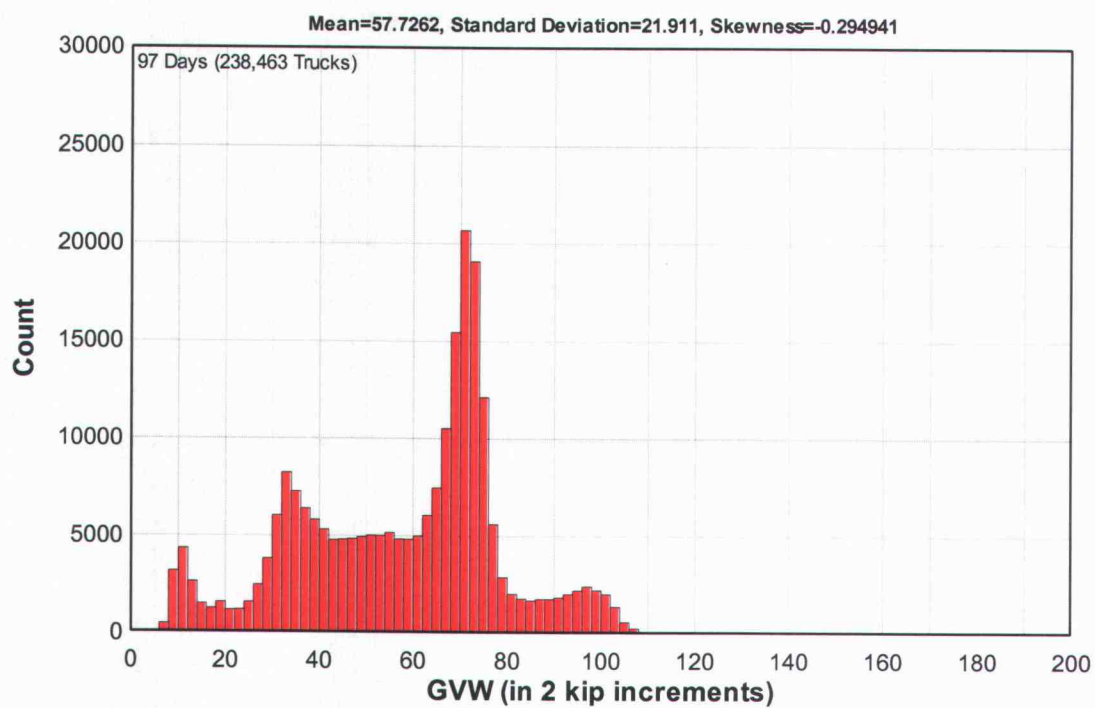
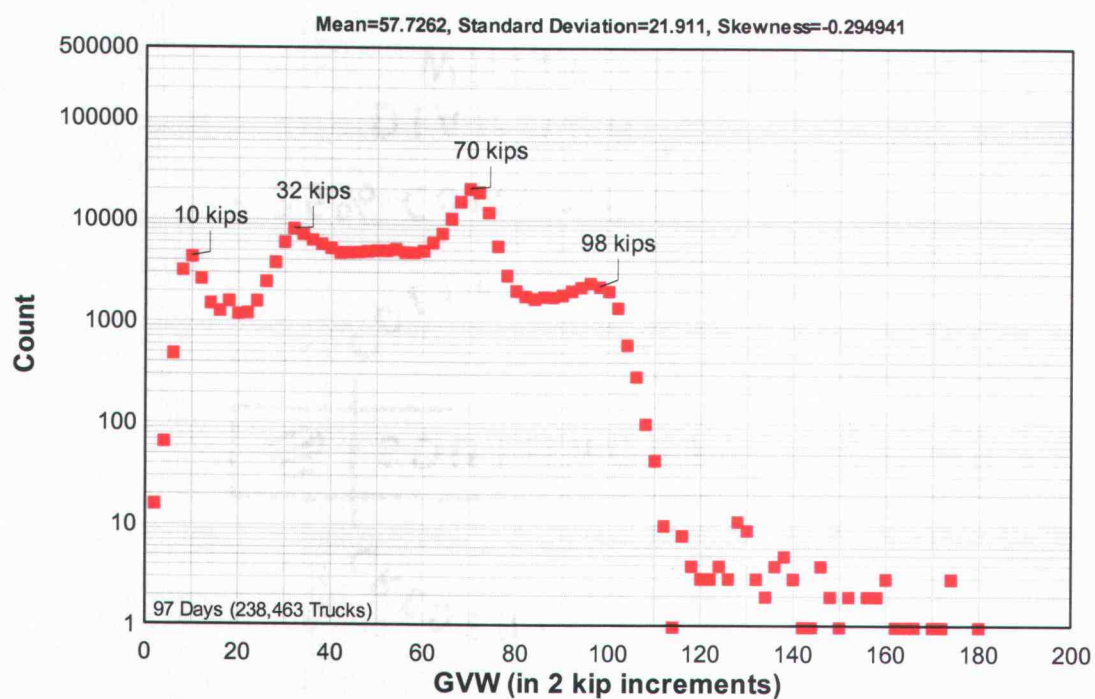


Fig. R5 – GVW histograms for all trucks captured by Wilbur WIM.

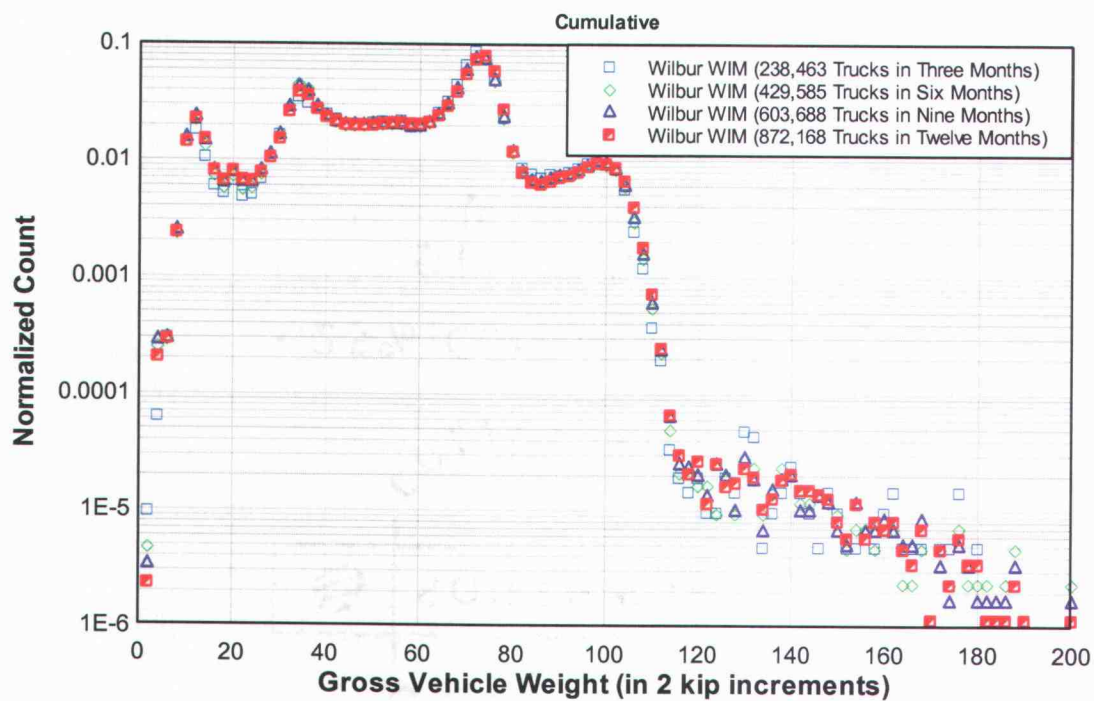


Fig. R6 – Accumulated WIM collection in 2003.

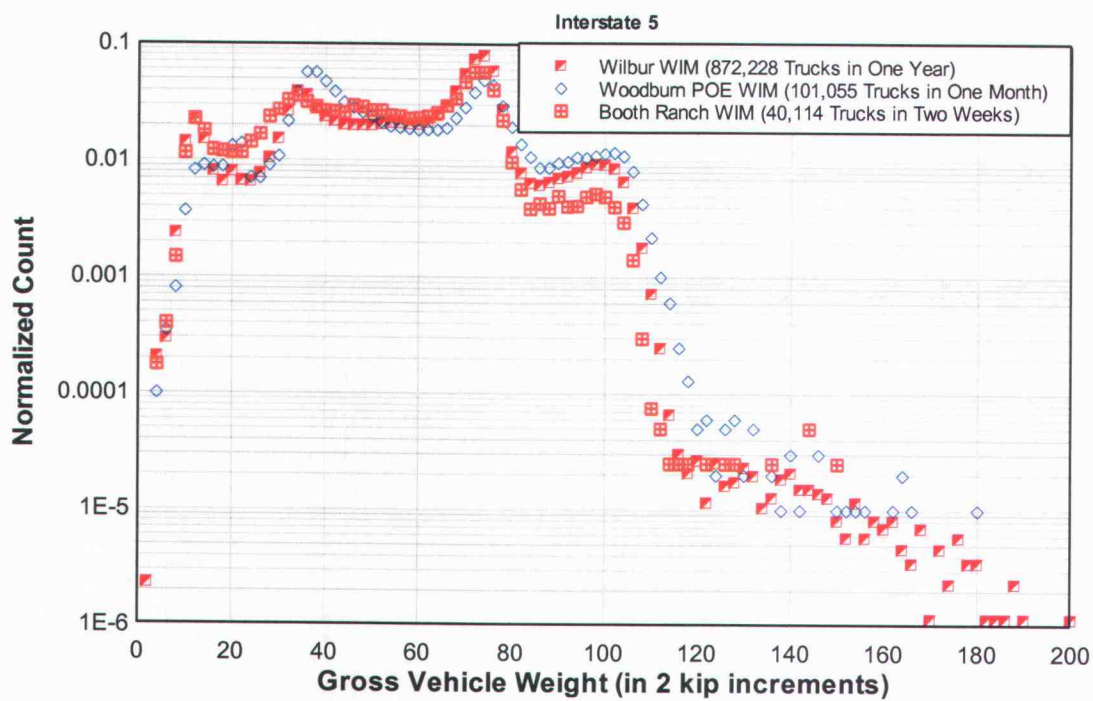


Fig. R7 – Comparison of WIM stations on Interstate 5.

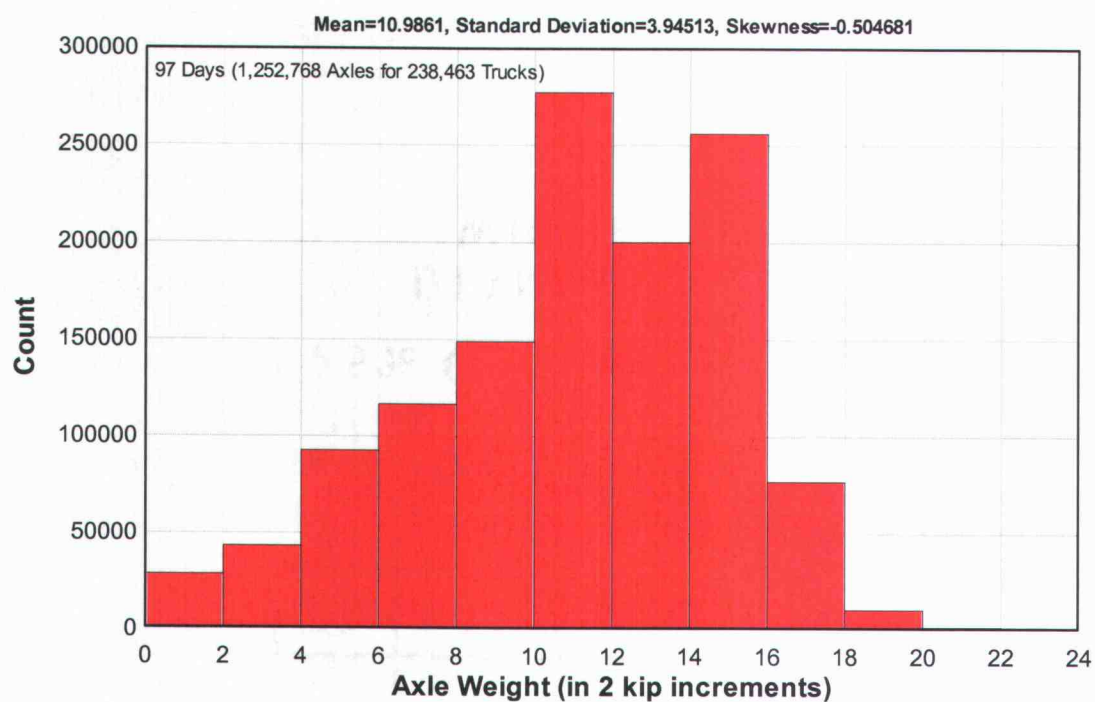
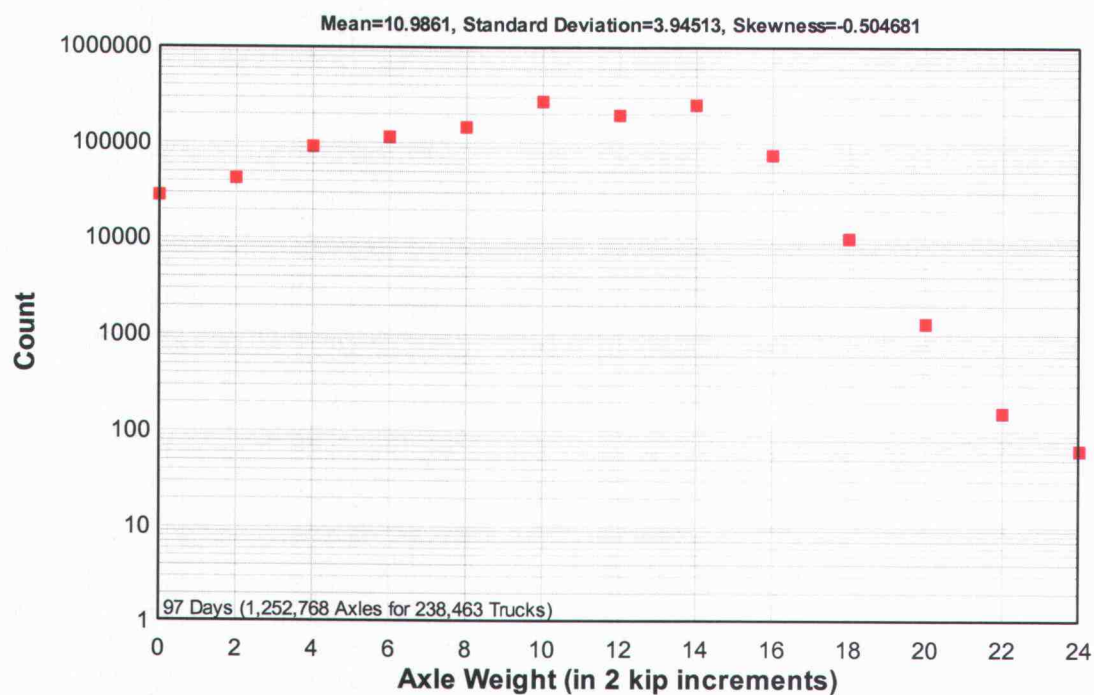


Fig. R8 – Axle weight histograms for all trucks captured by Wilbur WIM.

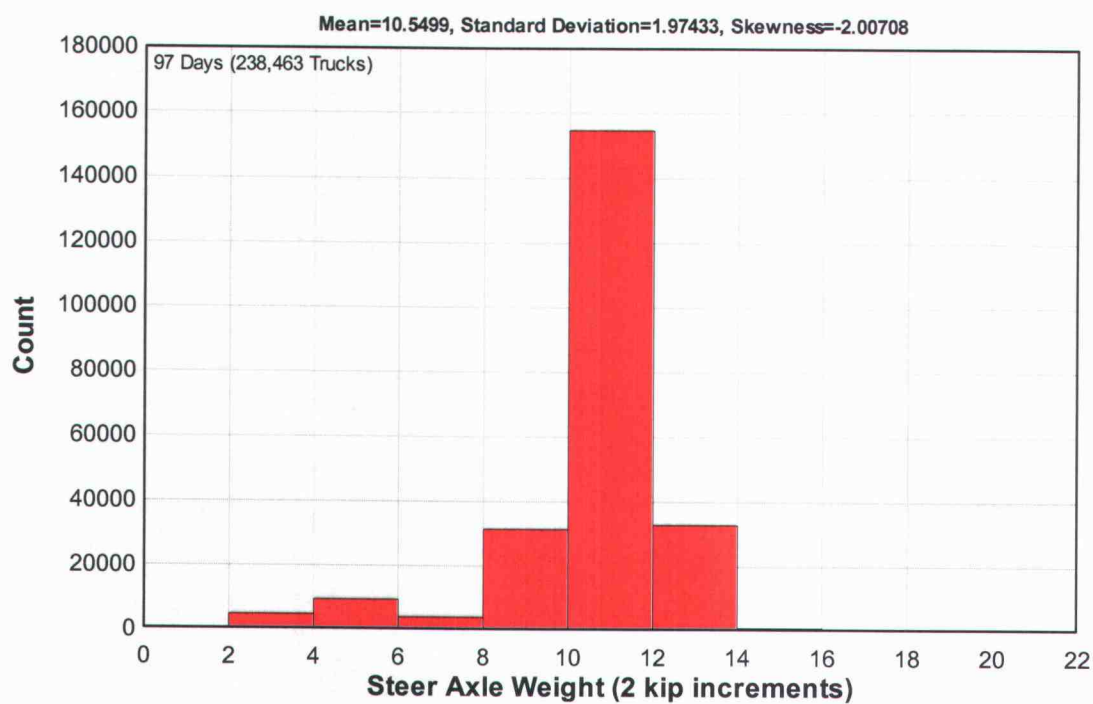
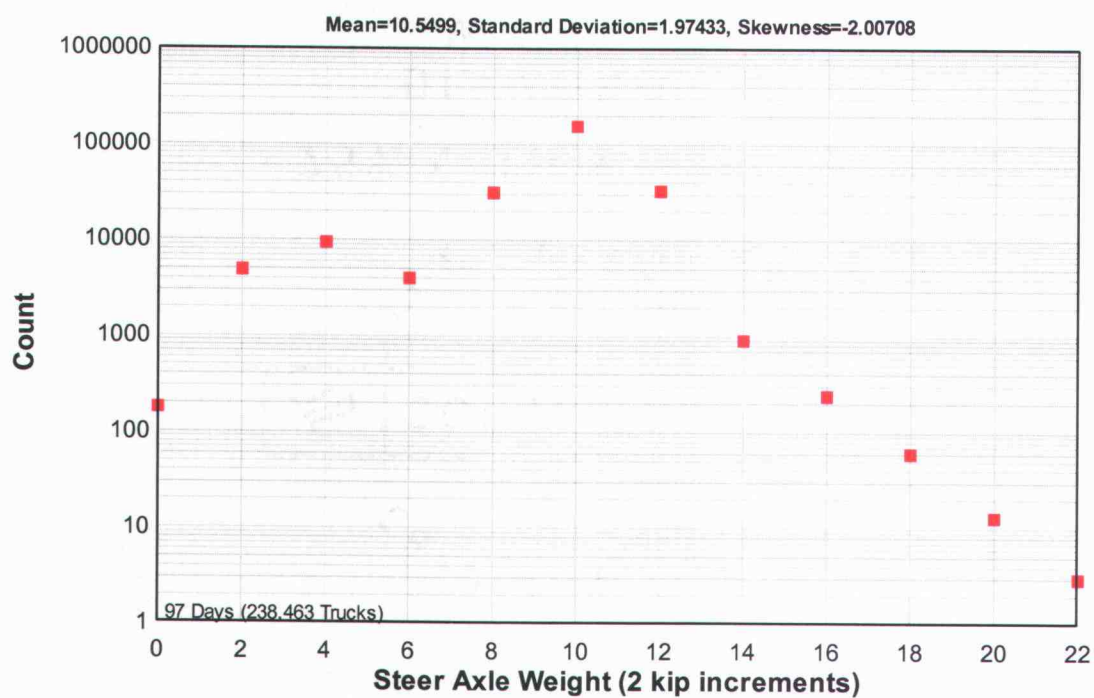


Fig. R9 – Steer axle weight histograms for all trucks captured by Wilbur WIM.

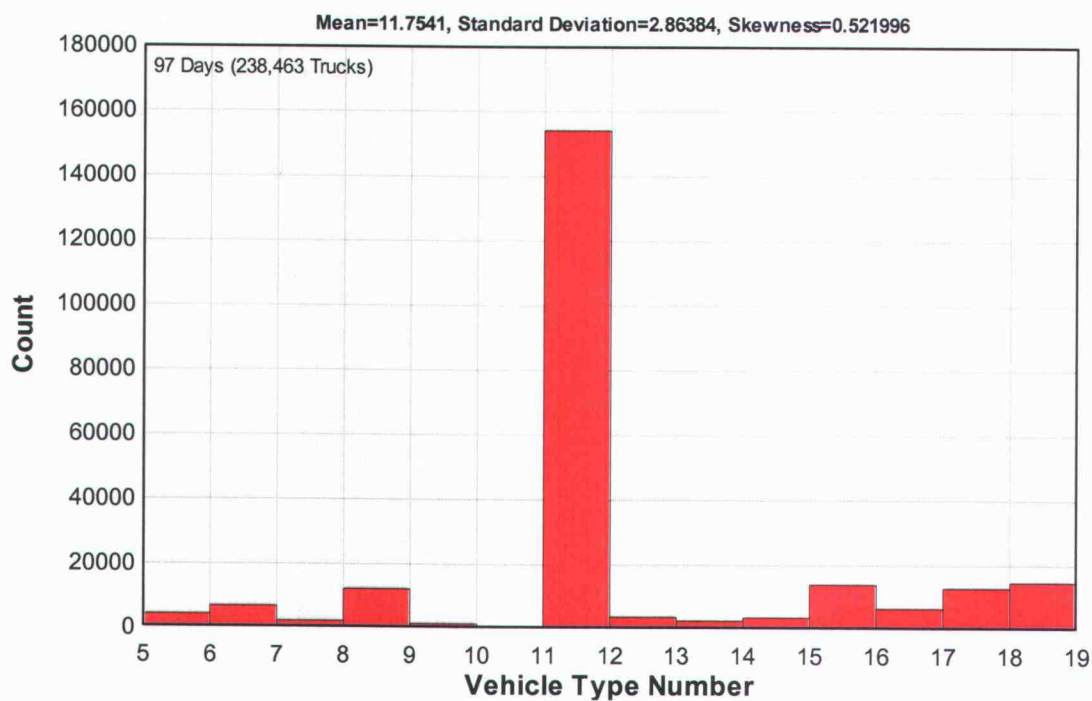
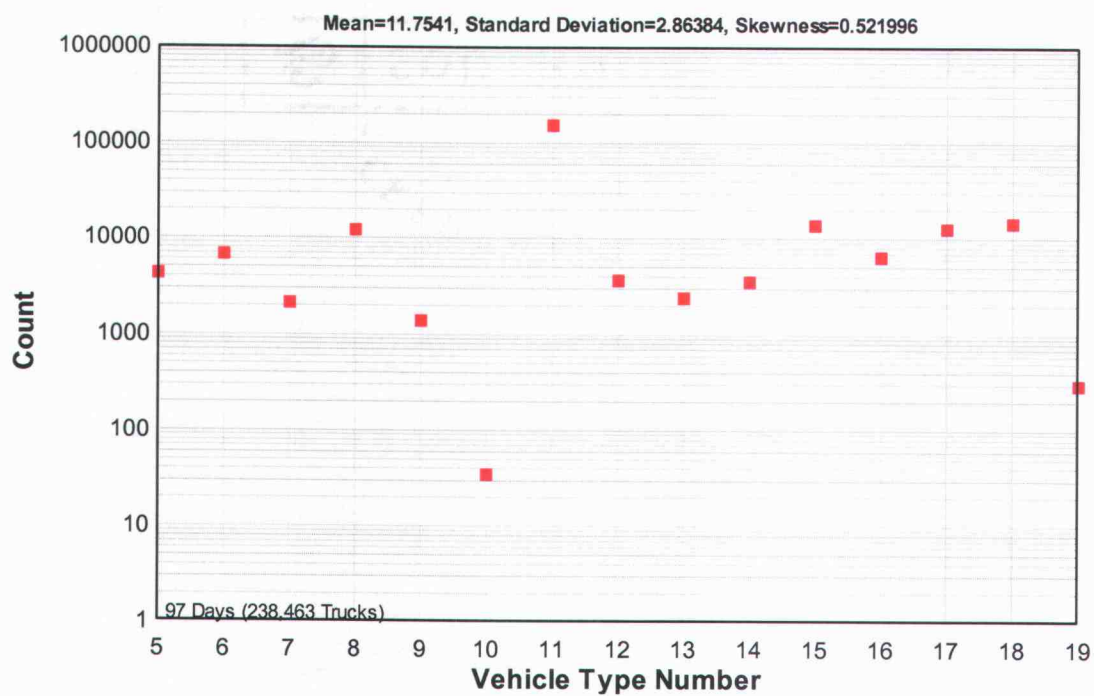


Fig. R10 – Histograms of vehicle type for all trucks captured by Wilbur WIM.

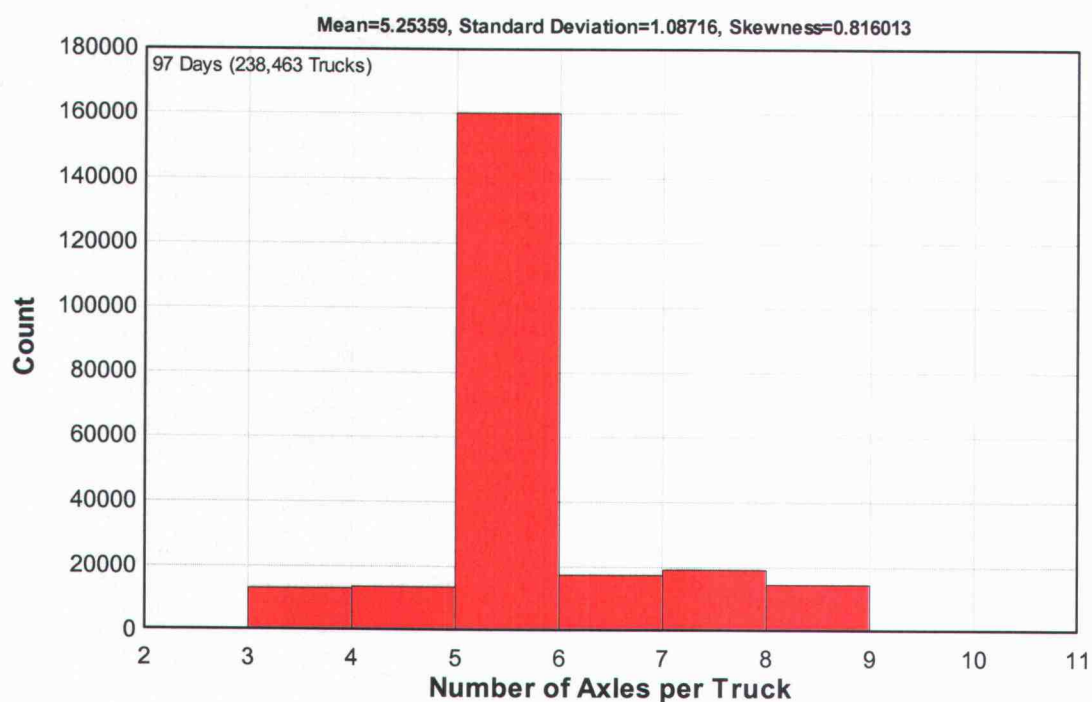
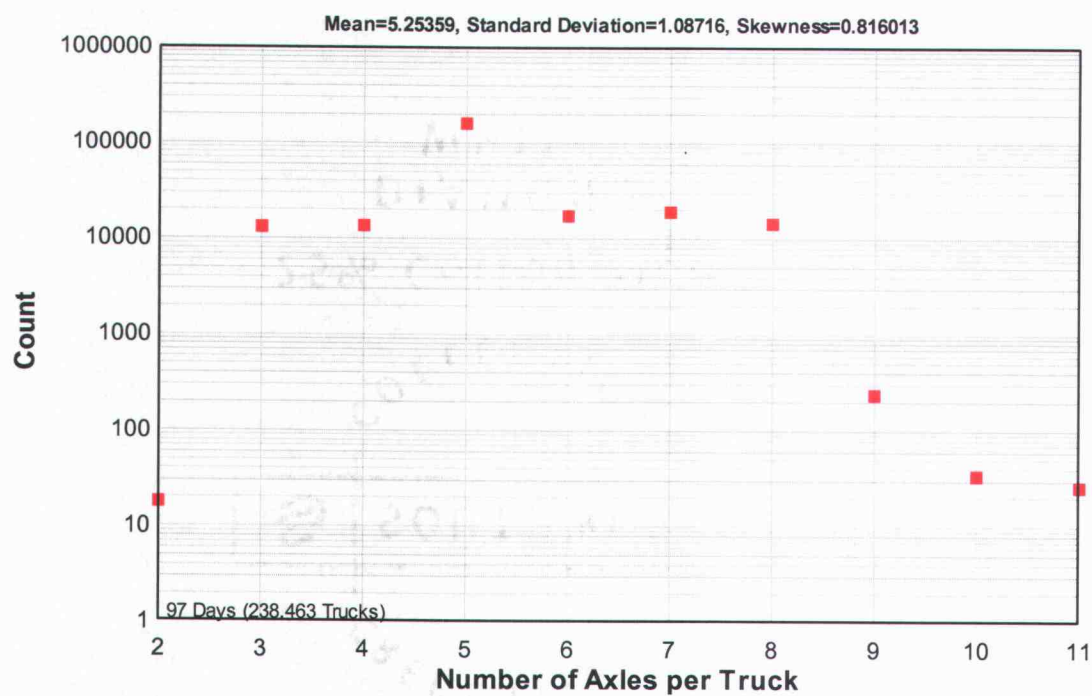


Fig. R11 – Histograms of axle number per vehicle for all trucks captured by Wilbur WIM.

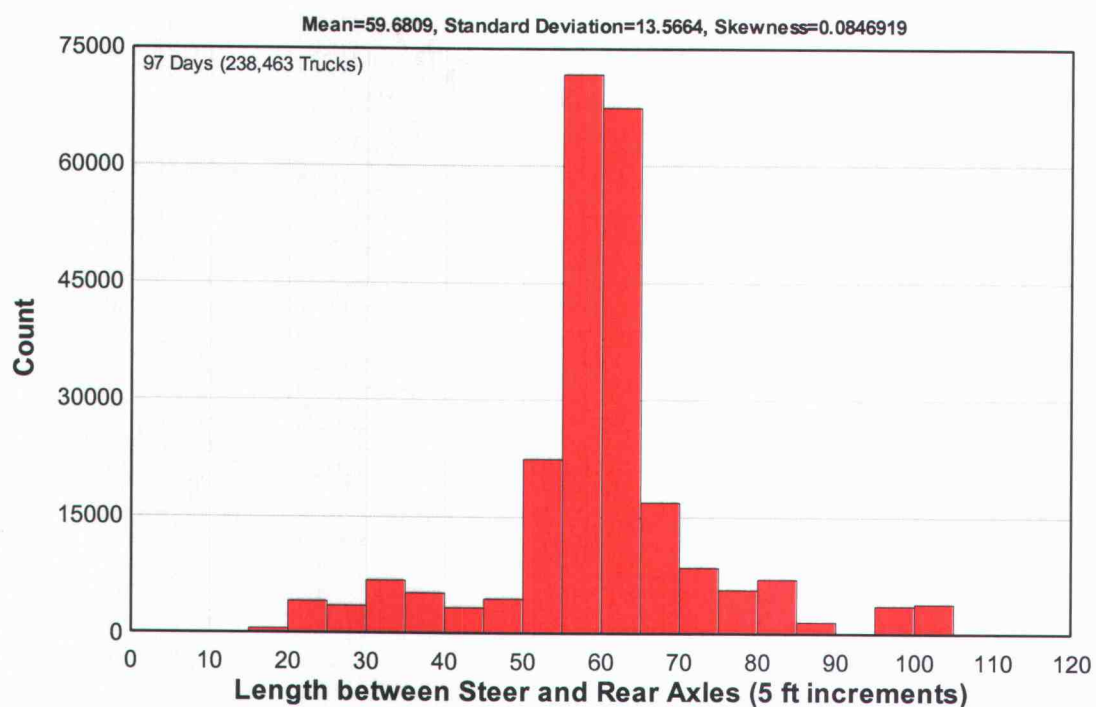
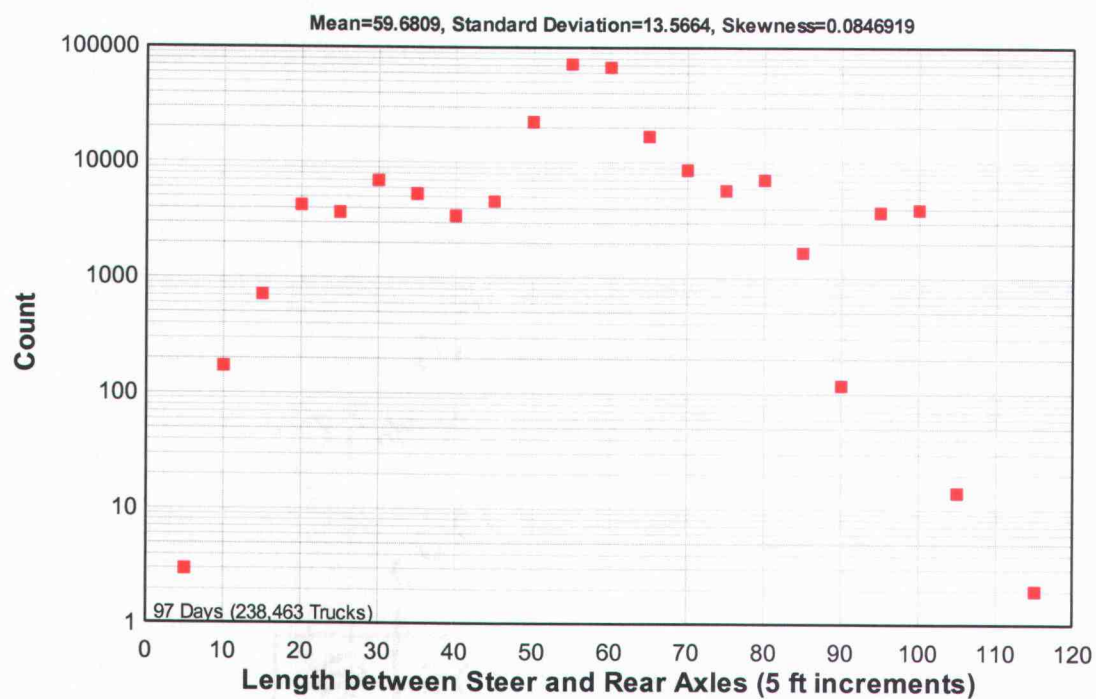


Fig. R12 – Histograms of steer to rear axle length for all trucks captured by Wilbur WIM.

The WIM vehicles from the first collection period at Wilbur (97 days) were classified into the permit tables. There are less than 15,000 vehicles of the nearly 240,000 vehicles that fall into Permit Table 3, 4 or 5 as shown in Figure R13. The vehicles captured at Woodburn POE in one month were also classified by Permit Table for comparison. As foreshadowed by the GWV comparison of the two stations (Figure R7), there are in fact more occurrences of vehicles in the higher Permit Tables, during a shorter collection period, at Woodburn POE as shown in Figure R14. This indicates that the occurrence rate for large loads is dependent on location.

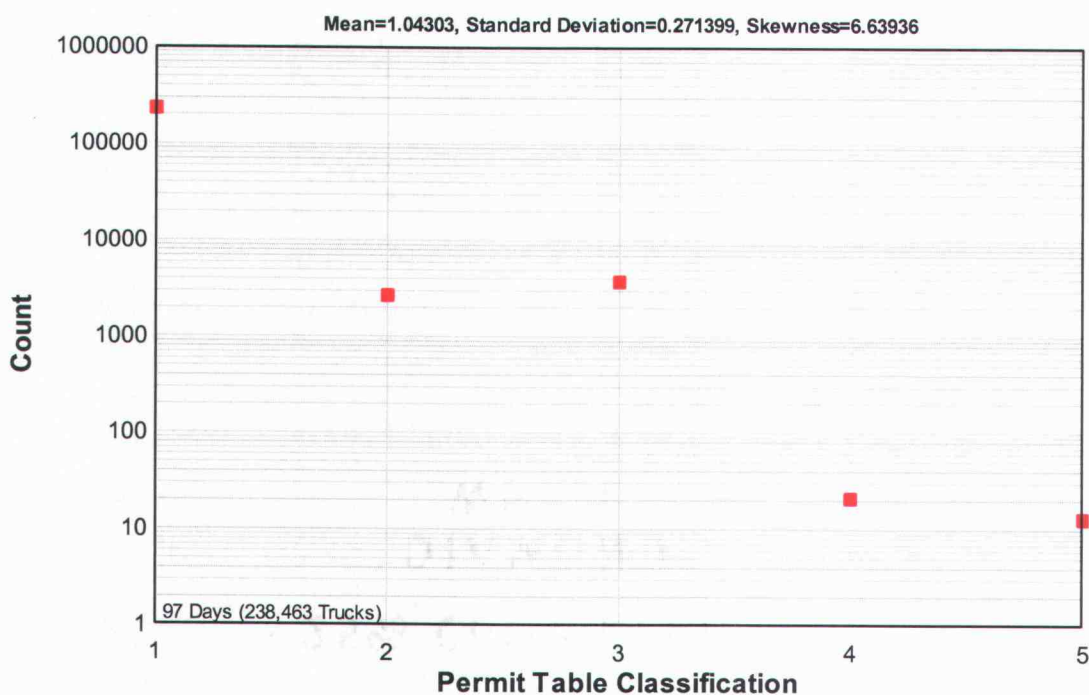


Fig. R13 – Histogram of Permit Table classification for all trucks captured by Wilbur WIM.

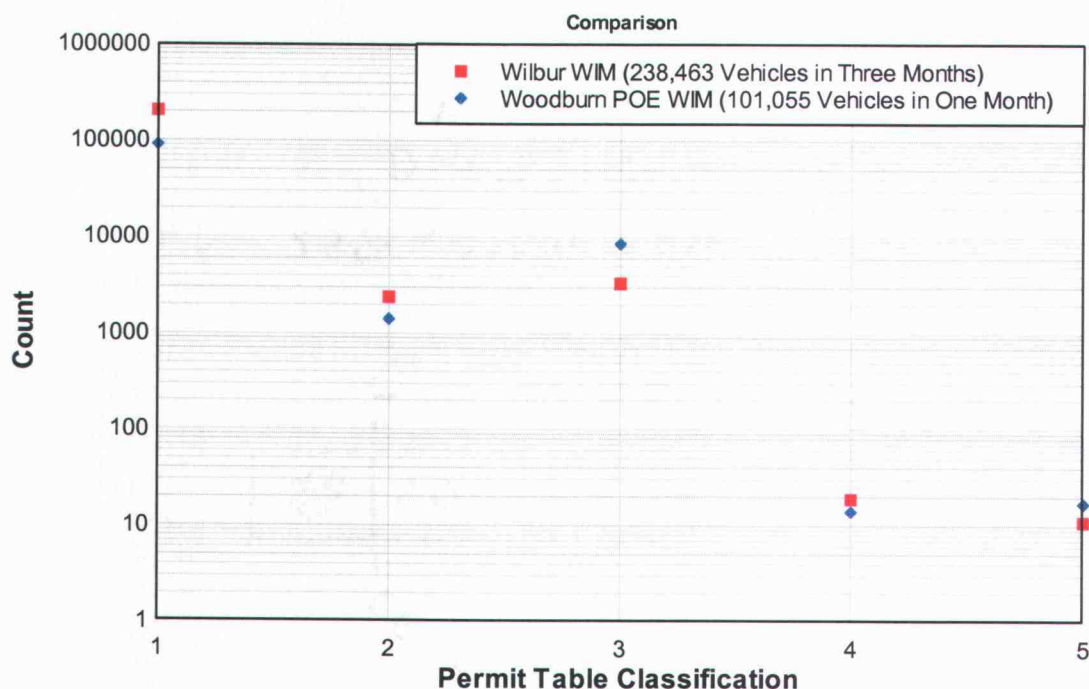


Fig. R14 – Comparison of WIM vehicle permit classifications.

The vehicles captured at the Wilbur WIM station from January 2003 to January 2004 are classified into the different permit tables for illustration purposes only since the program written does not account for any exceptions related to the permit tables. The entire year of Wilbur WIM data was separated into subsets for Permit Tables 3, 4 and 5 and will be used in subsequent figures and evaluations.

Live Load Effect

To determine the effects of truck loadings on a specific bridge, a FORTRAN program based on the slope-deflection method of structural analysis has been written where span lengths can be varied. A separate program is used for each bridge configuration, i.e., number of spans. It has been shown that a linear-elastic analysis is adequate for determining shear and moments in cracked RCDG bridges under service loads [Higgins *et*

al., 2004a]. From the database of Oregon's RCDG bridges built between 1947 and 1962, it was found that simply-supported and three-span continuous are the most common bridge configurations. Others occurring much less frequently are two-span, four-span, five-span, and six-span continuous bridges.

The truck data are input into the 2-D linear-elastic model of a particular bridge and the load effects are calculated at points of interest. The truck is moved in a thousand small increments (zeta) across the bridge until the last axle leaves the bridge. The entire history of the load effects is collected as the truck travels, and the maximum shear with corresponding moment as well as maximum moment with corresponding shear are extracted. The load effect history for each vehicle is of interest because as each axle group approaches a section, that axle group dominates the load effect. This is illustrated when the moment and shear are plotted together and when they are plotted separately as illustrated by the two parts of Figure R15. The analysis does not account for section changes in the girder, such as horizontal taper or vertical haunch. For bridges with taper or haunch, the geometry changes are typically within the quarter span of continuous supports. A preliminary investigation (See Appendix B) using SAP2000 [CSI, 2000] showed that the effect of horizontal taper at supports on the shear is less than 2% and on moment near continuous supports is approximately 15 %. Vertical haunch affected the shear and moment near supports by less than 3% and approximately 30%, respectively.

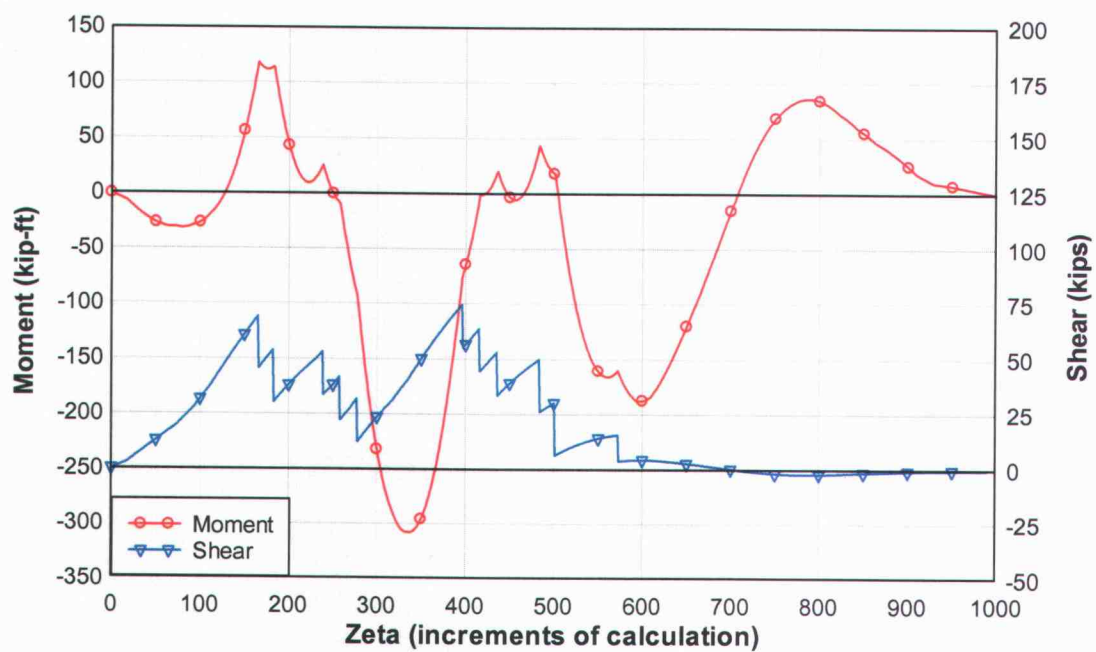
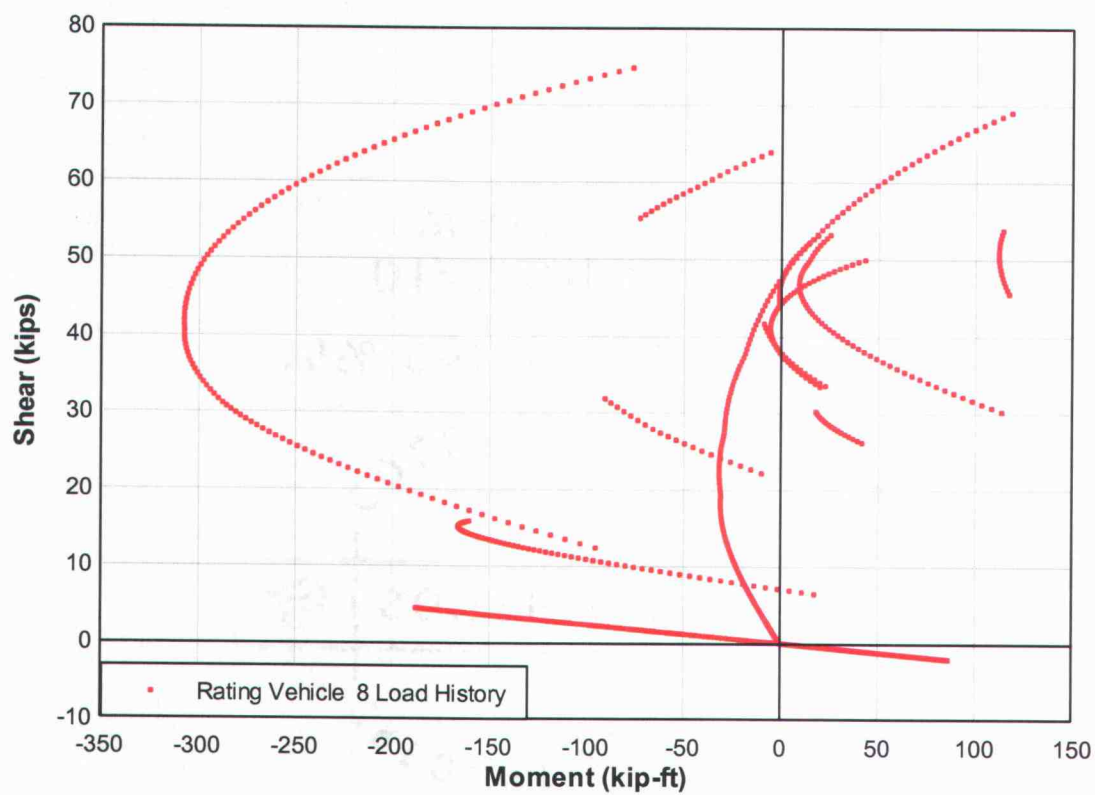


Fig. R15 – Load effect history of Rating Vehicle 8 on three (50 ft) - span continuous bridge.

Representative Rating Vehicle Live Load Effects

Currently, the ODOT Bridge Group uses eleven different vehicles when rating bridges. The description of these vehicles is shown in Appendix C. For simplicity, the vehicles are numbered from one (1) to eleven (11) in this study. In order to assess the load effects produced by the eleven ODOT Rating Vehicles as compared with actual permitted vehicles, analyses were performed for a range of bridge indeterminacies and span lengths. Results will enable a reduced number of rating vehicles to be used for assessments (of specifically one-time overloads) of RCDG bridges. Using the bridge database [Higgins *et al.*, 2004a] as a guide, four indeterminacies were included: simple, two-span continuous, three-span continuous, and four-span continuous. Span lengths ranging from short to long were investigated. End spans resting on abutments were considered simply supported. For the multi-span bridges, all spans were of equal length. The following cases were considered:

Single-Span simply-supported - 11 ft. span and 64 ft. span

Two-Span continuous – 25 ft. spans, 50 ft. spans and 70 ft. spans

Three-Span continuous – 50 ft. spans and 120 ft. spans

Four-Span continuous – 50 ft. spans and 70 ft. spans

Analysis results were collected at locations corresponding to diagonal cracking damage observed in the field. These included locations of relatively high shear. To simplify the number of locations, the maximum shear (V_{\max}) versus corresponding moment (M) at 4 ft. from the supports was used for the nine bridges. This corresponds roughly to the girder depth away from the support. Analysis results are shown in Appendix C. Also shown in these figures is the maximum moment (M_{\max}) versus corresponding shear (V) at the same location. These two points characterize the extremes of the load effect history. However,

due to the actual shape of the loading history as shown in Figure R15, the controlling load effect for capacity may be some intermediate value between these extremes.

The various ODOT Rating Vehicles as described imply representation of actual vehicles falling into specific permit tables. Three example plots are shown in Figures R16 to R18. Figure R16 shows that for a common span length of 50 ft., Rating Vehicles 10, 11, and 8 envelop the Permit Table 3, 4 and 5 WIM vehicles, respectively. Figure R17 shows that for long spans, Rating Vehicle 10 is no longer adequate to capture Table 3 load effects; likewise for Rating Vehicle 11 capturing Table 4 effects. Figure R18 indicates that for shorter spans, Rating Vehicle 7 is necessary to capture Table 4 and 5 WIM vehicle load effects, whereas Rating Vehicle 5 is needed to capture Table 3. Evaluation of the various load effects in Appendix C for the rating vehicles and their ability to describe WIM permit classifications is summarized in Table R1.

Table R1 – Rating Vehicles with representative load effects for permit categories.

Permit Table	Rating Vehicle Implied to Represent	Rating Vehicle That Represents Load Effects
Table 1 (Legal Loads)	1 thru 4	Not assessed
Table 3 (Continuous Trip)*	5 and 6	10 and 5 (and 11 for long spans)
Table 4 (Single Trip)	7	11 and 7 (and 8 for long spans)
Table 5 (Single Trip)	8	8 and 7

*Table 3 WIM vehicles were not separated into CTP and STP for this evaluation.

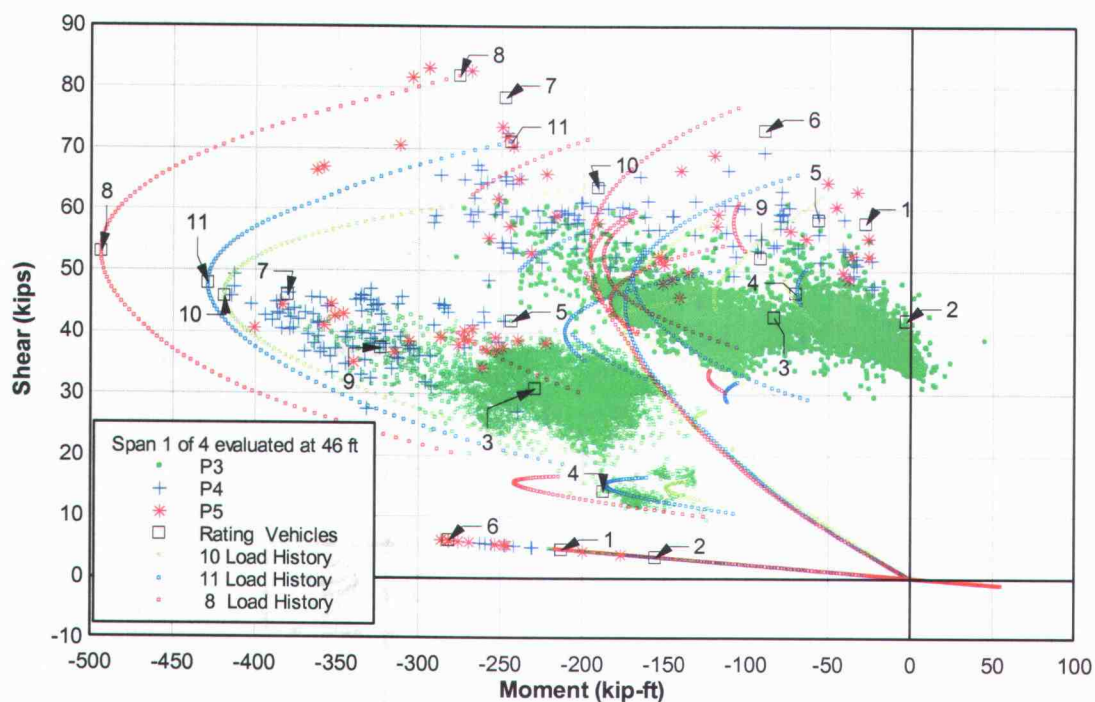


Fig. R16 – Maximum load effects for 1 year of Wilbur WIM permit vehicles (14,510) on a four (50ft) – span continuous bridge.

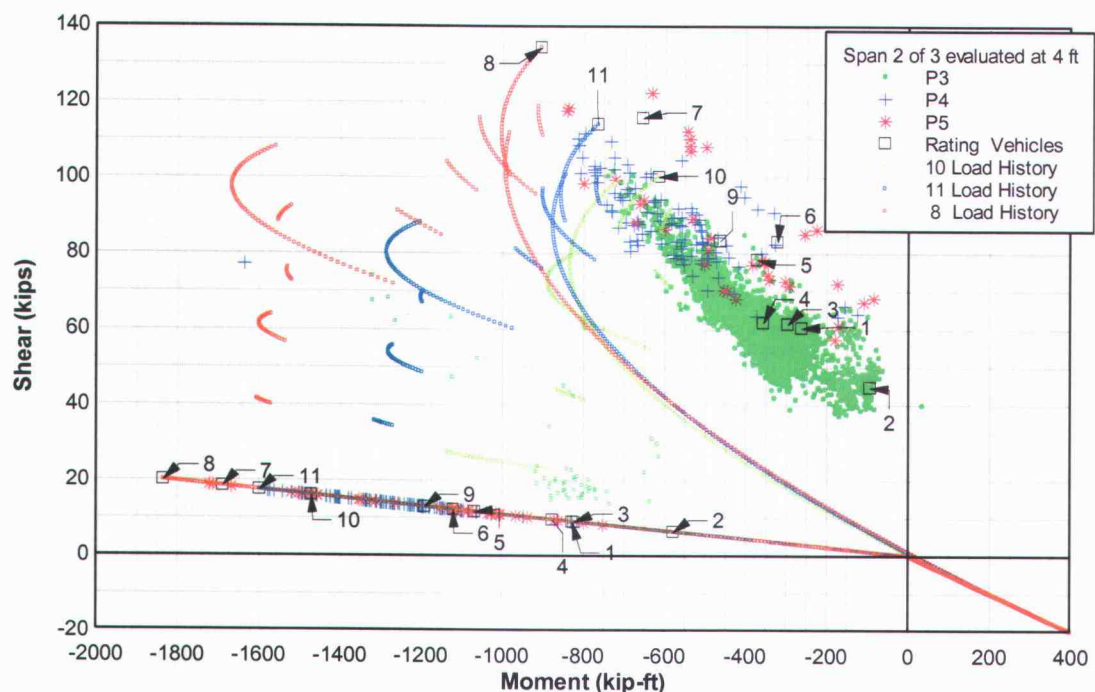


Fig. R17 – Maximum load effects for 1 year of Wilbur WIM permit vehicles (14,510) on a three (120 ft) – span continuous bridge.

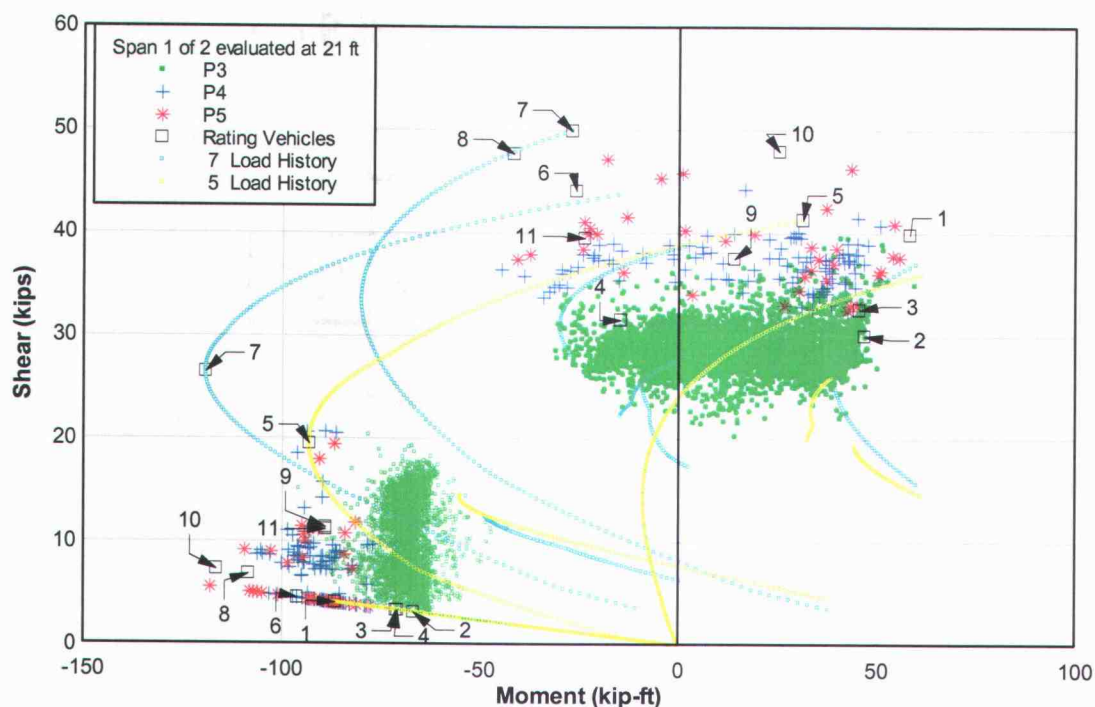


Fig. R18 – Maximum load effects for 1 year of Wilbur WIM vehicles (14,510) on a two (25 ft) – span continuous bridge.

Figures R16, R17 and R18 also make it apparent that there is no clear separation in the load effects produced by vehicles classified in Permit Tables 3, 4 and 5. Although Permit Tables imply that Permit Table 5 produces the largest load effects, many instances occur where a WIM vehicle corresponding to Permit Table 5 produces smaller load effects than a WIM vehicle corresponding to Permit Table 3. However, inspection of the WIM vehicles classified as Permit Table 5 (Appendix C) indicates that trucks commonly reached the higher table classification because of one heavy axle or axle group, whereas the WIM vehicle classified as Permit Table 3 that produced larger load effects was most likely fully loaded.

APPLICATION

The load effects calculated for the WIM vehicles and ODOT Rating Vehicles can be used to evaluate whether or not the capacity of a given section of a girder along the length of an entire bridge is adequate for the live load effects that are likely to occur during the life of the structure. The load effects were used to evaluate the service level performance and the capacity of a RCDG considering both one-time overloads and low-cycle fatigue. High cycle fatigue (HCF) will not be evaluated as field and laboratory work indicate that HCF loading, due to the low stress range in the stirrups, is unlikely to cause stirrup fracture [Higgins *et al.* 2004b]. A flowchart for the application process is illustrated in Figure R19. Service level performance evaluation is not included in the figure since it is only being performed in this study to explain the presence of diagonal cracks in the RCDG bridges and is not part of the methodology for assessment. The figure shows how the Oregon load spectrum, field testing, research and laboratory testing, bridge inspection and bridge drawings are integrated. The process is illustrated using a typical bridge.

Bridge Description

The McKenzie River (also called Spores) Bridge (ODOT #08175N) on I-5 northbound just north of Eugene, OR was part of the field testing performed [Higgins *et al.*, 2004b] and was identified as crack stage 3 by ODOT. It has a three-span continuous portion with all three spans 50 feet long. The bridge deck cross-section and exterior girder being analyzed are shown in Figure R20 and the profile is shown in Figure R21. The girder has a horizontally tapered web between the span quarter points on either side of continuous

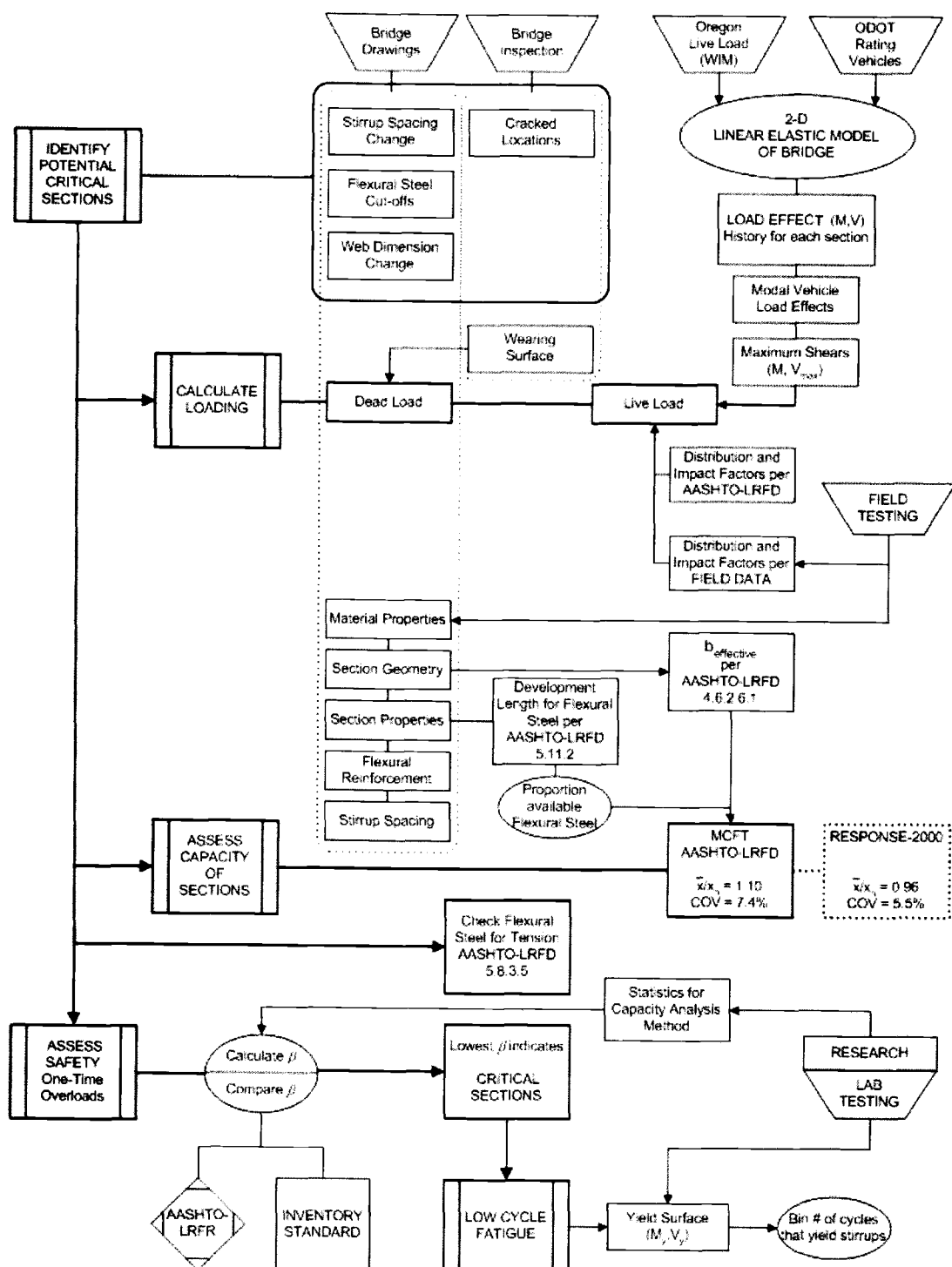


Fig. R19 – Flowchart for safety assessment and low cycle fatigue evaluation.

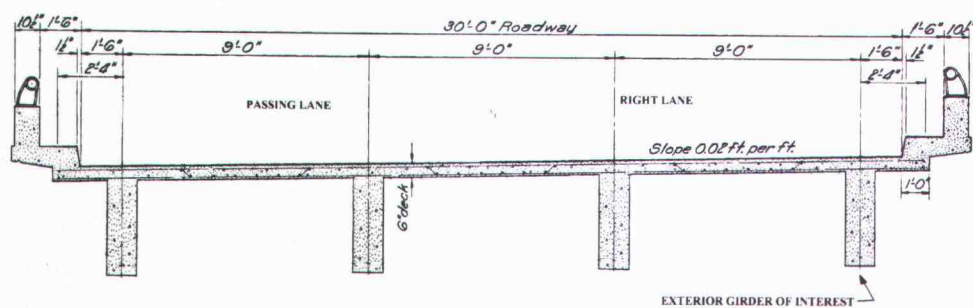


Fig. R20 – McKenzie River bridge deck cross-section.

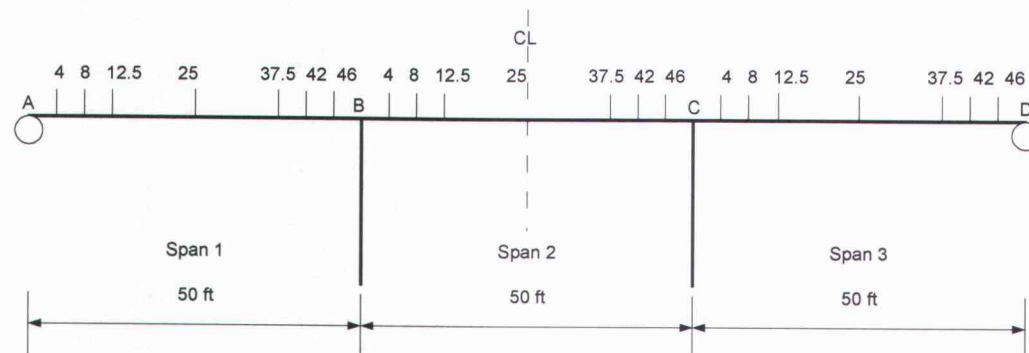


Fig. R21 – Profile view of McKenzie River bridge with cross-section locations (feet).



Fig. R22 – Existing cracks on the McKenzie River bridge exterior girder in span 1 near support B. The first diaphragm framing is 12.5 ft from support B centerline.

supports. The detailed bridge drawing is shown in Appendix D. A photo of the observed diagonal cracking on the exterior girder is shown in Figure R22.

Identify Potential Critical Sections

The first step is to identify girder sections that possibly control the capacity of the girder. Two sources for information are the bridge drawings and bridge inspection. The potentially critical sections will likely occur where there is a change in stirrup spacing, flexural reinforcing steel is cut-off, or there is a change in the web dimension. These can be determined from bridge drawings, and field verified as needed. The other indicator for a potential critical section is a diagonal tension crack in the girder based on field inspection. For example, the exterior girder of the McKenzie River bridge has diagonal cracks at approximately 4 ft. 8ft., and 12.5 ft. from the centerline of support B as shown in Figure R22. The drawings reveal that the tapered web section begins at 12.5 ft. from support B and that top and bottom flexural steel are cut-off at that location. There are seven stirrup changes in span 1. One is at about 4 ft. from support A and another is about 8 ft from support A. Not all stirrup change locations and flexural bar cut-off locations were evaluated for this example. The potentially critical locations that were assessed are depicted in Figure R21.

Calculate Loading

With the section locations determined for evaluation, the next step is calculating the dead load and live load at each section.

Dead Load

The permanent loading, referred to as dead load, is the self weight of the bridge members, deck, wearing surface and other components. The dead load is estimated from the bridge drawings. Additional information can be collected from field investigation such as the thickness of the wearing surface. The weight carried by each girder is taken as the total weight divided by the number of girders and this is applied as a distributed load along the length of the member. The dead load for components and wearing surfaces were not separated in the example, but could be if necessary.

Live Load

The live load effects on a bridge girder are determined from structural analysis of moving load models to determine the maximums at each section of interest. The static load effects are amplified for dynamic/impact effects using an impact factor. These forces are then assigned to girders by means of a distribution factor. Distribution factors represent how much of each lane load, or load effect of a truck, is distributed to an individual girder. The factor is dependent upon the bridge geometry and truck width as well as the lateral placement of the truck on the bridge.

The equations for live load distribution factors used in the AASHTO-LRFD Bridge Design Specification [2003] are dependent on the superstructure cross-section, span length, girder longitudinal stiffness and deck thickness for RCDG bridges. AASHTO-LRFD provides distribution factors for lane loads based on the 6 ft. wide HS vehicles (centerline of wheel-group to wheel-group). Observations from weigh station visits at Philomath and Woodburn (See Appendix A for full details) indicate that actual truck width ranges from

about 6'-3" to 7'-0". Large permit loads can be even wider. The distribution factors become larger as the width narrows. To be slightly conservative, 6 ft. is used for the truck width when calculating AASHTO-LRFD distribution factors applied to the WIM vehicle effects.

Distribution and impact factors calculated from AASHTO-LRFD could be overly-conservative for a specific bridge. Field data can be collected to more reasonably reflect in-situ distribution and impact factors. Based on instrumented stirrups with strain gages at multiple cracked locations, a distribution factor for shear can be estimated. Using a test vehicle and driving it over the bridge at different speeds, an impact factor was also determined [Higgins *et al.*, 2004b]. Since an overly-conservative assessment may lead to unnecessary and costly repairs and closures [Stewart *et al.*, 2002], and field data are available for the McKenzie River bridge, two cases for each of the application examples will be calculated. Distribution factors and impact factors will be applied to the WIM load spectrum load effects using the AASHTO-LRFD method in the first case. In the second case, distribution factors and impact factors determined from field investigations for the McKenzie River bridge will be used. The distribution and impact factors are summarized in Table R2.

Table R2 – Distribution and impact factors for McKenzie River Bridge exterior girder.

	Impact Factor	Distribution Factors (Lane Fraction)	
		Moment	Shear
AASHTO-LRFD	1.33	$DF_M = 0.867$	$DF_V = 0.884$
Field Study*	1.317	Right Lane = 0.61 Passing Lane = 0.15	Right Lane = 0.61 Passing Lane = 0.15

* Field study factors are based on stirrup strains. Moment and shear are assumed to have same distribution for diagonal crack locations.

A previous study for developing the truck load model used in the AASHTO code revealed that for two lane bridges, the maximum effects are obtained for two side-by-side identical trucks (i.e., perfect correlation between truck weights) [Nowak and Hong, 1991]. Therefore, the AASHTO distribution factors account for this multiple presence. To simplify this multiple presence situation for the field data case on a two-lane bridge with both lanes traveling in the same direction, the shear load histogram is plotted with arithmetic scale (before distribution and impact factors are applied) to determine the most commonly occurring (modal) shear produced. Figure R23 is the histogram for shear at 8 ft. away from support B (first continuous support) using the 97 days of Wilbur WIM data described above (Figures R5, and R8 to R13), using the three-span continuous linear-elastic model where all three spans are 50 ft. It is clearly shown that the modal shear of 32 kips occurs much more often than other shears. Therefore, it is assumed that a vehicle producing this shear can reasonably be found to be concurrent with any other vehicle on the bridge. Moreover, if the vehicle on the bridge produces a smaller shear than the modal shear, the vehicle is assumed to be passing. If the vehicle produces a larger shear than the modal shear, it is assumed to be in the right or driving lane. However, the shear produced by Rating Vehicle 2 is 38.6 kips, and since there is not a Rating Vehicle producing a smaller shear, it will be used to represent the modal truck. Load effects representative of Rating Vehicle 2 occurred over 4,000 times in a three month period so the likelihood of concurrent vehicles is high (Figure R23).

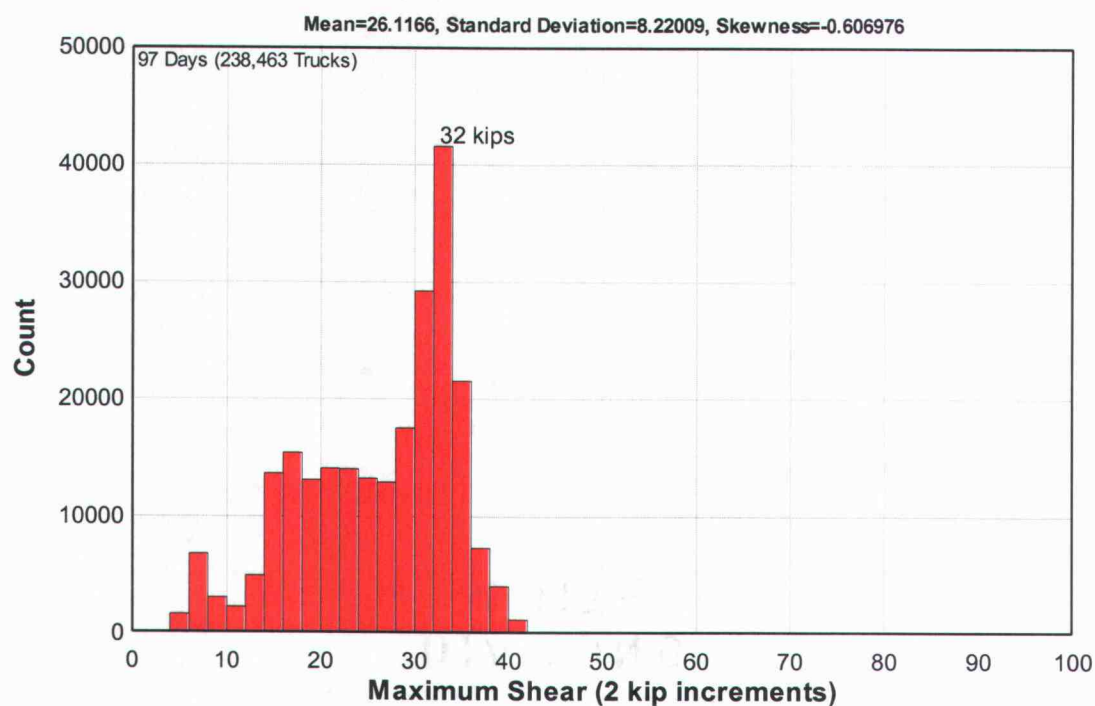
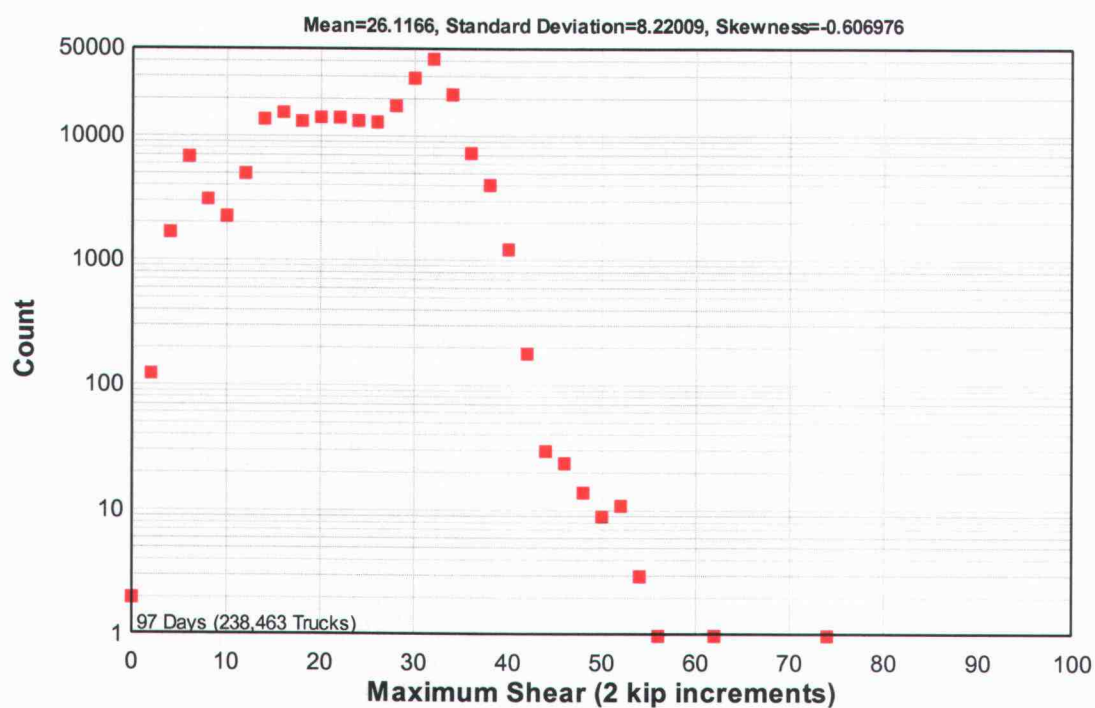


Fig. R23 – Modal shear produced at 42 ft in span 1 of three (50 ft) - span continuous bridge.

The largest data set is the Wilbur WIM data collected from January 2003-January 2004. Wilbur is also the closest WIM station to the McKenzie River Bridge (approximately 60 miles south), whereas Woodburn POE is approximately 80 miles north. Since the tail vehicles in the distribution are likely to produce the largest load effects, the year of data has been classified into Permit Tables 3, 4 and 5 to reduce the amount of calculation. To reduce calculation further, the rating vehicles determined to represent the WIM vehicles classified in those tables can be used in the safety assessment.

Service Level Performance

Service level performance is defined here as the initial onset of diagonal-tension cracking due to unfactored loads. Though not directly part of the assessment method, it identifies the likely-hood of diagonal cracking for a bridge. To investigate loads that may initiate diagonal cracking in the bridge, the shear force from load effects was compared with the shear force to cause cracking. In the presence of large moments, for which adequate longitudinal reinforcement is provided, the shear to cause diagonal cracking (V_{cr}) [ACI-ASCE, 1962] is:

$$V_{cr} = 1.9bd\sqrt{f'_c} \quad [R4]$$

where b (in) is the beam web width, d (in) is the depth of the shear section and f'_c is the 28-day concrete compressive strength (psi). From recent laboratory testing of full-scale girders of the vintage and type used in this bridge, V_{cr} was determined to be an average of 1.4 times $bd_e\sqrt{f'_c}$ where d_e is the depth from the compression face to the centroid of the flexural steel [Higgins *et al.*, 2004b].

The exterior girder section 8 ft. away from support face BA (the first interior support) was evaluated and is in a high moment region. V_{cr} was calculated for the widened section due to horizontal taper near the continuous support locations ($b_v=15.5\text{in}$ and $d_v=41.2\text{in}$) and has been adjusted by subtracting the dead load shear as calculated from the bridge drawings. The service level performance of the exterior girder in Figure R24 shows the shear force from each WIM vehicle at 8 ft. away from the continuous support using AASHTO-LRFD distribution factors. Figure R25 shows the shear force from each WIM vehicle on the bridge combined with the vehicle producing the modal shear at 8 ft. away from support face BA and distribution factors determined from field study of McKenzie River bridge. Note that in each case, the shears were determined without impact factors to illustrate that even without a dynamic amplification, cracking is likely to occur. The truck count is shown on a logarithmic scale. Figures R24 and R25 show that in one year, thousands of WIM vehicles classified as Permit Table 3, 4 and 5 exceeded V_{cr} . Finally, the eleven rating vehicles used by the ODOT Bridge Group when performing bridge ratings are shown as vertical lines for reference. It becomes clear that vehicles from Permit Tables 3, 4, and 5, in both the AASHTO-LRFD case and the field data case, are sufficient to produce diagonal cracking of the girder.

Further, the field case without multiple presence is considered. Calculation of the shear produced by Rating Vehicle 2 multiplied by the field data impact factor and only the right lane distribution factor results in a shear of 30.52 kips which still exceeds the cracking shear. From this, it is estimated using the logarithmic scale in Figure R23, that easily over 10,000 trucks per year produce or exceed the cracking shear for the girder. Based on this

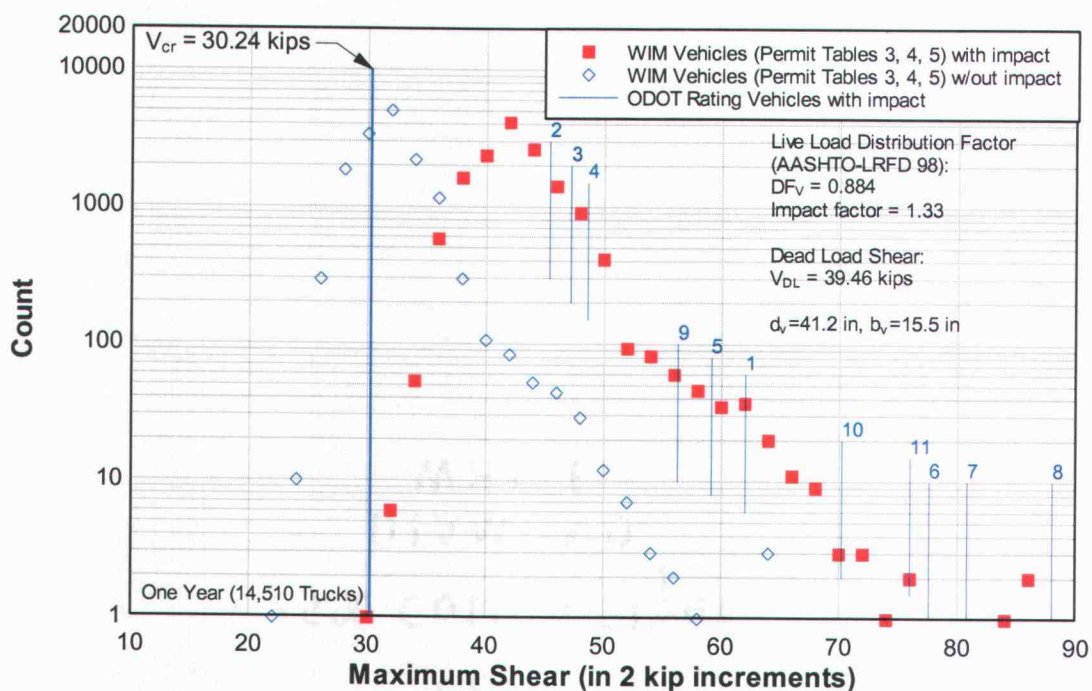


Fig. R24 – Service level performance histogram for diagonal cracking for the McKenzie River bridge at 42 ft. in span 1 (AASHTO-LRFD).

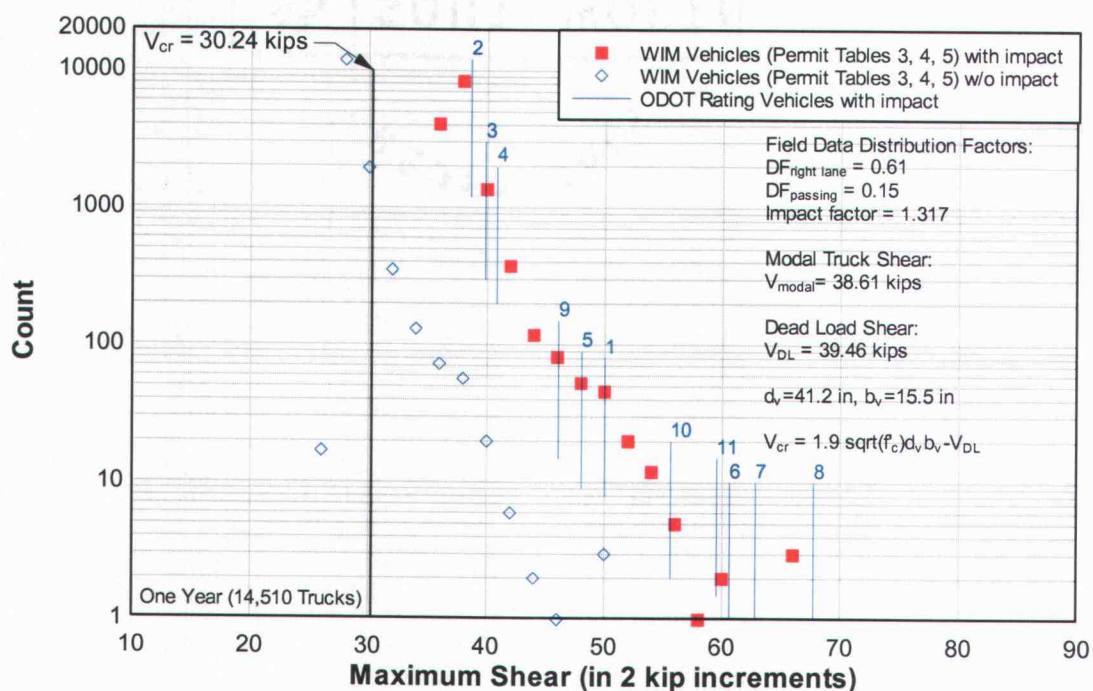


Fig. R25 - Service level performance histogram for diagonal cracking for the McKenzie River bridge at 42 ft. in span 1 (Field data).

assessment, it is apparent that cracking as shown in Figure R22 is to be expected for the loading conditions.

Calculate Capacity

The next step for assessment is to calculate the capacity. An appropriate method to calculate capacity for the structural member is required. For RCDGs the interaction between moment and shear is essential to predicting the capacity. Modified compression field theory [Vecchio and Collins, 1988] takes into account this interaction and a simplified form is adopted in the AASHTO-LRFD specification. The AASHTO-MCFT is more fully described in the AASHTO-LRFD 5.8.3.4.2 Commentary. Full-scale laboratory testing of large RC girders (designed to reflect RCDG bridges in Oregon) [Higgins *et al.*, 2004b] showed that AASHTO-99 MCFT is a simple method for reasonably predicting the ultimate capacity of conventionally reinforced concrete members of the size and type found in the 1950's population of RCDG bridges in the ODOT inventory. Experimental data from full-scale testing of twenty-three (23) specimens resulted in an average experimental-to-predicted shear strength ratio of 1.10 with a coefficient of variation (COV) of 7.4 % [Higgins *et al.*, 2004b]. Figure R26 shows the results of the predictions using AASHTO-99 MCFT on Normal probability paper. A Normal distribution was assumed. Another method for shear capacity prediction developed by Bentz [2000] is called *Response 2000TM* (R2K) and is based on MCFT. Laboratory results for the same twenty-three specimens gave an average experimental-to-predicted shear strength ratio of 0.96 with a COV of 5.5 %

[Higgins *et al.*, 2004b]. The laboratory testing statistics of these two methods are summarized in Table R3.

Table R3 – Shear prediction statistics from laboratory testing [Higgins *et al.*, 2004b].

	Average ratio Experimental to Predicted Shear Strength	COV
<i>Response2000TM</i> R2K	0.96	0.05
AASHTO-99 MCFT	1.10	0.074

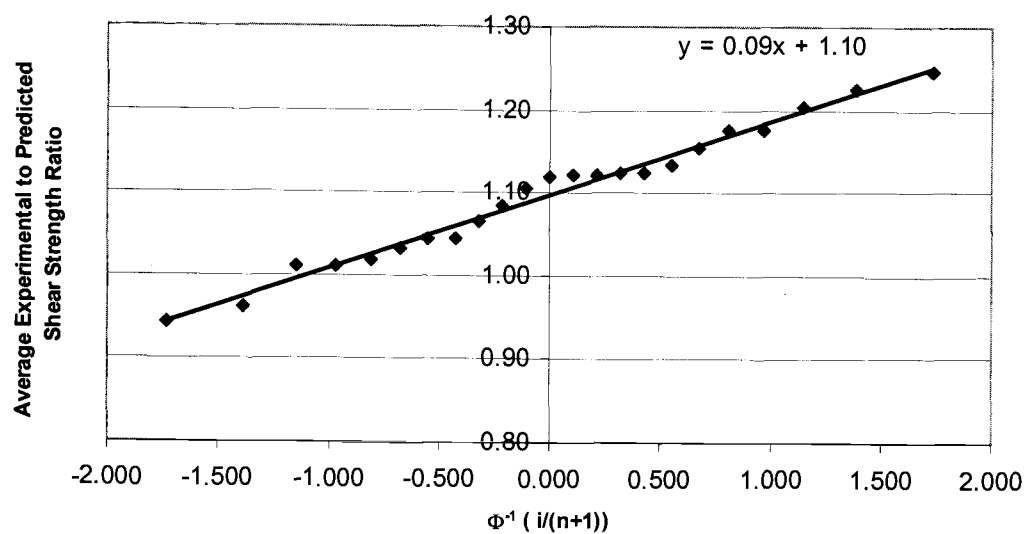


Fig. R26 – Laboratory results plotted on Normal probability paper.

Once the section and material properties, geometry, longitudinal reinforcing, and stirrup spacing are known at the location of interest, the program *Response 2000TM* can be used to determine the nominal shear and moment (V_n - M_n) curve for capacity as described by either AASHTO-LRFD MCFT or sectional MCFT analysis. Hereafter, results from *Response 2000TM* will be referred to as R2K. Two parameters for each section for input into *Response 2000TM* require special note: the effective flange width (b_{eff}) and the developed area of steel (A_s). Using the bridge drawings, b_{eff} is calculated using AASHTO-LRFD 4.6.2.6.1. In order to account for shear lag, a linear transition between zero and full b_{eff} was considered in a quarter-span length from the supports (approximately $3d$ away from the support for this example).

Since the flexural reinforcement plays an important role in the shear capacity of a member, the development length becomes of critical importance. Development length required for the flexural steel was calculated per AASHTO-LRFD 5.11.2. It should be noted that the longitudinal steel in the flange of the T-beam (steel to resist negative moment) does not have more than 12 inches of fresh concrete below the steel because the bridges in this study were constructed in two casting sequences with a cold joint and shear keys at the flange/web interface. At each cross-section of interest along the girder length, the length of steel available for development is divided by the development length required. This ratio is used to proportion the area of steel at the cross-section that is effective for flexural resistance. This method was also used by Collins [2003] for analysis of the laboratory specimens.

As an example, the capacity was calculated using AASHTO-MCFT for the cross-section at 42 ft. in span 1. The section has flexural reinforcement located in the deck and base of the web. Due to the cut-off locations of the flexural reinforcement, only four #11 bars were fully developed in the flange and three #11 bars in the bottom of the section. The stirrup spacing was 9 in. and the effective flange width was considered 50 in. to account for shear lag. The web was 15.5 in. since the section is within the horizontally tapered stem region. The cross-section is shown in Figure R27. *Response 2000TM* is used to calculate both the AASHTO-MCFT and R2K moment-shear (M-V) interaction curves. It is observed that at this location where the moment is transitioning from positive to negative there is a disconnect in the AASHTO-MCFT capacity curves at zero moment (refer to Figure R28). The section was obviously designed for the flexural steel in the flange to be in tension (i.e., negative moment), but loading in a bridge can likely cause moment sign reversal at this location. It is unrealistic for the shear capacity to have two different values at this point. In contrast, the R2K M-V interaction curve shows continuity through this transition region. Full-scale laboratory testing of RCDGs with a moving load showed that R2K is conservative in this low moment region [Nicholas, 2004]. Therefore, it is recommended that either R2K be used to predict capacity in this region or that a simple modification to the AASHTO-MCFT M-V curves be made. The modification for AASHTO-MCFT entails changing the shear value at zero moment for the smaller M-V interaction curve to the shear value at zero moment for the larger M-V interaction curve as illustrated by the dashed line in Figure R28. Since R2K was found to be conservative near points of inflection (zero moment) and the recommended modification to AASHTO-MCFT is below the R2K prediction, this should be a viable solution for capacity prediction in situations where the moment changes sign in transition regions due to vehicular loading.

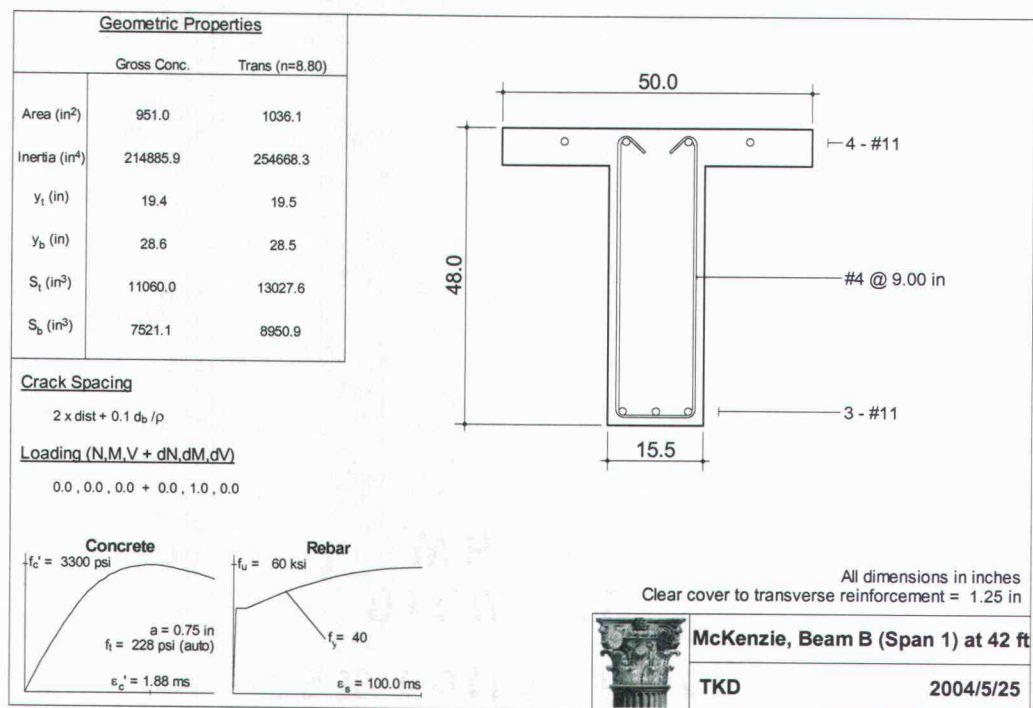


Fig. R27 – Cross-section for McKenzie River Bridge at 42 ft in span 1 (*RESPONS 2000*TM).

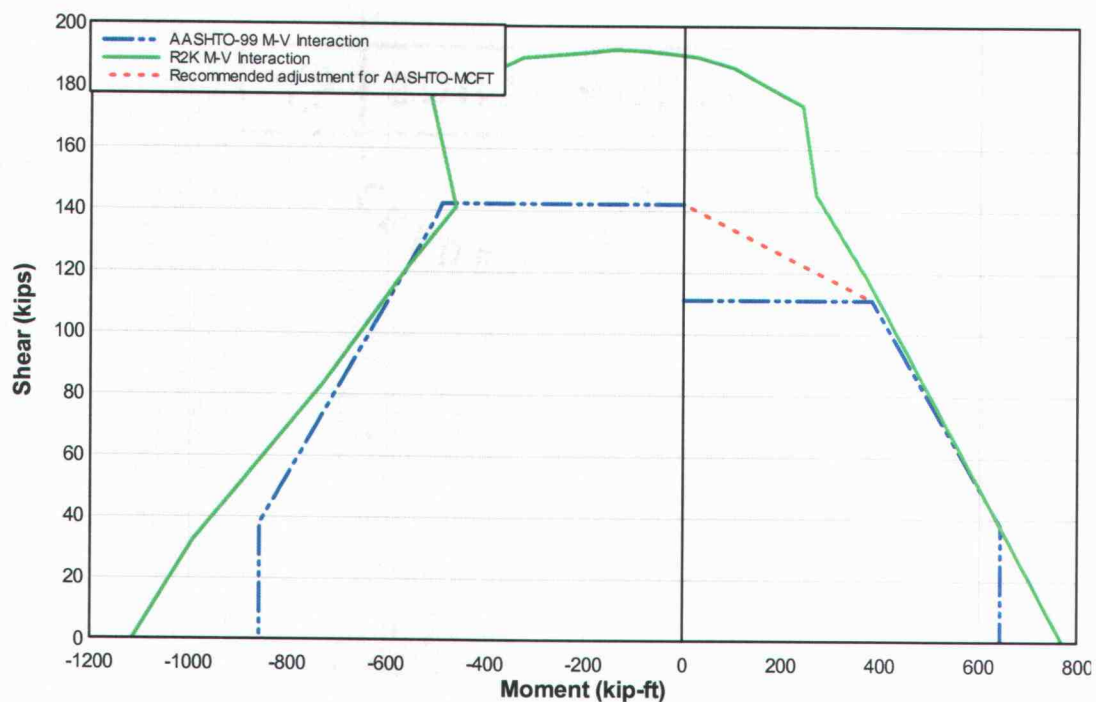


Fig. R28 – Disconnect of AASHTO-MCFT compared to R2K at points of inflection.

From the experimental statistics for AASHTO-99 MCFT, assuming normal distributions, the moment-shear interaction curves at the average, and 1, 2, and 3 standard deviations (σ) below the average, can be drawn. These are used in the following safety assessment for one-time overloads.

Safety Assessment – One time Overloads

An assessment of safety for a bridge girder is performed by comparing the load effects produced at selected cross-sections with the available resistance provided by that section. An effective method for making relative comparisons for safety or reliability is the calculation of the second-moment reliability index (β). For this example, the uncertainty and variability are considered for the resistance (or capacity) while the load (or demand) is considered to be known (deterministic). Figure R29 illustrates how β is calculated. The nominal capacity from AASHTO is shown, along with the average and standard deviations at 1σ , 2σ and 3σ , all of which are functions of the statistics described in Table R3. Since the distribution for the capacity is assumed Normal, β is simply the number of standard deviations from the coordinate of intersection on the average capacity curve (M_μ , V_μ) to the moment (M) and shear (V) as calculated in Equations R5 and R6. The entire truck history is shown, but only the controlling moment and shear combination is sketched in Figure R29. The slope (m) of the line projected from the controlling load effect coordinate is determined from the ratio of the live load shear (V_{LL}) divided by the live load moment (M_{LL}) as shown in Equation R7. This is the slope at which the load effect will increase or decrease if all axle weights in the truck were amplified by a constant value. The y-intercept (V_o) of this projected line is a function of the live load, distribution factors and the dead load as shown in Equation R8.

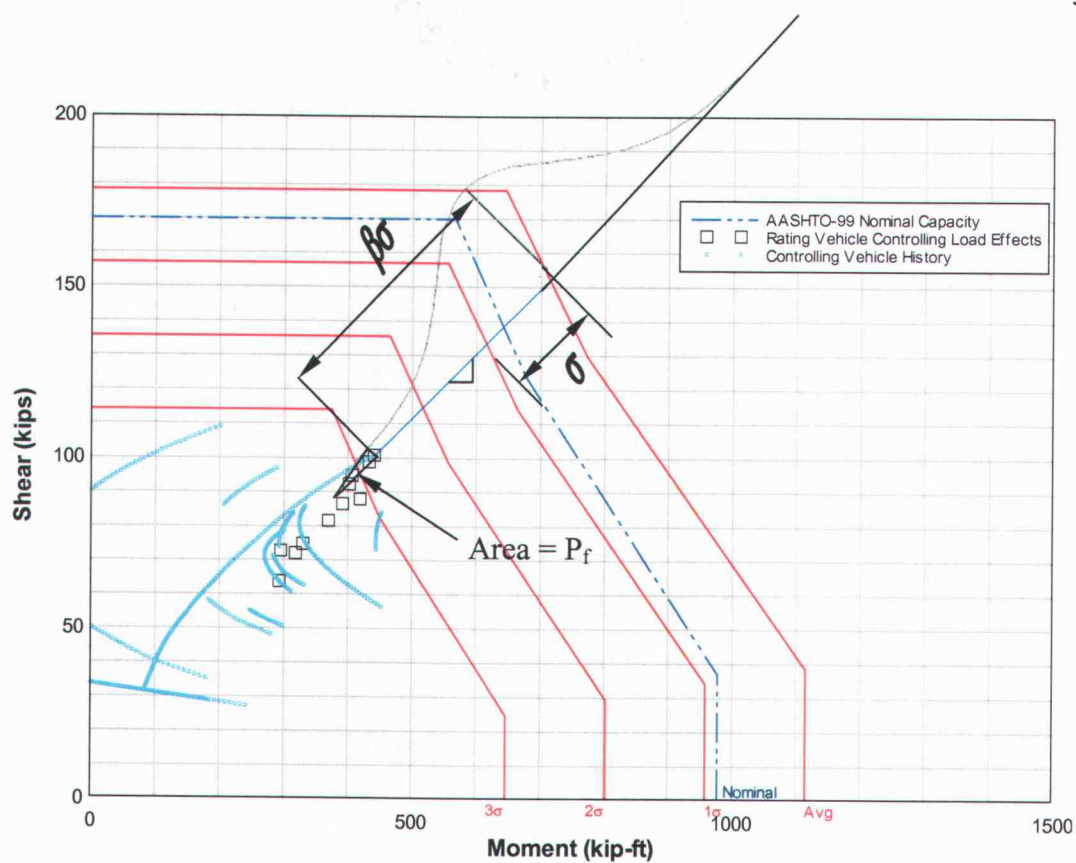


Fig. R29 – Illustration of how the reliability index is calculated.

$$M = M_{LL} DF_M IM + M_{DL} \quad [R5]$$

$$V = V_{LL} DF_V IM + V_{DL} \quad [R6]$$

$$m = V_{LL} / M_{LL} \quad [R7]$$

$$V_o = -mM + V \quad [R8]$$

where, IM is the impact factor and DF is the distribution factor for moment and shear as indicated by the subscript. The probability of failure (p_f) or more suitably in this use, the probability of exceedence, is the area under the normal curve left of the (M , V) coordinate,

and is related to β through Equation R3. Equation R9 is in general probability terms for a discrete value of X ,

$$p_f = P(X \leq x) = \Phi((x - \mu) / \sigma). \quad [R9]$$

For this two dimensional case, x is the coordinate (M, V) , μ is the coordinate $(M\mu, V\mu)$, and σ is shown in Figure R29.

Calculate the Reliability Index

A FORTRAN program was written to aide in the calculation of p_f and β . This program checks each of the moment and shear pairs produced at the cross-section as the truck models are moved across the bridge and stores the minimum value of β . The smallest β indicates the controlling load effect at the location.

The safety assessment is performed for the McKenzie River bridge at the potential critical locations at 4 ft. ($\sim d$), 8 ft. ($\sim 2d$), 12.5 ft. (quarter-point), 25 ft. (mid-span), etc. (refer to Figure R21). The tapered web between quarter-points on either side of continuous supports was considered for the resistance calculation. Cross-sections of the girder at each location are shown in Appendix D. The β values calculated for the eleven ODOT Rating Vehicles are plotted versus the location of the section in Figure R30. One critical location is indicated where β dips to the lowest value (~ 2.5).

The location is in the first span, 8 ft. from the continuous support (the same section evaluated for cracking). Rating Vehicle 8 resulted in the smallest β for the section. It

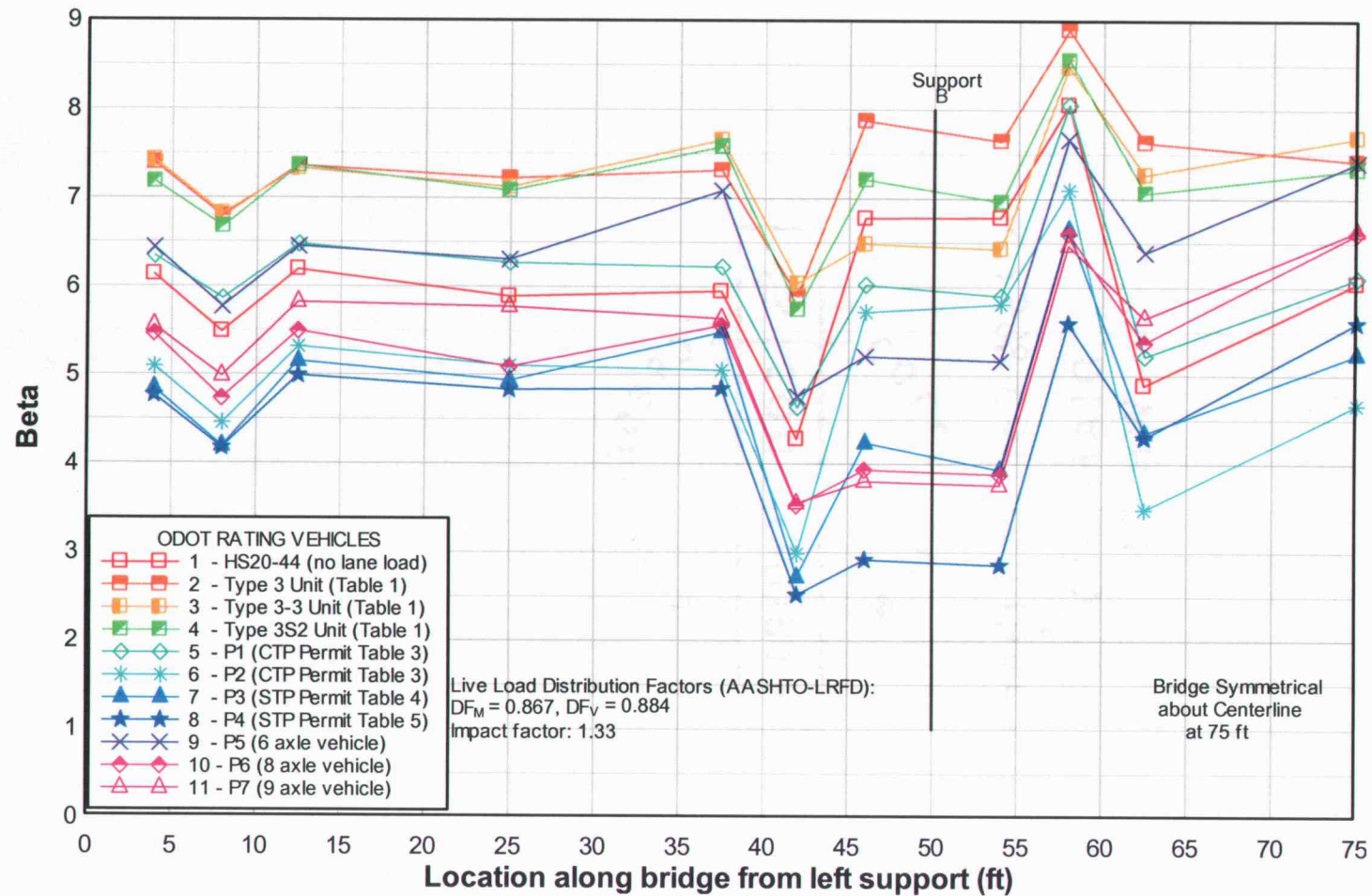


Fig. R30 – Safety assessment for exterior girder of McKenzie River bridge (08175N) using ODOT Rating Vehicles.

produced the smallest β in both the positive and negative moment regions. Three WIM vehicles classified as Permit Table 5 resulted in nearly the same β . For this section, the load effect V_{\max} with corresponding moment controlled. β at 42 ft. in span 1 is calculated from Figures R31 and R32 for the AASHTO-LRFD and field data cases, respectively. The comparison of the AASHTO-LRFD and field data cases shows that using distribution values collected for the specific bridge and using loading specific to the State will result in much larger β values, possibly more representative of in-situ conditions. The AASHTO-MCFT M-V interaction curve has been adjusted to transition the capacity in the disconnected region. It is clear that if the M-V interaction was not adjusted, some rating vehicles would have indicated β less than 1.0 and in some cases exceeded the nominal capacity.

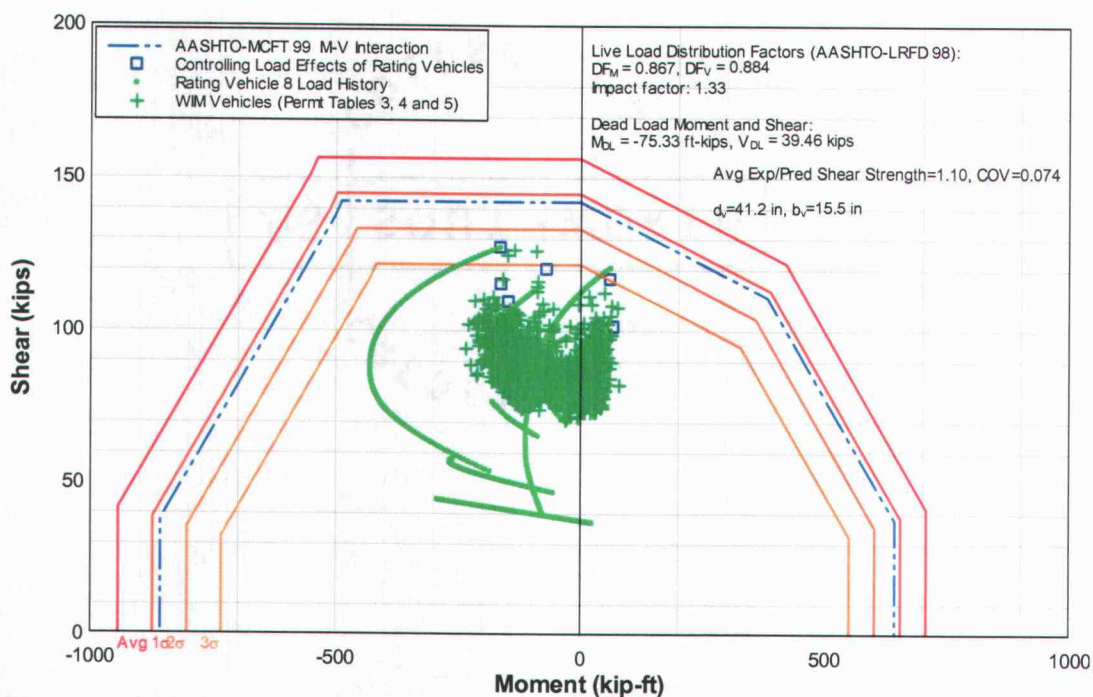


Fig. R31 - Safety assessment for the exterior girder for the cross-section at 42 ft. in span 1. Live load distribution and impact factors from AASHTO-LRFD are applied.

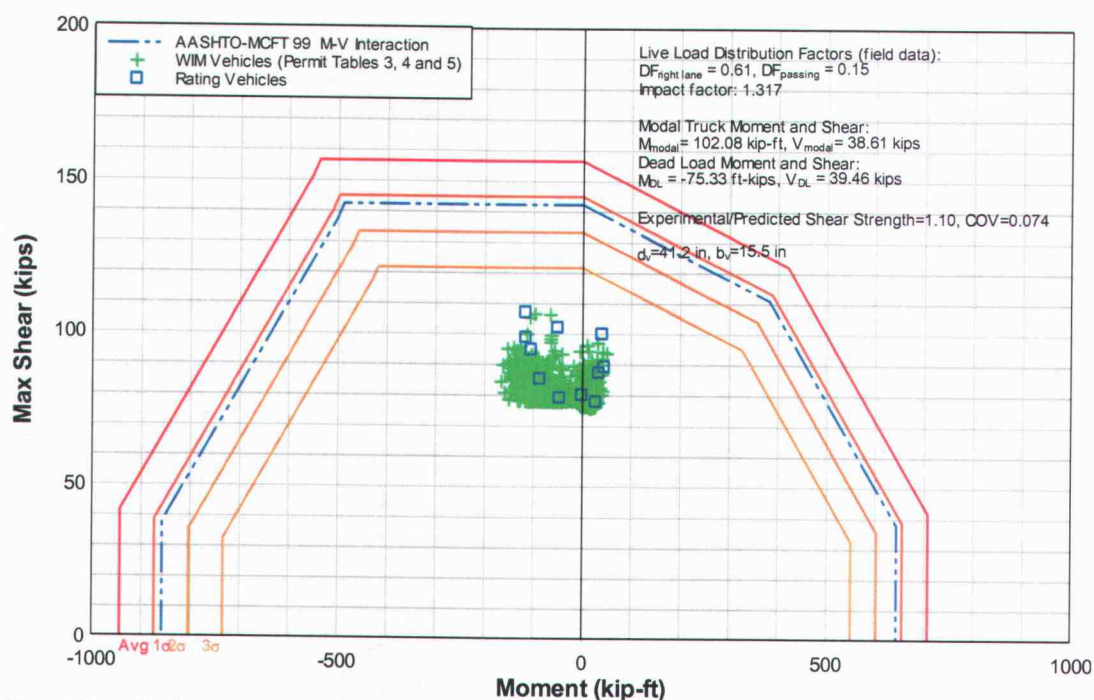


Fig. R32 - Safety assessment for the exterior girder for the cross-section at 42 ft. in span 1. Live load distribution and impact factors from field data.

The critical section is where flexural steel is cut-off in both the flange (deck) and the web. The critical section considered for this bridge is at 42 ft. in span. This section will be further evaluated for low-cycle fatigue.

Compare the Reliability Index

Determining the critical section for a girder of the many possibilities by comparing β is the primary use of the reliability index. The index can also be used for comparison between components and other RCDG bridges for ranking. To establish a target reliability index for the bridge inventory, a suite of bridges should be assessed. The suite of bridges should also be rated using the AASHTO 2003 Manual for Condition Evaluation and Load and Resistance Factor Rating of Highway Bridges (LRFR). The LRFR is calibrated for a target reliability index of 2.5. Comparison of the safety assessment to unity in the LRFR will

help gauge what index should be selected. Other guiding factors are experience, performance, bridge age, and loading history.

The LRFR provides reliability based rating evaluation in contrast to past practice (Guide Specifications for Strength Evaluation of Steel and Concrete Bridges 1989). The LRFR adopts a target reliability index of 2.5 calibrated to past AASHTO operating level load ratings. The calculations for loads and resistance use many AASHTO-LRFD principles. The main difference is the load and resistance factors are specified for rating based on evaluation.

For comparison, the rating factor for one of the critical sections was calculated using the LRFR. The section at 42 ft. in span 1 was selected. Therefore, the load effects from Rating Vehicle 8 were used. A Permit Load Rating was performed. The result for checking Rating Vehicle 8 at the critical section gave a Permit Load Rating of 0.83 for Moment and 0.55 for Shear. Since the ratings are less than unity, this vehicle should not be allowed on the bridge. This would indicate that the LRFR β of 2.5 and that of the safety assessment can not be directly compared. It also indicates that a β of 2.5 in the safety assessment may not provide an adequate level of safety as compared with the LRFR.

Low-Cycle Fatigue

Once the critical section (or critical sections as in this example) is determined, the section can be evaluated for repeated loading. To address the issue of low-cycle fatigue (LCF), it is necessary to identify the number of trucks, when combined with the dead load, to produce load effects sufficient to cause yielding in the stirrups. Further, it is necessary to

identify the magnitude of these loads in relation to the nominal capacity. The nominal capacity for AASHTO-99 MCFT is drawn with a resistance factor (ϕ) of 1.0. The curve is then redrawn at 95%, 90%, 85%, and 80% of ultimate capacity. The yield surface, moments and shears that cause yielding in the stirrups as determined from analysis [Robelo, 2004] is plotted. Due to the nature of the yield surface, only the maximum shears and their corresponding moments need be produced from the load spectrum for this evaluation. Vehicles that fall above yield are binned for each 5%-capacity and are plotted in a histogram for comparison with laboratory testing results for LCF.

Load effects produced by the WIM vehicles in one year as collected at Wilbur and classified as Permit Tables 3, 4 and 5 are calculated for the two critical locations identified by the safety assessment. The two cases for distribution factors and impact factors are presented for each section.

The LCF evaluation for the section at 42 ft in span 1 of the McKenzie River bridge is illustrated in Figure R33 for the AASHTO-LRFD case and Figure R34 for the field data case. Of these cases, only the section at 42 ft in span 1 with AASHTO-LRFD distribution and impact factors applied (Figure R33) produced load effects sufficient to yield the stirrups. There were only five events that exceeded the yield threshold; three in the 85% of capacity range and two in the 80% of capacity range. The histogram of the results is shown in Figure R35.

If it is assumed the annual values for truck load effects are stationary and there is statistical independence, then the annual value of occurrences can be extrapolated to estimate bridge

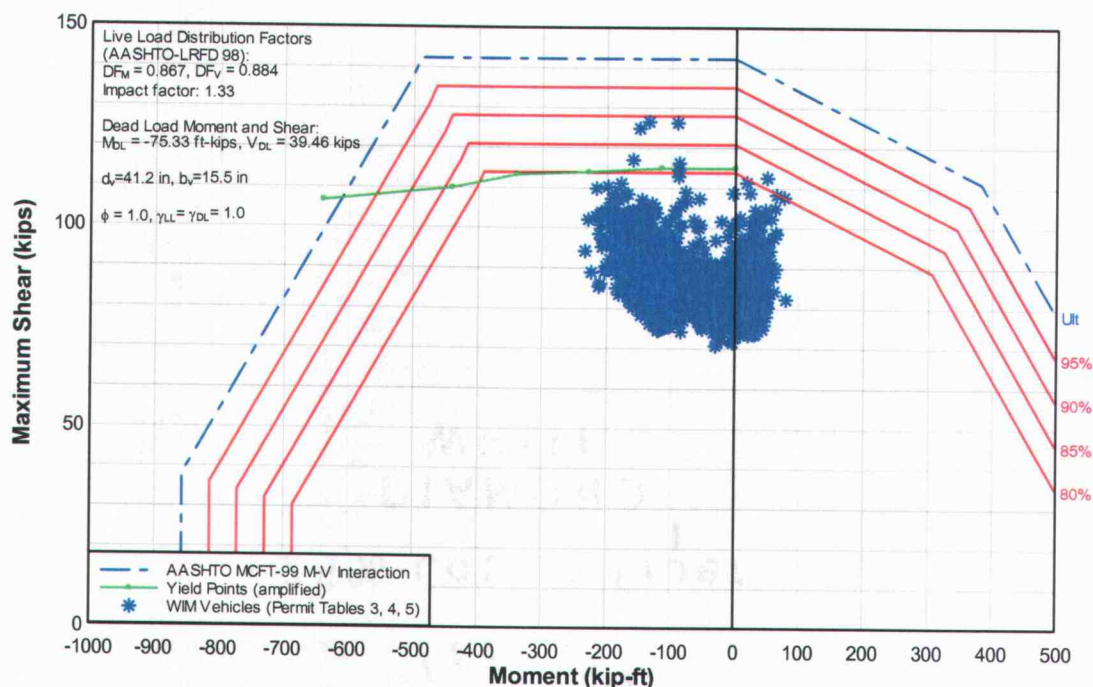


Fig. R33 – Low cycle fatigue evaluation for exterior girder of McKenzie R. bridge at 42 ft. in span 1 (AASHTO-LRFD). One year (14,510) Wilbur WIM permit vehicles.

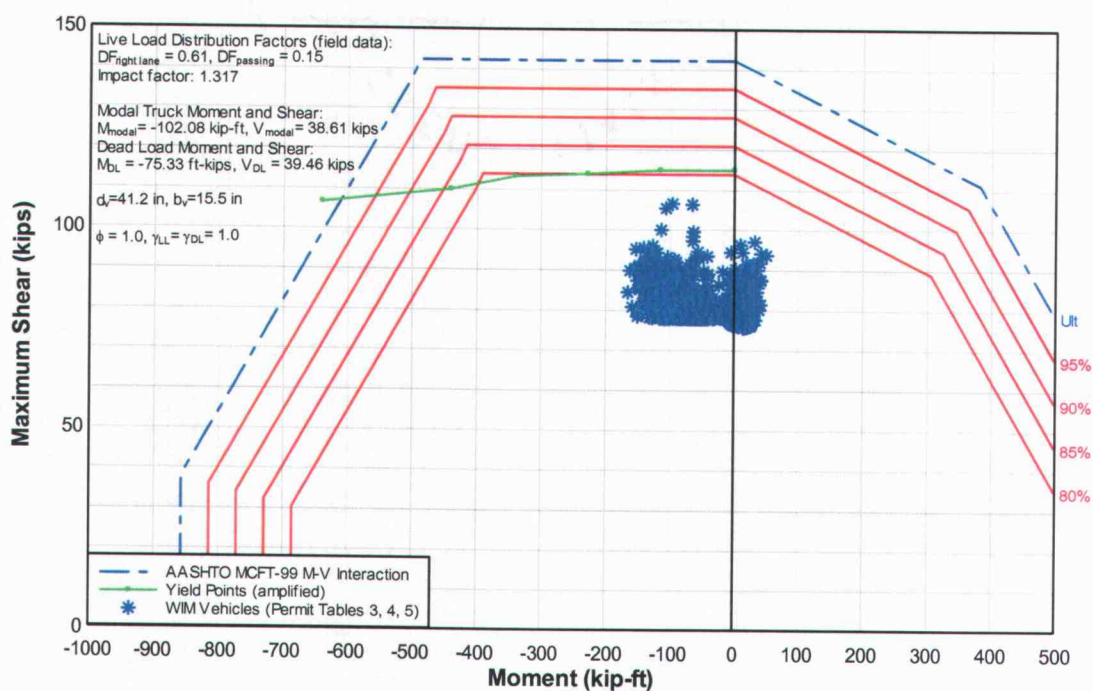


Fig. R34 – Low cycle fatigue evaluation for exterior girder of McKenzie R. bridge at 42 ft. in span 1 (field data). One year (14,510) Wilbur WIM permit vehicles.

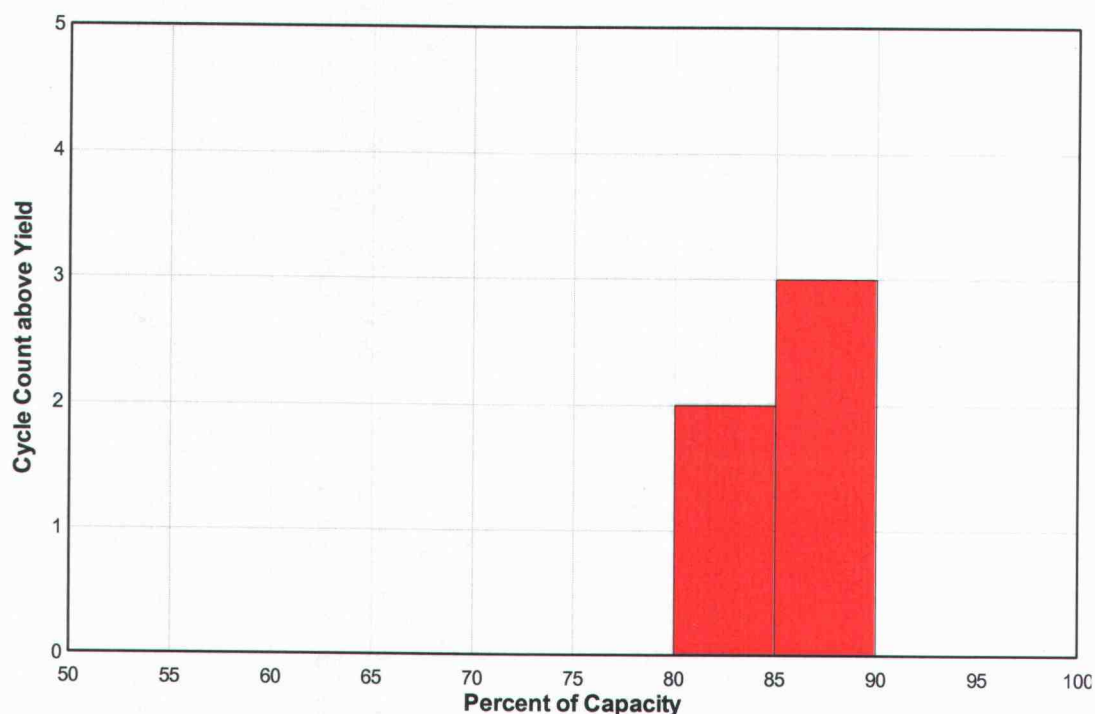


Fig. R35 – Annual cycles with load effects greater than the amplified yield points. Results from low cycle fatigue evaluation at 42 ft. in span 1 for exterior girder of the McKenzie R. bridge (AASHTO-LRFD).

life when compared to the LCF data from full-scale testing in the laboratory [Higgins *et al.*, 2004b]. Judgment as to the number of cycles that may already have occurred must be made in order to estimate remaining bridge life. The methodology for estimating life given a number of overloads is described in Higgins *et al.* [2004b].

CONCLUSIONS

Assessment of an existing bridge is needed when the structure exhibits signs of distress. Assessment practices require refinement in the calculation of loading and resistance, while maintaining an acceptable level of risk, to minimize costs associated with repair, replacement and weight restrictions. The methodology presented integrates full-scale laboratory testing for capacity, which found that the capacity requires assessment of shear and moment capacity simultaneously, and field data, with an Oregon specific truck loading. A live load model (load spectrum) was developed for Oregon, followed by a service level evaluation to explain the presence of diagonal tension cracks in vintage 1950's RCDG bridges. An assessment methodology was also presented that integrates the vehicular loading specific to Oregon with field data and full-scale laboratory testing findings for evaluation of RCDG bridges.

Investigation of weigh-in-motion data revealed that the rating vehicles used by the ODOT Bridge Group do in fact envelope the load effects produced by the WIM data. It also revealed that there are no clear distinctions between load effects produced by vehicles within the various permit table classifications.

Service level performance evaluation demonstrated that the McKenzie River bridge is expected to have diagonal tension cracks. Since this bridge is characteristic of the many bridges in Oregon's inventory, it is anticipated that many of the 1950's vintage RCDG bridges would exhibit this type of cracking.

Phase 1 of the assessment methodology was a safety assessment for one-time overloads at critical sections of a bridge girder. Full-scale laboratory testing of RCDGs revealed that the capacity of a typical girder was reasonably predicted using the AASHTO simplified form of modified compression field theory (MCFT) which accounts for shear and moment interaction. A recommendation was made for section capacity near points of inflection. The statistical characterization for AASHTO-MCFT, based on full-scale testing, was considered for the section capacity and compared to the load effect, which was considered to be deterministic. A reliability index (β) was calculated to identify critical sections. The section with the smallest reliability index was the most critical. After application of the safety assessment methodology to multiple bridges in the ODOT bridge inventory and comparison to the current load and resistance factor rating specification for highway bridges, a target β can be selected for Oregon's RCDG bridges that will represent an acceptable level of risk to be maintained system-wide.

Phase 2 of the assessment methodology addresses the issue of low-cycle fatigue (LCF). LCF occurs when load effects produce shears and moments sufficient to cause yielding of the stirrups. The most critical section identified in Phase 1 of the methodology is evaluated to determine the number of WIM vehicles (per year) that produces load effects that cause stirrup yielding and at what percentage of the ultimate capacity. If the truck load effects are assumed stationary and to have statistical independence, then the annual number of cycles at the various amplitudes, when compared to the LCF data from full-scale laboratory testing, enables estimation of bridge life.

The assessment methodology can be applied to other structural members (ie., bent caps and columns) using appropriate capacity models recommended by future research efforts. Once applied to the bridge system, use of both the safety assessment and LCF evaluation will enable engineers to rationally establish load restrictions based on an owner selected target reliability index developed for the bridge inventory, prioritize bridges (or segments of a bridge) for repair or replacement, and evaluate how repeated events that yield stirrups may reduce the life of a bridge.

RECOMMENDATIONS AND FUTURE WORK

The following recommendations and suggestions for future work are divided into two categories. The first is for load data collection and analysis, and the second is for applications of the assessment methodology.

Load Data

- Modify WIM data collection format to eliminate spurious data to eliminate unnecessary post-processing and facilitate compilation and integration of new data.
- Obtain additional information concerning axle weights and spacing for all overweight permits issued. This will allow for possible inclusion of additional data in the extreme distribution tails (large load effects with infrequent occurrence) which WIM may not capture.
- Update the model each year to check for changes in the load spectrum. In addition, check that the rating vehicles are still representative of in-situ truck traffic. The fact that Rating Vehicle 6 controlled over all the other Rating Vehicles during the safety assessment of one of the critical sections (Figure R33) may indicate that the number of Rating Vehicles can be reduced after further investigation.
- Analyze available data for other routes in Oregon, particularly I-84 and US Highway 97 to compare with the load spectrum examined for I-5 in this study.
- Evaluate The AASHTO HL-93 design vehicle and lane load during assessments to use for comparison with the LRFR specification.
- Finally, load effects on other bridge components in addition to girders, (ie., bentcaps, columns, etc.) should also be calculated for a system assessment.

- If desired, the live load effects can be characterized statistically. It was determined in the course of this study that the shears from Permit Tables 3, 4 and 5 are best characterized by a Lognormal distribution (see Appendix A). The characterization should account for the variability in each part of the load effect calculation (Equations R5 and R6) since the live load, dead load, distribution factors, and impact factors, are all random variables with variability and uncertainty as a result of the methods used for measurements and calculations. This could prove untenable as the shear and moment are not fully correlated near continuous supports, and the controlling load effect (from the truck history) will vary depending on the capacity curve to which it is compared.

Application

- Determine a target reliability index for Oregon's RCDG bridge inventory by performing safety assessments of numerous bridges in Oregon using the previously described methodology in concert with load rating per AASHTO-LRFR [2003].
- The proposed method is applicable to bent caps, but analysis methods available to predict capacity are not currently adequate and insufficient data exist to characterize the statistical variability. Other structural components, in particular the bent caps, may govern the capacity of a bridge as a system. Therefore, a safety assessment for the bent caps comparing load effects to the best method for predicting capacity for the bent caps as determined from full-scale testing should also be developed.

REFERENCES

- ACI-ASCE Committee. (1962). "Shear and Diagonal Tension," pt. 2, 326, *J. ACI*, vol. 59, no. 2, pp. 277-333.
- Agarwal, A. C., and Wolkowicz, M. (1976). *Interim report on 1975 commercial vehicle survey*. Res. And Dev. Div., Ministry of Transp., Downsview, Ontario, Canada.
- Akgül, F., and Frangopol, D.M. (2004). "Bridge rating and reliability correlation: A comprehensive study for different bridge types." *J. Struct. Eng.*, 130(7), 1063-1074.
- Akgül, F., and Frangopol, D. M (2003a). "Rating and Reliability of Existing Bridges in a Network. *J. Bridge Engineering*. 8(6), 383-393.
- AASHTO. (1989). "Guide Specifications for Strength Evaluation of Steel and Concrete Bridges", Washington, D. C.
- AASHTO. (1996). "Standard Specification for Highway Bridges," 16th Edition, Washington, D. C.
- AASHTO. (2003). "LRFD Bridge Design Specifications," 2nd Edition, Washington, D. C.
- AASHTO, (2003). "Manual for Condition Evaluation and Load and Resistance Factor Rating (LRFR) of Highway Bridges", Washington, D. C.
- American Concrete Institute. (2002). ACI 318, "Building Code Requirements for Structural Concrete", Farmington Hills, Michigan.
- Ang, A. H.-S., and Tang, W. H. (1984). Probability Concepts in engineering planning and design, Vol. II, Wiley, New York.
- Bentz, E. C. (2000). "Sectional Analysis of Reinforced Concrete Members," PhD Thesis, Department of Civil Engineering, University of Toronto.
- Collins, M. P. (2003). Personal correspondence with C. Higgins at Oregon State University.

- Ellingwood, B., Galambos, T.V., MacGregor, J.G., and Cornell, C.A. (1980). "Development of a Probability Based Load Criterion for American National Standard A58," *NBS Special Publication SP577*, National Bureau of Standards, Washington, D.C.
- Estes, A.C., and Frangopol, D.M. (1999). "Repair optimization of highway bridges using a system reliability approach." *J. Struct. Eng.*, 125(7), 766-775.
- Estes, A.C., and Frangopol, D.M. (2003). "Updating Bridge Reliability Based on Bridge Management Systems Visual Inspection Results." *J. Struct. Eng.*, Vol 8, No.6, pp 374-382.
- Fifer, D. (2002). Personal correspondence.
- Higgins, C., Yim, S., Miller, T., Robelo, M., and Potisuk, T. (2004). "Remaining Life of Reinforced Concrete Beams with Diagonal-Tension Cracks". *Report No. FHWA-OR-RD-04-12*, Federal Highway Administration, Washington, D. C.
- Higgins, C., Rosowsky, D., Miller, T., Yim, S., Daniels, T., Forrest, R., Lee, A., Nicholas, B., Potisuk, T., and Robelo, M. (2004b). "A Reliability Based Assessment Methodology for Diagonally Cracked Reinforced Concrete Deck Girder Bridges: An Integrated Approach". Federal Highway Administration, Submitted.
- Moses, F., and Ghosn, M. (1985). "A comprehensive study of bridge loads and reliability." *Report No. FHWA/OH-85/005*, Dept. of Civ. Engrg., Case Western Reserve Univ., Cleveland, Ohio.
- Nicholas, B. (2004). "Shear-Moment Capacity of Conventionally Reinforced Concrete Bridge Girders Subjected to Moving Loads". Project Report, Department of Civil, Construction and Environmental Engineering, Oregon State University.
- Nowak, A. S., and Collins, K. R. (2000). Reliability of Structures, McGraw-Hill, New York.
- Nowak, A.S. and Hong, Y.K. (1991), "Bridge Live Load Models," *ASCE Journal of Structural Engineering*, 117(9):2757-2767.
- RESPONSE 2000, Bentz, E. (2000)

Robelo, M. (2004). "Analysis of Diagonally Cracked Conventionally Reinforced Concrete Girders in the Service Load Range". MS Thesis, Department of Civil, Construction and Environmental Engineering, Oregon State University.

SAP2000, Version 7.40, Computers and Structures Inc., Berkeley, CA.

Stewart, M.G., Rosowsky, D.V., and Val, D. (2002). "Reliability-based bridge assessment using risk-ranking decision analysis." *Struct. Safety*, 23(2001), 397-405.

Stewart, M.G., and Val, D. (1999). "Role of load history in reliability-based decision analysis of ageing bridges." *J. Struct. Eng.*, 125(7), 776-783.

Stewart, M.G., and Val, D. (2003). "Multiple Limit States and Expected Failure Costs for Deteriorating Reinforced Concrete Bridges." *J. Struct. Eng.*, Vol. 8, No. 6, Nov/Dec, 405-415.

Vecchio, F. J., and Collins, M. P. (1986). "Modified Compression-Field Theory for Reinforced Concrete Elements Subjected to Shear", *J. ACI*, March-April, pp. 219-231.

APPENDICES

APPENDIX A
TRUCK LOADING

IMPORTANT TRUCK LOADING TERMINOLOGY

MCTD: Motor Carrier Transportation Division of the Oregon Department of Transportation.

GVW: Gross Vehicle Weight – The weight of a vehicle or vehicle combination and any load thereon.

Single Axle Weight – Total weight on one or more axles whose centers are not more than 40 inches apart. Federal Single Axle Weight limit is 20,000 lbs.

Tandem Axle Weight – Total weight on two or more consecutive axles more than 40 inches but less than 96 inches apart. Federal Tandem Axle Weight limit is 34,000 lbs.

Bridge Formula: $W = 500 [LN / (N - 1) + 12N + 36]$, where L = length (ft), and N = axles, W = weight (lbs) The single or tandem axle weight limits *supercede* the bridge formula for all axles not more than 96 inches apart. *Bridge Formula Exception:* Two consecutive sets of tandem axles may carry 34,000 lbs each if the overall distance between the first and last axles of these tandems is 36 ft or more. See handout for more detail.

Overweight Permit: Required for trucks over 80,000 lbs or “legal axle weights” that are single non-divisible loads. (ie, Tables 2 to 5 +)

Extended Weight Permit: For divisible loads with maximum weight of 105,500 lbs (Table 2).
Good for one year. Expected to comply to Maps 1, 4, and 7 showing length limits.

Permit Weight Tables: Truck configuration and load distribution in any grouping meets the table values. Table 1 based on Bridge Formula.
Tables 3 to 5 created by Oregon.

Table 1: Legal loads (max GVW 80,000 lbs, single axle 20,000 lbs/ tandem 34,000lbs)ORS818.010

Table 2: Extended Weight permits up to 105,500 lbs, but must have legal axles. Smaller axle groupings must still **pass Table 1**. (Just accommodates *longer* vehicles).

Table 3: Consists of both Continuous Trip *heavyhauls* with GVW less than 98 kips and Single Trips (beyond 98 kips GVW). Based on two wheelbase formulas:

For 18 ft or less of wheelbase,
(1000)*(wheelbase + 40ft).
Otherwise,
(1200)*(wheelbase + 40ft).

Table 4: Single Trips only. Based on two wheelbase formulas:
For 18 ft or less of wheelbase,
(1200)*(wheelbase + 40 ft).

Otherwise,
 $(1400) * (\text{wheelbase} + 40 \text{ ft}).$

Table 5: Allows even more weight on a shorter wheel base. Single Trips only.
 Based on three wheelbase formulas:

For wheelbase between 8 and 10 feet,
 $(6500) * (\text{wheelbase}).$
 $10 \text{ ft} < \text{wheelbase} < 30 \text{ ft},$
 $(2200) * (\text{wheelbase} + 20 \text{ ft}).$
 For wheelbase $> 30 \text{ ft},$
 $(1600) * (\text{wheelbase} + 40 \text{ ft}).$

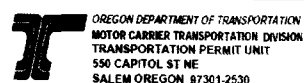
Super Load: Anything that falls outside of Weight Table 5 must be cleared by engineering. For example, Triple axle over 65 kips or GVW over 304,000 lbs. Road use assessment fees are already prepared for loads up to 240,000 lbs. Anything over this must be computed by the department.

STP: Single Trip Permit- Issued for portions of Weight Table 3, and all of Weight Tables 4 and 5. (Bonus Weights) Permit is valid for about one week. Route must be declared.

CTP: Continuous Trip Permit – May travel wherever and as often in one year. (98,000 max GVW, 21,500 lbs/axle or 43,000 lbs/tandem) Expected to comply to Route Map 2.

Bonus Weight: A truck qualifies when it has at least 9 axles in the combo with 4 consecutive tandems (24,000/axle, 48,000/tandem)

Reference Document located at <http://www.leg.state.or.us/ors/>.



Permit Weight Table 1

The following exceptions apply to the table of weights shown below:

Exception 1: Two consecutive tandem axles may weigh up to 34,000 pounds each if:

Minimum Axle Spacing Required	Interstate Highways	Non-Interstate Highways
30 feet or more	Permit Required	No Permit Required
36 feet or more	No Permit Required	No Permit Required

Exception 2: A group of four axles consisting of a set of tandem axles and two axles spaced nine feet or more apart may have a loaded weight of more than 65,500 pounds and up to 70,000 pounds if:

Minimum Axle Spacing Required	Interstate Highways	Non-Interstate Highways
35 feet or more	Permit Required	No Permit Required

- Minimum axle spacing is the distance between the first and last axle of any group shown above.

Wheelbase In Feet *	Number of Axles						Wheelbase In Feet *	Number of Axles					
	2	3	4	5	6	7 Or More		2	3	4	5	6	7 Or More
4	34,000	34,000	34,000	34,000	34,000	34,000	31	40,000	59,000	62,500	67,500	72,500	78,000
5	34,000	34,000	34,000	34,000	34,000	34,000	32	40,000	60,000	63,500	68,000	73,000	78,500
6	34,000	34,000	34,000	34,000	34,000	34,000	33	40,000	60,000	64,000	68,500	74,000	79,000
7	34,000	34,000	34,000	34,000	34,000	34,000	34	40,000	60,000	64,500	69,000	74,500	80,000
8 & less	34,000	34,000	34,000	34,000	34,000	34,000	35	40,000	60,000	65,500	70,000	75,000	80,000
Over 8	38,000	42,000	42,000	42,000	42,000	42,000	36	40,000	60,000	66,000	70,500	75,500	80,000
9	39,000	42,500	42,500	42,500	42,500	42,500	37	40,000	60,000	66,500	71,000	76,000	80,000
10	40,000	43,500	43,500	43,500	43,500	43,500	38	40,000	60,000	67,500	71,500	77,000	80,000
11	40,000	44,000	44,000	44,000	44,000	44,000	39	40,000	60,000	68,000	72,500	77,500	80,000
12	40,000	45,000	50,000	50,000	50,000	50,000	40	40,000	60,000	68,500	73,000	78,000	80,000
13	40,000	45,500	50,500	50,500	50,500	50,500	41	40,000	60,000	69,500	73,500	78,500	80,000
14	40,000	46,500	51,500	51,500	51,500	51,500	42	40,000	60,000	70,000	74,000	79,000	80,000
15	40,000	47,000	52,000	52,000	52,000	52,000	43	40,000	60,000	70,500	75,000	80,000	80,000
16	40,000	48,000	52,500	58,000	58,000	58,000	44	40,000	60,000	71,500	75,500	80,000	80,000
17	40,000	48,500	53,500	58,500	58,500	58,500	45	40,000	60,000	72,000	76,000	80,000	80,000
18	40,000	49,500	54,000	59,000	59,000	59,000	46	40,000	60,000	72,500	76,500	80,000	80,000
19	40,000	50,000	54,500	60,000	60,000	60,000	47	40,000	60,000	73,500	77,500	80,000	80,000
20	40,000	51,000	55,500	60,500	66,000	66,000	48	40,000	60,000	74,000	78,000	80,000	80,000
21	40,000	51,500	56,000	61,000	66,500	66,500	49	40,000	60,000	74,500	78,500	80,000	80,000
22	40,000	52,500	56,500	61,500	67,000	67,000	50	40,000	60,000	75,500	79,000	80,000	80,000
23	40,000	53,000	57,500	62,500	68,000	68,000	51	40,000	60,000	76,000	80,000	80,000	80,000
24	40,000	54,000	58,000	63,000	68,500	74,000	52	40,000	60,000	76,500	80,000	80,000	80,000
25	40,000	54,500	58,500	63,500	69,000	74,500	53	40,000	60,000	77,500	80,000	80,000	80,000
26	40,000	55,500	59,500	64,000	69,500	75,000	54	40,000	60,000	78,000	80,000	80,000	80,000
27	40,000	56,000	60,000	65,000	70,000	75,500	55	40,000	60,000	78,500	80,000	80,000	80,000
28	40,000	57,000	60,500	65,500	71,000	76,500	56	40,000	60,000	79,500	80,000	80,000	80,000
29	40,000	57,500	61,500	66,000	71,500	77,000	57 or more	40,000	60,000	80,000	80,000	80,000	80,000
30	40,000	58,500	62,000	66,500	72,000	77,500	more						

The loaded weight of any group of axles, vehicle, or combination of vehicles shall not exceed that specified in the table of weights shown above or any of the following:

- The manufacturer's side wall tire rating but not to exceed 600 pounds per inch of tire width.
- 600 pounds per inch of tire width.
- 20,000 pounds on any one axle, including any one axle of a group of axles.
- 34,000 pounds on any tandem axle.
- The sum of the permissible axle, tandem axle, or group of axle weights shown above, whichever is less.

Note exceptions 1 and 2 above.

7/95 6150 (8-02)

Distance measured to the nearest foot: when exactly 1/2 foot or more, round up to the next larger number.

SIKE 00057

Fig. A1 – Legal weight table [Oregon Motor Carrier].



OREGON DEPARTMENT OF TRANSPORTATION
MOTOR CARRIER TRANSPORTATION DIVISION
550 CAPITOL ST NE
SALEM OR 97301-2530

PERMIT WEIGHT TABLE 2

WHEELBASE	5 Axles	6 Axles	7 Axles	8 or More Axles
47	77500	81000	81000	81000
48	78000	82000	82000	82000
49	78500	83000	83000	83000
50	79000	84000	84000	84000
51	80000	84500	85000	85000
52	80500	85000	86000	86000
53	81000	86000	87000	87000
54	81500	86500	88000	91000
55	82500	87000	89000	92000
56	83000	87500	90000	93000
57	83500	88000	91000	94000
58	84000	89000	92000	95000
59	85000	89500	93000	96000
60	85500	90000	94000	97000
61	86000	90500	95000	98000
62	87000	91000	96000	99000
63	87500	92000	97000	100000
64	88000	92500	97500	101000
65	88500	93000	98000	102000
66	89000	93500	98500	103000
67	90000	94000	99000	104000
68	90000	95000	99500	105000
69	90000	95500	100000	105500
70	90000	96000	101000	105500
71	90000	96500	101500	105500
72	90000	96500	102000	105500
73	90000	96500	102500	105500
74	90000	96500	103000	105500
75	90000	96500	104000	105500
76	90000	96500	104500	105500
77	90000	96500	105000	105500
78	90000	96500	105500	105500

See Weight Table 1, if using less than five axles or 47 feet wheelbase.

735-6111(2-00)

• DISTANCE MEASURED TO THE NEAREST FOOT. WHEN EXACTLY 1/2 FOOT OR MORE, ROUND UP TO THE NEXT LARGER NUMBER •

STK # 300558

Fig. A2 – Extended legal weight table [Oregon Motor Carrier].



OREGON DEPARTMENT OF TRANSPORTATION
MOTOR CARRIER TRANSPORTATION DIVISION
550 CAPITOL ST NE
SALEM OR 97301-2530

PERMIT WEIGHT TABLE

3

WHEELBASE

[illegible]

735-8112 (10-99)

● DISTANCE MEASURED TO THE NEAREST FOOT. WHEN EXACTLY 1/2 FOOT OR MORE, ROUND UP TO THE NEXT LARGER NUMBER.

STK # 300569

Fig. A3 – Permit Table 3 [Oregon Motor Carrier].

Fig. A3 (Continued) – Permit Table 3 [Oregon Motor Carrier].



OREGON DEPARTMENT OF TRANSPORTATION
MOTOR CARRIER TRANSPORTATION DIVISION
560 CAPITOL ST NE
SALEM OR 97301-2530

PERMIT WEIGHT TABLE

4

[illegible]

735-8113 (10-99)

● DISTANCE MEASURED TO THE NEAREST FOOT. WHEN EXACTLY 1/2 FOOT OR MORE, ROUND UP TO THE NEXT LARGER NUMBER. ●

STK # 300560

Fig. A4 – Permit Table 4 [Oregon Motor Carrier].

Fig. A4 (Continued) – Permit Table 4 [Oregon Motor Carrier].



OREGON DEPARTMENT OF TRANSPORTATION
MOTOR CARRIER TRANSPORTATION DIVISION
550 CAPITOL ST NE
SALEM OR 97301-2530

PERMIT WEIGHT TABLE

5

[illegible]

735-8114 (10-99)

● DISTANCE MEASURED TO THE NEAREST FOOT. WHEN EXACTLY 1/2 FOOT OR MORE, ROUND UP TO THE NEXT LARGER NUMBER ●

STK # 3005b1

Fig. A5 – Permit Table 5 [Oregon Motor Carrier].

Fig. A5 (Continued) – Permit Table 5 [Oregon Motor Carrier].

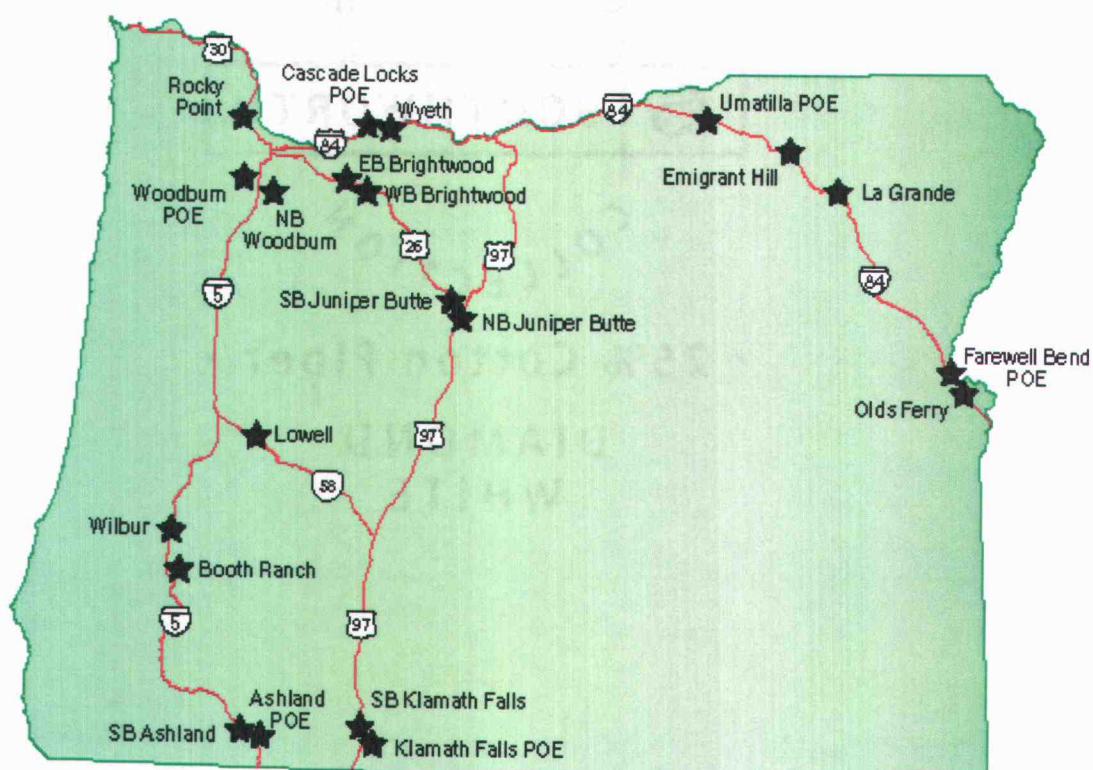


Fig. A6 – Location of WIM stations in Oregon.

[<http://www.odot.state.or.us/trucking/its/green/sites.htm>]

OREGON DEPARTMENT OF TRANSPORTATION JOINT STATE/COUNTY PERMIT						
CARRY THIS PERMIT IN THE CAB OF THE POWER UNIT AT ALL TIMES						
Permit No: STP239729	Issue Date	Issue Time	Effective Date	Date of Expiration	Total Fee	
Location: HOSTFAX	09/10/2002	0207P	09/16/2002	09/25/2002	\$164.15	
Permittee: (Name and Address)			Commodity			
DAILY EXP INC			TURBINE RUNNER SHAFT			
P O BOX 39						
CARLISLE	PA 17013	Carrier File #:	USDOT: 0010558			
Load Length	Width	Height	Overall Length	Rear Overhang	Front Overhang	
LEGAL	10'00"	14'00"	136'00"	LEGAL	LEGAL	
Legal Weight Table	Extended Weight Table		Heavy Haul Weight Table 5	Gross Weight	Axles	
				251,400	13	
Description of Vehicles: 4-J3-S3-B3 W/58 FT TRAILER						
Year	Make	Vin	License	State	Unit No.	
1999	PETBT	1XP5PBEX3X0490969	P38568	IL	187237	

Fig. A7 – Example of an overweight permit.

Activity Report																						
12/18/2002 12:04:00 AM to 12/18/2002 11:59:54 PM																						
Date/Time	Day	Scale	Locatio	Scale	Gross	Warnings	Type	Axles	Commodity	WM	Reason	Wgt 1	Wgt 2	Wgt 3	Wgt 4	Wgt 5	Wgt 6	Wgt 7	Wgt 8	Wgt 9	Wgt 10	Wgt 11
12/18/2002 03:56:19 AM	Wed	WOODBURN	2409	767			12	5	0002	wir	OBYPAS	100	163	166	167	171	0	0	0	0	0	0
12/18/2002 04:53:42 AM	Wed	WOODBURN	2409	189			5	3	0002	wml	WBLOWM	90	59	40	0	0	0	0	0	0	0	0
12/18/2002 04:55:54 AM	Wed	WOODBURN	2409	758			15	6	0002	wml	WBLOWM	92	93	118	117	162	176	0	0	0	0	0
12/18/2002 04:57:39 AM	Wed	WOODBURN	2409	369			11	5	0002	wml	WBLOWM	98	73	71	64	63	0	0	0	0	0	0
12/18/2002 04:58:57 AM	Wed	WOODBURN	2409	912			18	8	0002	wml	OBYPAS	81	101	84	121	137	143	132	113	0	0	0
12/18/2002 05:01:45 AM	Wed	WOODBURN	2409	928			18	8	0002	wml	OBYPAS	92	127	128	108	115	166	110	82	0	0	0
12/18/2002 05:03:06 AM	Wed	WOODBURN	2409	859			18	8	0002	wml	OBYPAS	91	134	129	120	111	164	61	49	0	0	0
12/18/2002 05:04:04 AM	Wed	WOODBURN	2409	962			17	7	0002	wir	OBWIND	85	155	148	104	103	194	173	0	0	0	0
12/18/2002 05:04:50 AM	Wed	WOODBURN	2409	458			11	5	0002	wml	WBLOWM	82	103	97	87	89	0	0	0	0	0	0
12/18/2002 05:05:07 AM	Wed	WOODBURN	2409	784			15	6	0002	wml	WBLOWM	88	90	163	150	153	140	0	0	0	0	0
12/18/2002 05:05:46 AM	Wed	WOODBURN	2409	717			11	5	0002	wml	WBLOWM	93	159	158	160	147	0	0	0	0	0	0
12/18/2002 05:06:17 AM	Wed	WOODBURN	2409	506			11	5	0002	wir	WBLOWM	113	101	97	97	98	0	0	0	0	0	0
12/18/2002 05:07:29 AM	Wed	WOODBURN	2409	750			15	6	0002	wml	WBLOWM	97	156	140	113	116	128	0	0	0	0	0
12/18/2002 06:11:53 AM	Wed	WOODBURN	2409	993			18	8	0002	wml	OBYPAS	95	147	147	111	126	132	129	106	0	0	0
12/18/2002 06:13:22 AM	Wed	WOODBURN	2409	954			16	7	0002	wml	OBYPAS	90	187	149	153	137	121	117	0	0	0	0
12/18/2002 06:13:37 AM	Wed	WOODBURN	2409	209			5	3	0002	wml	WBLOWM	97	65	47	0	0	0	0	0	0	0	0
12/18/2002 06:13:44 AM	Wed	WOODBURN	2409	720			11	5	0002	wml	WBLOWM	90	159	151	156	164	0	0	0	0	0	0
12/18/2002 06:13:53 AM	Wed	WOODBURN	2409	695			1	5	0002	c70	WAFRNT	110	295	290	0	0	0	0	0	0	0	0
12/18/2002 06:14:10 AM	Wed	WOODBURN	2409	548			11	5	0002	wml	WBLOWM	81	125	124	112	106	0	0	0	0	0	0
12/18/2002 06:14:35 AM	Wed	WOODBURN	2409	701			11	5	0002	wml	WBLOWM	98	166	171	131	135	0	0	0	0	0	0
12/18/2002 06:15:37 AM	Wed	WOODBURN	2409	0			3	6	0002	c70	O-NONE	0	0	0	0	0	0	0	0	0	0	0
12/18/2002 06:15:39 AM	Wed	WOODBURN	2409	740			11	5	0002	wml	WBLOWM	94	160	156	154	176	0	0	0	0	0	0
12/18/2002 06:16:04 AM	Wed	WOODBURN	2409	0			5	5	0002	c70	O-NONE	0	0	0	0	0	0	0	0	0	0	0
12/18/2002 06:16:37 AM	Wed	WOODBURN	2409	915			3	7	0002	c70	O-NONE	107	364	351	93	0	0	0	0	0	0	0
12/18/2002 06:16:40 AM	Wed	WOODBURN	2409	663			12	5	0002	wml	WBLOWM	88	177	168	122	108	0	0	0	0	0	0
12/18/2002 06:17:06 AM	Wed	WOODBURN	2409	690			11	5	0002	wml	WBLOWM	92	152	150	136	160	0	0	0	0	0	0
12/18/2002 06:18:00 AM	Wed	WOODBURN	2409	1017			18	8	0002	wml	OBYPAS	107	82	164	165	122	155	106	116	0	0	0
12/18/2002 06:18:29 AM	Wed	WOODBURN	2409	525			11	5	0002	wml	WBLOWM	74	104	106	116	125	0	0	0	0	0	0
12/18/2002 06:18:36 AM	Wed	WOODBURN	2409	714			3	5	0002	c70	O-NONE	107	337	270	0	0	0	0	0	0	0	0
12/18/2002 06:19:31 AM	Wed	WOODBURN	2409	847			3	7	0002	c70	O-NONE	100	366	381	0	0	0	0	0	0	0	0

Fig. A8 – Example of REALTIME data.

(3869) LANE #1 TYPE 11 GVW 73.2 kips LENGTH 72 ft
 18-K ESAL 2.763 SPEED 60 mph MAX GVW 80.0 kips Thu Jan 30 00:01:11.25 2003

|<----- 57.2ft ----->|
 o o o o o
 14.8 15.8 15.5 15.2 11.9

(3870) LANE #1 TYPE 14 GVW 72.0 kips LENGTH 75 ft
 18-K ESAL 1.857 SPEED 53 mph MAX GVW 80.0 kips Thu Jan 30 00:01:22.66 2003

|<----- 68.4ft ----->|
 o o o o o
 11.8 14.0 16.5 9.8 10.0 9.9

(3873) LANE #1 TYPE 11 GVW 68.5 kips LENGTH 67 ft
 18-K ESAL 2.144 SPEED 59 mph MAX GVW 80.0 kips Thu Jan 30 00:01:38.13 2003

|<----- 56.8ft ----->|
 o o o o o
 13.8 14.7 14.7 14.3 11.2

(3874) LANE #1 TYPE 11 GVW 57.8 kips LENGTH 73 ft AVI TAGS: 000545492067
 18-K ESAL 1.148 SPEED 59 mph MAX GVW 80.0 kips Thu Jan 30 00:01:45.97 2003


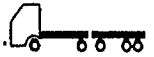

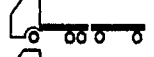

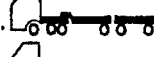

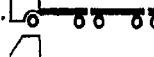




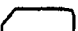
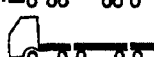

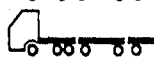







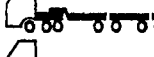
|<----- 58.9ft ----->|
 o o o o o
 10.8 10.4 13.1 13.4 10.1

(3875) LANE #1 TYPE 11 GVW 72.4 kips LENGTH 67 ft
 18-K ESAL 2.620 SPEED 56 mph MAX GVW 80.0 kips Thu Jan 30 00:01:49.89 2003

|<----- 59.3ft ----->|
 o o o o o
 15.0 14.9 15.2 15.2 12.0

Fig. A9 – Example of raw WIM data.

CLASSIFICATIONS USED IN OREGON'S WEIGH - IN - MOTION STUDY

Vehicle Type		Vehicle Type	
1. 	Cars	13. 	(2-3) Other 5 Axle Combinations
2. 	Panels	14. 	(3-2)
3. 	Pickups	15. 	(3-2-2) 8 axle Combinations
4. 	Light Vehicles w/ trailers	16. 	(2-2-2)
5. 	2 axle, Single Units	17. 	(2-2-3)
6. 	2 axle Buses	18. 	(2-2-2-2) Triples
7. 	3 axle Single Units	19. 	(3-2-2) Other 7 Axle Combinations
8. 	(2-3-1) 3 axle Combinations	20. 	(2-2-3)
9. 	3 axle Buses	21. 	(3-2-3) 8 axle Combinations
10. 	(2-2-2) 4 axle Combinations	22. 	(3-2-2-2)
11. 	(2-2) 4 axle Single Units	23. 	(3-2-2-3) 9 axle or more Combinations
12. 	(3-2) 5 axle Semis	24. 	(3-2-2-2)
	(2-2-2-2) 5 axle Twins		

These are examples of configurations; there are other possible combinations not illustrated.

Fig. A10 – Classifications used for WIM collection in Oregon [Oregon Motor Carrier].

Philomath Weigh Station, Hwy 20/34, 09 April 03																			
Cargo Description	GVW (kips)	Width (ft)	No. Axles	Length (ft)	Individual Axle Weights (kips)								Axle Spacings (ft)						
					wt1	wt2	wt3	wt4	wt5	wt6	wt7	wt8	spc1	spc2	spc3	spc4	spc5	spc6	spc7
Logs	79.2	6'-3"	5	51.25	17	17	16.7	16.7	11.8	0	0	0	4.75	23.5	4.75	18.25	0	0	0
Chips	88.1	6'-2"	6	61.5	14.1	14.1	14.1	16.6	16.6	12.6	0	0	4.75	5	30.75	4	17	0	0
Logs	86	6'-3"	6	52.25	16.9	16.9	14	14	12.3	11.9	0	0	4.5	26	4.5	5	12.25	0	0
Lumber	102.3	6'-3"	8	84.5	10.4	11	12.1	14.9	14.9	14	13.5	11.5	4	11	13.5	4	28	4	20
Logs	85.6	6'-4"	6	50.75	17	17.1	14	14	12.3	11.2	0	0	4	25	4.5	5	12.25	0	0
Lumber	96.4	6'-7"	8	68.75	10.1	12.2	12.2	12.2	14	14	10.6	11.1	5	5	5	30.75	4.5	5	13.5
Woodburn POE, I-5 South Bound, 15 April 03																			
Cargo Description	GVW (kips)	Width (ft)	No. Axles	Length (ft)	Individual Axle Weights (kips)								Axle Spacings (ft)						
					wt1	wt2	wt3	wt4	wt5	wt6	wt7	wt8	spc1	spc2	spc3	spc4	spc5	spc6	spc7
Steel Beams	67.5	6'-6"	5	63.5	14.8	14.2	14	13.4	11.1	0	0	0	10.25	31.5	4.25	17.5	0	0	0
Petroleum	100	6'-6"	7	67.25	13	13.9	13.4	13	17	17.1	12.6	0	4	19	4	20.25	4	16	0
Rock Sifter	80.6	7'-0"	5	56	16	16.3	18.1	18	12.2	0	0	0	5	25.5	4.5	21	0	0	0
Lumber Posts	106	6'-3"	7	83.75	14.1	14.5	16.8	17.1	15.6	16	11.9	0	15.75	12.25	9.75	23	4.5	18.5	0
Covered	102.6	6'-5"	8	75.25	12	13	11.2	12	12	16.1	16	10.3	4	18.25	4	4	24	4.25	16.75
Concrete Pumper	74.7	6'-6"	4	25.25	21	21	16.4	16.3	0	0	0	0	4.25	15.5	5.5	0	0	0	0
Notes:																			
Weights were measured in axle groups on a static scale.																			
Distances were measured with a tape measure between axle centerlines.																			
Units are kips and ft																			

Fig. A11 – Data collected at weigh station visits.

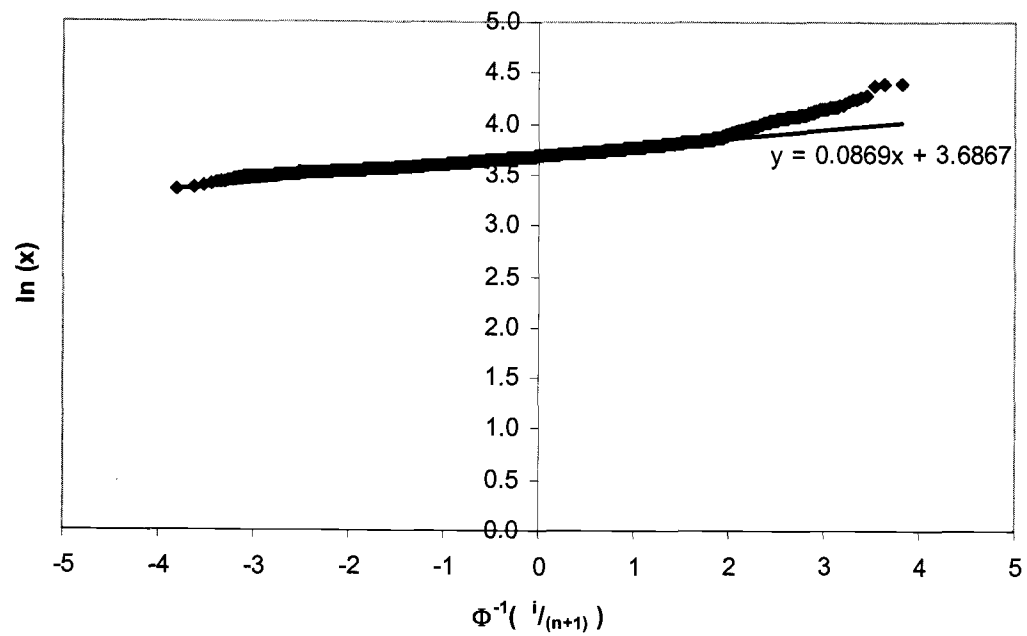


Fig. A12 – Maximum shear produced at 5 ft. away from support B of the McKenzie River bridge plotted on Lognormal probability paper. One year of Wilbur WIM vehicles classified as Permit Table 3, 4 and 5.

APPENDIX B
HAUNCH/TAPER STUDY

**LIVE LOAD EFFECTS ON A THREE-SPAN CONTINUOUS BRIDGE:
MODEL CHECK AND EXPLORATION OF TAPER AND HAUNCH**

Prepared by:

Theresa K. Daniels, Graduate Research Assistant

danielth@engr.orst.edu

Oregon State University

PURPOSE

The purpose of this exercise is to check the slope-deflection model used in the FORTRAN program which assumes constant modulus of elasticity (E) and moment of inertia (I), to determine load effects; shear and moment. Secondly, explore the effect of taper and haunch on the load effects.

PRODECURE

A 3-span continuous bridge with all spans 50 feet is used for the study. Load effects are determined at support centerlines and at 5 and 15 feet away as well as at mid-spans. Three loadings are used for comparison; A 1 kip moving point load, the AASHTO HS20-44 design vehicle (both spacings are 14 ft) (Figure B1), and the Permit 4 vehicle (Figure B8). The vehicle axle weights and spacings are shown in Appendix AM2. Two programs are used for analysis; FORTRAN and SAP2000. The results from FORTRAN are first compared to a prismatic model in SAP2000.

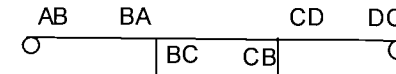
The FORTRAN results are modified with sign changes and mirror images in order to reflect the same sign convention used in SAP2000 and to account for the vehicle being "driven" over the model in only one direction.

To explore the effects of taper and haunch, a search is performed in the State of Oregon bridge database which produces two histograms. The first one is for bridges that have a tapered web (i.e., change in web thickness, b), and a second for bridges with a haunched web (i.e., change in web height, h). Taper/ $b = 0.00$ and Haunch/ $h = 0.00$ is represented by the prismatic model. Tapered and haunched section changes begin at the span quarter points. A tapered section is modeled in SAP2000 to represent the actual web changes in the McKenzie River Bridge which has a Taper/ $b = 0.54$. To finish out the possible range of ratios, a second bridge (No. 07832) that has similar span lengths with a Taper/ $b = 0.93$ is modeled. Two haunched sections are modeled in SAP2000 for a Haunch/ $h = 0.51$ (bridge No. 07519) and the Mary's River Bridge with Haunch/ $h = 0.86$.

RESULTS

For quick reference, a summary of the percent change from prismatic to various haunch and taper ratios taken at key points is tabulated in Table B1. Plots follow comparing the percent difference in load effects of all vehicles between the prismatic section and the tapered or haunched sections (Figures B1 to B4). The portion displayed is for the portion of the envelope that is the maximum at that position. It should be noted that a positive (+) percent change indicates that the value decreased from that of the prismatic section and a negative (-) percent change indicates an increase. Following each percent difference plot are the respective moment or shear envelopes for each loading.

Table B1 - Summary of percent change at key points dependent on loading and haunch or taper ratios.



		Percent Change																	
Ratio	Loading	AB		Mid-span		BA		BC		Mid-span		CB		CD		Mid-span		DC	
		V	M	V	M	V	M	V	M	V	M	V	M	V	M	V	M	V	M
Taper/b = 0.54	1 kip	0.00%	0.00%	-2.03%	3.04%	0.00%	-11.89%	0.00%	-11.89%	0.00%	3.56%	0.00%	-11.89%	0.00%	-11.89%	-2.03%	3.04%	0.00%	0.00%
	HS20-44	0.68%	0.00%	-2.20%	3.54%	-0.64%	-11.43%	-0.09%	-11.43%	0.22%	4.19%	-0.09%	-11.43%	-0.64%	-11.43%	-2.20%	3.54%	0.68%	0.00%
	Permit 4	1.01%	0.00%	-3.05%	3.94%	-1.14%	-10.28%	-0.95%	-10.28%	-3.65%	4.65%	-0.95%	-10.28%	-1.14%	-10.28%	-3.05%	3.94%	1.01%	0.00%
Taper/b = 0.93	1 kip	0.00%	0.00%	-3.19%	4.77%	0.00%	-18.70%	0.00%	-18.70%	0.00%	5.45%	0.00%	-18.70%	0.00%	-18.70%	-3.19%	4.77%	0.00%	0.00%
	HS20-44	1.07%	0.00%	-3.48%	5.54%	-0.99%	-17.87%	-0.14%	-17.87%	0.32%	6.37%	-0.14%	-17.87%	-0.99%	-17.87%	-3.48%	5.54%	1.07%	0.00%
	Permit 4	1.59%	0.00%	-4.72%	6.18%	-1.76%	-15.98%	-1.50%	-15.98%	-5.77%	7.07%	-1.50%	-15.98%	-1.76%	-15.98%	-4.72%	6.18%	1.59%	0.00%
Haunch/h = 0.51	1 kip	0.00%	0.00%	-5.74%	8.59%	0.00%	-33.05%	0.00%	-33.05%	0.00%	10.30%	0.00%	-33.05%	0.00%	-33.05%	-5.74%	8.59%	0.00%	0.00%
	HS20-44	1.74%	0.00%	-5.87%	9.21%	-1.52%	-29.04%	-0.03%	-29.04%	-0.06%	10.92%	-0.03%	-29.04%	-1.52%	-29.04%	-5.87%	9.21%	1.74%	0.00%
	Permit 4	6.35%	0.00%	-2.70%	14.46%	1.80%	-18.99%	2.74%	-18.99%	-3.89%	16.71%	2.74%	-18.99%	1.80%	-18.99%	-2.70%	14.46%	6.35%	0.00%
Haunch/h = 0.86	1 kip	0.00%	0.00%	-7.12%	10.65%	0.00%	-41.17%	0.00%	-41.17%	0.00%	13.54%	0.00%	-41.17%	0.00%	-41.17%	-7.12%	10.65%	0.00%	0.00%
	HS20-44	2.06%	0.00%	-7.10%	11.13%	-1.87%	-35.41%	-0.02%	-35.41%	-0.13%	14.24%	-0.02%	-35.41%	-1.87%	-35.41%	-7.10%	11.13%	2.06%	0.00%
	Permit 4	6.95%	0.00%	-4.52%	16.40%	1.12%	-24.80%	2.35%	-24.80%	-6.14%	20.02%	2.35%	-24.80%	1.12%	-24.80%	-4.52%	16.40%	6.95%	0.00%

OBSERVATIONS

Linear Model Check

Driving the vehicle, especially the large Permit 4 vehicle, in only one direction in the linear model (produced in FORTRAN) affects the shear envelope results due to asymmetry of the loading.

For All Loadings

Additional concrete in the section attracts more moment to the supports while reducing the positive moment near mid-spans.

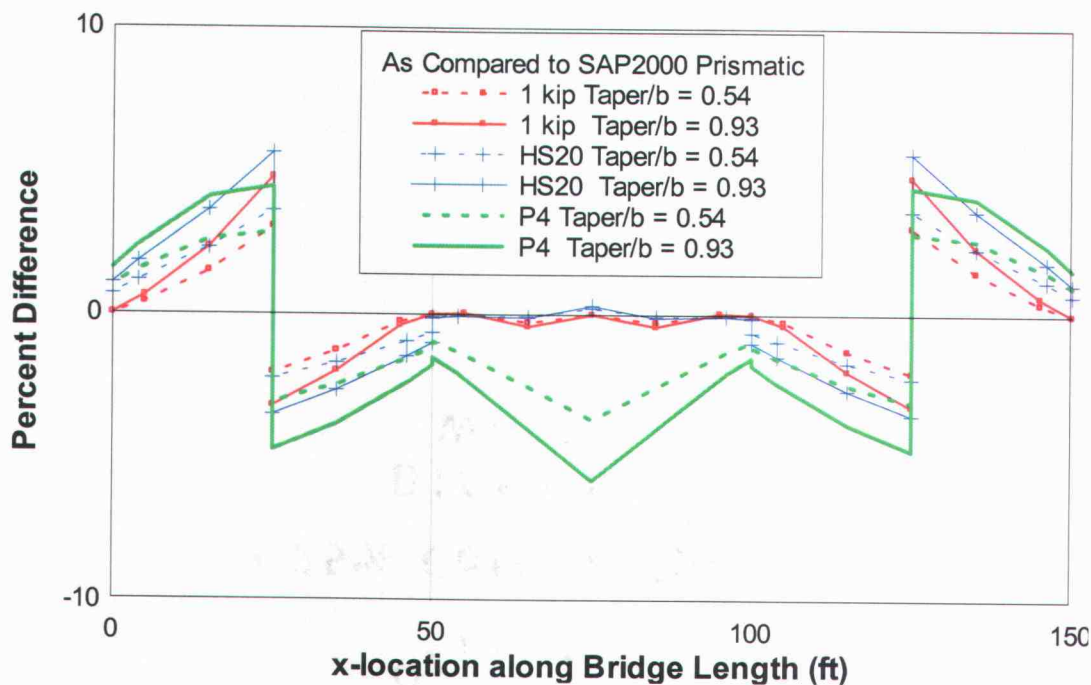


Fig. B1 - Percent change in shear for tapered sections of a three (50 ft)-span continuous bridge.

Taper

Tapered sections have a consistent percent change increase in shear at the supports. The percent change in shear for all loading types and taper ratios is less than 2 % at the supports and less than 6% at mid-spans. The positive moment near mid-spans decreases by less than 10%. The negative moment increases by approximately 12% at the supports for a taper ratio of 0.54 and 18% for a ratio of 0.93.

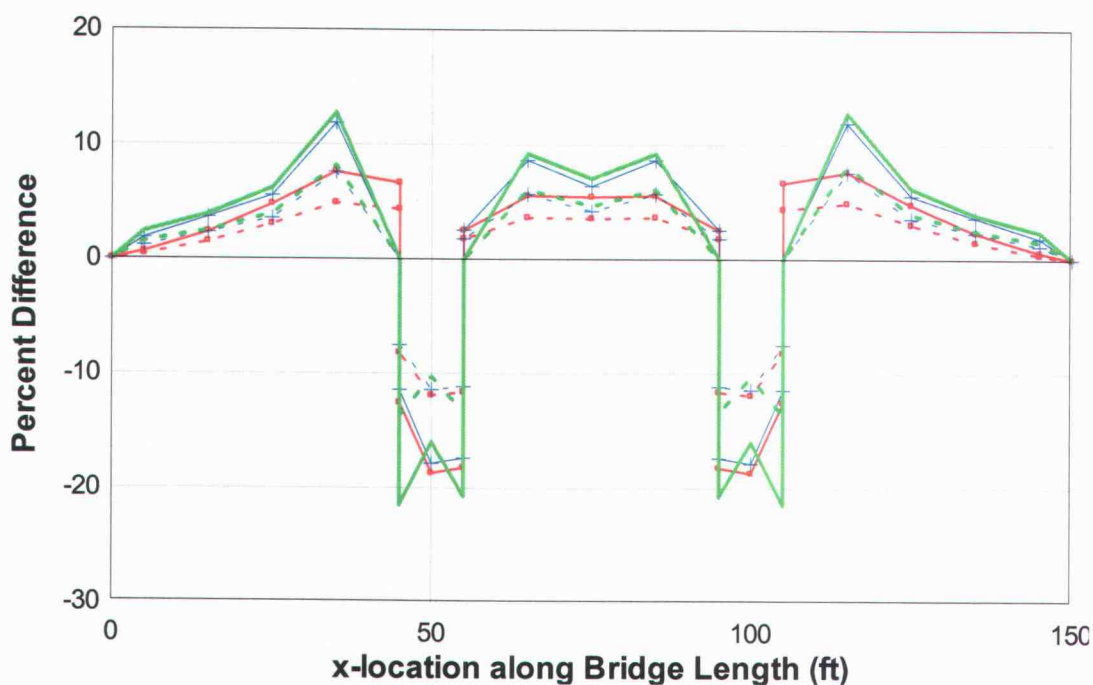


Fig. B2 - Percent change in moment for tapered sections of a three (50 ft)-span continuous bridge.

Haunch

Haunched sections have shear increases and decreases of less than 3% at interior supports. The simply supported ends decrease 0-7% depending on the loading, but appear unaffected by the size of the haunch ratio. However, the change in moment does depend on the

loading and haunch ratio. The positive moment decreases 10-20% at mid-spans, while the negative moment increases 20-40% at the interior supports.

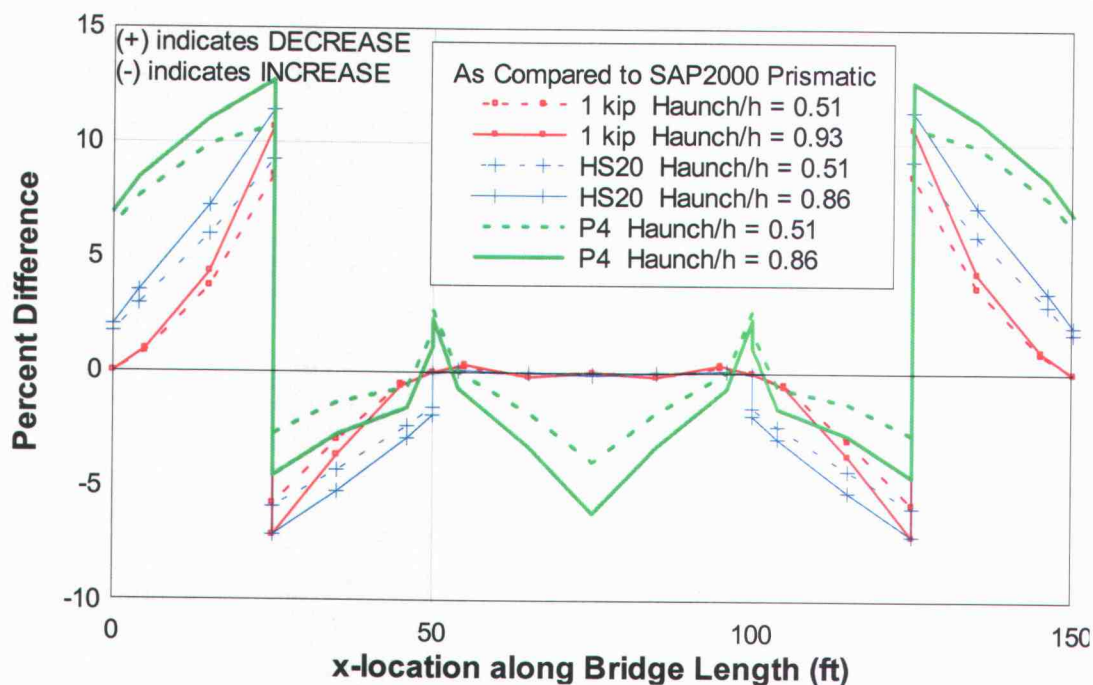


Fig. B3 - Percent change in shear for haunched sections of a three (50 ft)-span continuous bridge.

CONCLUSIONS

Model Check

The linear FORTRAN model appears to be performing well when compared to the prismatic SAP2000 model. It should be noted however, that for completeness, the vehicles should be run in both directions when calculating the load effects.

Taper

It also appears that a horizontal taper has a more consistent (linear) effect on the shear from varying vehicles since the shear changes consistently regardless of taper ratio or loading. The change in shear is minimal at the supports (less than 2%) and can be ignored. Though the positive moment decreases up to 10% near mid-spans, the negative moment increases from 12-18% depending on the ratio, and should be considered since this amount will likely impact the design.

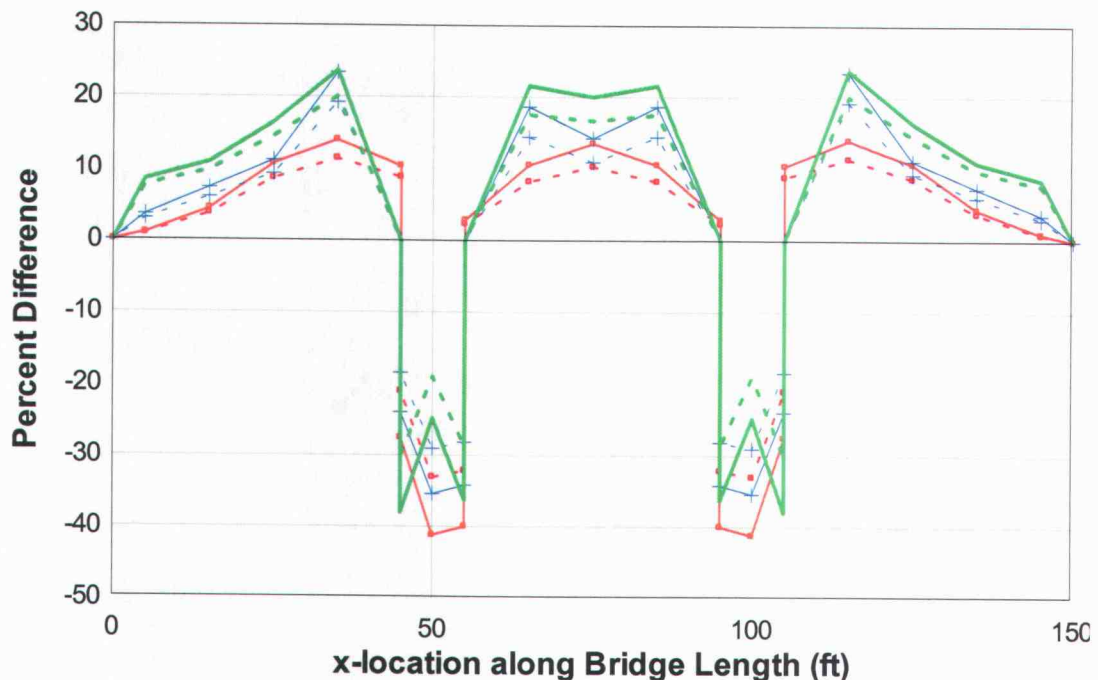


Fig. B4 - Percent change in moment for haunched sections of a three (50 ft)-span continuous bridge.

Haunch

Shear in a haunched section is affected most at mid-spans. The shear decreases at the end supports and increases by less than 3% at the interior supports. Therefore, since design is

usually controlled by shear at the supports, the change can be ignored. Since the positive moments near mid-span decrease they too can be ignored. However, the negative moment requires special attention with increases between 20 and 40% depending on the loading and the haunch ratio.

FURTHER STUDY

Further study is needed to determine if the change in the moment of inertia (I) is adequate to handle the change in load effect, therefore making the changes null, if loads and design are determined assuming a prismatic section. In addition, further study is still needed on the effect of cracked sections. Since the cracked moment of inertia (I_{cr}) changes when the concrete cracks, the distribution of the load effects for a statically indeterminate structure may also change significantly.

APPENDIX C
RATING VEHICLES

HS20-44 - Design vehicle

3 axle vehicle

Gross Weight = 72 kips

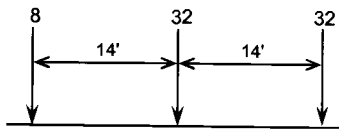


Fig. C1 - Rating Vehicle 1

Type 3 Unit - legal vehicle conforming to Weight Table 1

3 axle vehicle

Gross Weight = 50 kips

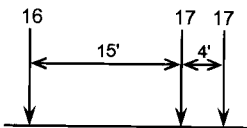


Fig. C2 - Rating Vehicle 2

Type 3-3 Unit - legal vehicle conforming to Weight Table 1

5 axle vehicle

Gross Weight = 80 kips

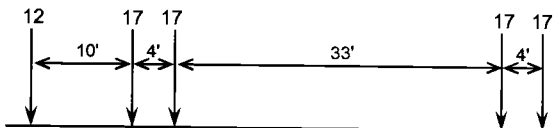


Fig. C3 - Rating Vehicle 3

Type 3S2 Unit - legal vehicle conforming to Weight Table 1

6 axle vehicle

Gross Weight = 80 kips

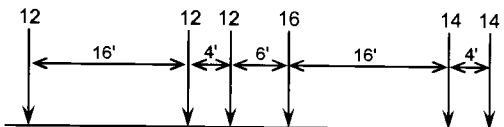


Fig. C4 - Rating Vehicle 4

Permit 1 - continuous trip permit vehicle conforming to Weight Table 3
 5 axle vehicle
 Gross Weight = 98 kips

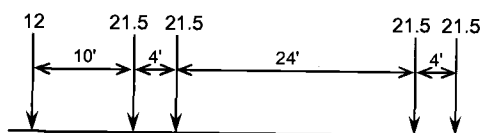


Fig. C5 - Rating Vehicle 5

Permit 2 - continuous trip permit vehicle conforming to Weight Table 3
 5 axle vehicle
 Gross Weight = 98 kips

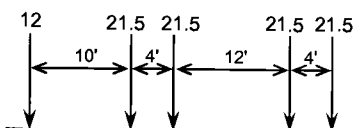


Fig. C6 - Rating Vehicle 6

Permit 3 - single trip permit vehicle conforming to Weight Table 4
 8 axle vehicle
 Gross Weight = 163 kips

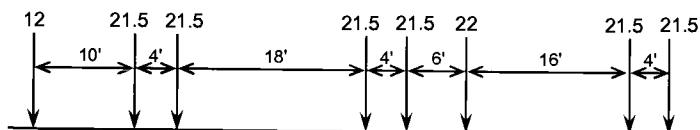


Fig. C7 - Rating Vehicle 7

Permit 4 - single trip permit vehicle conforming to Weight Table 5
 11 axle vehicle
 Gross Weight = 228 kips

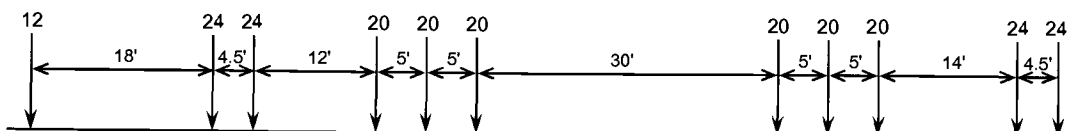


Fig. C8 - Rating Vehicle 8

Permit 5

6 axle vehicle

Gross Weight = 120.5 kips

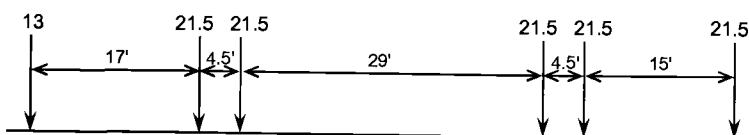


Fig. C9 - Rating Vehicle 9

Permit 6

8 axle vehicle

Gross Weight = 150.5 kips

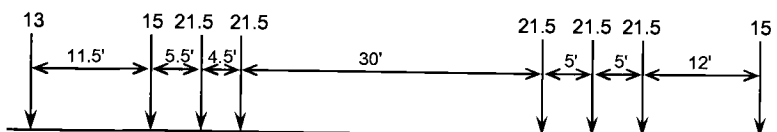


Fig. C10 - Rating Vehicle 10

Permit 7

9 axle vehicle

Gross Weight = 185 kips

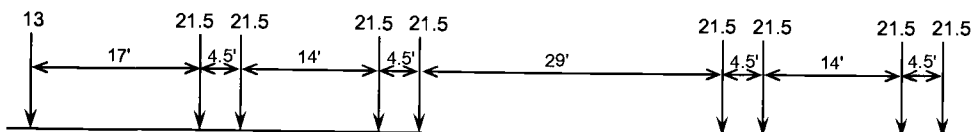


Fig. C11 - Rating Vehicle 11

Table C1 – ODOT Rating Vehicles in table form.

GVW	SPD	TYP	P	LENGTH	NAXLE	Axle Weights (kips)											Axle Spacings (ft)									
						AXL1	AXL2	AXL3	AXL4	AXL5	AXL6	AXL7	AXL8	AXL9	AX10	AX11	SPC1	SPC2	SPC3	SPC4	SPC5	SPC6	SPC7	SPC8	SPC9	SP10
72	55	0	0	28	3	32	32	8	0	0	0	0	0	0	0	0	14	14	0	0	0	0	0	0	0	0
50	55	0	0	19	3	17	17	16	0	0	0	0	0	0	0	0	4	15	0	0	0	0	0	0	0	0
80	55	0	0	51	5	17	17	17	17	12	0	0	0	0	0	0	4	33	4	10	0	0	0	0	0	0
80	55	0	0	46	6	14	14	16	12	12	12	0	0	0	0	0	4	16	6	4	16	0	0	0	0	0
98	55	0	0	42	5	21.5	21.5	21.5	21.5	12	0	0	0	0	0	0	4	24	4	10	0	0	0	0	0	0
98	55	0	0	30	5	21.5	21.5	21.5	21.5	12	0	0	0	0	0	0	4	12	4	10	0	0	0	0	0	0
163	55	0	0	62	8	21.5	21.5	22	21.5	21.5	21.5	12	0	0	0	0	4	16	6	4	18	4	10	0	0	0
228	55	0	0	103	11	24	24	20	20	20	20	20	24	24	12	4.5	14	5	5	30	5	5	12	4.5	18	18
120.5	55	0	0	70	6	21.5	21.5	21.5	21.5	21.5	13	0	0	0	0	0	15	4.5	29	4.5	17	0	0	0	0	0
150.5	55	0	0	73.5	8	15	21.5	21.5	21.5	21.5	21.5	15	13	0	0	0	12	5	5	30	4.5	5.5	11.5	0	0	0
185	55	0	0	92	9	21.5	21.5	21.5	21.5	21.5	21.5	21.5	13	0	0	0	4.5	14	4.5	29	4.5	14	4.5	17	0	0

Table C2 – Wilbur WIM vehicles classified as Permit Table 5 in 2003.

GVW	SPD	TYP	P	LENGTH	NAXLE	Axle Weights (kips)											Axle Spacings (ft)									
						AXL1	AXL2	AXL3	AXL4	AXL5	AXL6	AXL7	AXL8	AXL9	AX10	AX11	SPC1	SPC2	SPC3	SPC4	SPC5	SPC6	SPC7	SPC8	SPC9	SP10
156.3	49	19	5	100.4	10	8.5	22.9	20.5	23.3	17.6	17.1	13.2	13.3	13.4	6.6	0	7.2	12.9	7.2	27.3	7.2	12.9	7.2	7.2	11.5	0
109.3	58	11	5	58.7	5	24.5	24.7	21.2	22.2	16.7	0	0	0	0	0	0	7.5	27.1	7.5	16.6	0	0	0	0	0	0
96.5	55	17	5	73.5	7	1.1	1.1	17.5	20.7	22.6	22.5	11.1	0	0	0	0	7.2	11.5	7.2	24.5	7.2	15.9	0	0	0	0
66.9	47	11	5	53.4	5	1.1	1.1	21.3	22.4	21	0	0	0	0	0	0	8.1	19.4	8.1	17.8	0	0	0	0	0	0
174.5	54	19	5	101.8	11	11.8	14.4	16.8	24	24.6	17.8	12.4	13	13.1	15.3	11.3	6.9	9.6	6.9	6.9	26.1	6.9	6.9	8.3	6.9	16.5
147.1	50	19	5	92	9	9.2	10.5	24.6	24.6	18.3	18.7	14.5	16.1	10.4	0	0	7.1	11.3	7.1	25.5	7.1	9.9	7.1	17	0	0
102.9	55	11	5	55.5	5	22.7	24.5	20.7	22.7	12.3	0	0	0	0	0	0	7.5	25.5	7.5	15	0	0	0	0	0	0
160.5	48	19	5	90.9	9	14.5	14	24.5	24.5	19.6	20.7	15.2	15.6	11.9	0	0	7.2	11.5	7.2	26	7.2	8.7	7.2	15.9	0	0
131.3	57	17	5	65.5	7	18.1	21.6	22.8	21.1	22.1	13.4	12	0	0	0	0	7	7	26.5	7	7	11.1	0	0	0	0
96.3	55	11	5	55.8	5	18.3	23.7	20	22.5	11.9	0	0	0	0	0	0	7.5	25.6	7.5	15.1	0	0	0	0	0	0
69.8	59	5	5	23.9	3	24.5	23.7	21.6	0	0	0	0	0	0	0	0	7	16.9	0	0	0	0	0	0	0	0
106.2	53	15	5	70.7	6	6.4	19.9	22.4	22.5	24.4	10.6	0	0	0	0	0	13.5	7.5	25.6	7.5	16.5	0	0	0	0	0
173.7	45	19	5	77.4	10	14.1	15	14.1	13.9	23.4	23.5	21.4	20.8	13.3	14.2	0	9.9	7	7	15.5	7	7	7	8.4	8.4	0
98.6	49	15	5	30.1	6	14.7	14.8	12.9	18.6	18.9	18.6	0	0	0	0	0	6	6	6	6	6	0	0	0	0	0
158.5	40	18	5	62.3	8	11.5	19.1	18.2	24.4	24.4	19.7	20.3	20.9	0	0	0	13	7.2	13	7.2	7.2	7.2	7.2	0	0	0
74	8	15	5	24.8	6	1.1	15.2	16.7	14.6	14.4	12	0	0	0	0	0	6.8	4.3	4.3	4.3	5.1	0	0	0	0	0
136.2	40	18	5	51.1	8	13.5	13.9	13.8	13.6	17.3	19.7	18.9	25.4	0	0	0	6.6	6.6	7.9	6.6	6.6	10.5	6.6	0	0	0
97.4	56	11	5	55.4	5	20.1	23.4	20.1	21.5	12.3	0	0	0	0	0	0	7.5	25.5	7.5	15	0	0	0	0	0	0
74.6	55	11	5	16	5	13.5	16.2	17.8	15.1	11.9	0	0	0	0	0	0	2.2	6.5	2.2	5.2	0	0	0	0	0	0
136.2	40	18	5	51.2	8	13.6	13.9	13.8	11.2	20.8	22.9	16.5	23.5	0	0	0	6.6	6.6	6.6	6.6	6.6	10.5	7.9	0	0	0
125.6	55	17	5	78.1	7	14.3	14.1	13.9	13.5	22.8	24.7	22.3	0	0	0	0	8.8	7.4	7.4	32.4	7.4	14.7	0	0	0	0
118.3	52	18	5	81.2	8	7.9	9.1	19.8	21.9	21.8	21.2	9.2	7.3	0	0	0	6.9	12.4	6.9	27.5	6.9	6.9	13.8	0	0	0
106.2	52	14	5	71.2	6	3.2	20.1	23.8	23.7	24.5	10.9	0	0	0	0	0	13.6	7.6	25.8	7.6	16.7	0	0	0	0	0
101.2	52	14	5	71.1	6	6.8	17.4	21.6	20.9	23.8	10.7	0	0	0	0	0	13.6	7.6	25.7	7.6	16.6	0	0	0	0	0
94.7	53	11	5	57.5	5	18.8	24.4	18.8	21.6	11	0	0	0	0	0	0	7.4	29.5	7.4	13.3	0	0	0	0	0	0
81.5	37	8	5	23	4	24.3	21.8	19.8	15.6	0	0	0	0	0	0	0	6.1	10.9	6.1	0	0	0	0	0	0	0
98.2	59	15	5	29.3	6	17	18.6	12.3	15.8	16.8	17.7	0	0	0	0	0	5.9	5.9	5.9	5.9	5.9	0	0	0	0	0
149.3	53	19	5	94.1	9	11.7	11	24.2	24.3	16.2	18.2	17.5	17.7	8.4	0	0	7.2	10.1	7.2	26.1	7.2	11.6	7.2	17.4	0	0
95.9	54	11	5	51.2	5	20.4	24.3	21.2	20	10.1	0	0	0	0	0	0	7.3	20.5	7.3	16.1	0	0	0	0	0	0
105.8	46	15	5	60.6	6	6.6	22.3	24.2	21.7	19.1	11.9	0	0	0	0	0	9.3	7.8	20.2	7.8	15.5	0	0	0	0	0
140.3	37	18	5	56.7	8	10	16.3	16	18	20.1	18.1	19.6	22.1	0	0	0	9.7	6.9	11.1	6.9	6.9	6.9	8.3	0	0	0
174.3	41	19	5	76.4	10	14.9	15	15.1	15.1	22.2	23.3	20.6	19.8	13.7	14.5	0	9.7	6.9	6.9	15.3	6.9	6.9	6.9	8.3	8.3	0
142.6	36	18	5	56.8	8	10.7	15.9	15.8	19.1	19.6	17.4	22.1	22.1	0	0	0	9.7	6.9	11.1	6.9	6.9	6.9	8.3	0	0	0
138.4	36	18	5	56.5	8	10.5	15.9	16.1	18.7	18.7	17.2	19.6	21.7	0	0	0	9.6	6.9	11	6.9	6.9	6.9	8.3	0	0	0
126.3	50	17	5	65	7	18.2	19.6	22.6	21.3	23.1	10.9	10.6	0	0	0	0	6.9	6.9	27.7	6.9	6.9	9.7	0	0	0	0

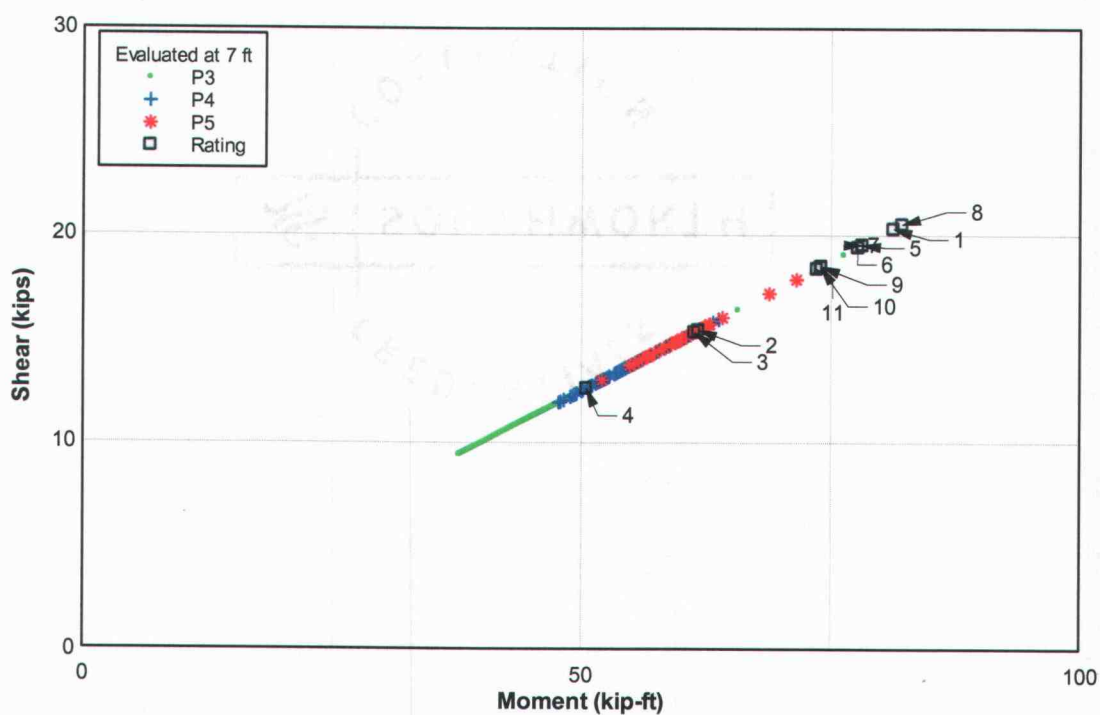


Fig. C12 - Maximum shear and moment load effects produced by one year of Wilbur WIM vehicles classified as Permit Tables 3, 4 and 5 and the eleven rating vehicles for a single (11 ft) span simply-supported bridge evaluated at 7 ft from left support in span one.

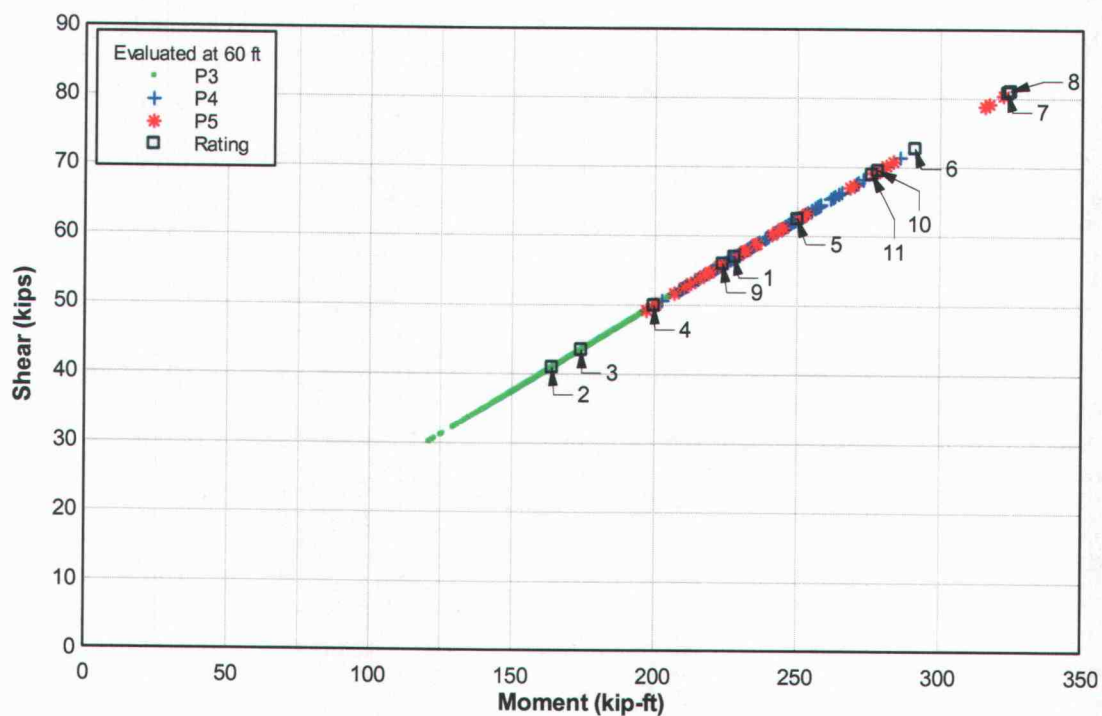


Fig. C13 - Maximum shear and moment load effects produced by one year of Wilbur WIM vehicles classified as Permit Tables 3, 4 and 5 and the eleven rating vehicles for a single (64 ft) span simply-supported bridge evaluated at 60 ft from left support in span one.

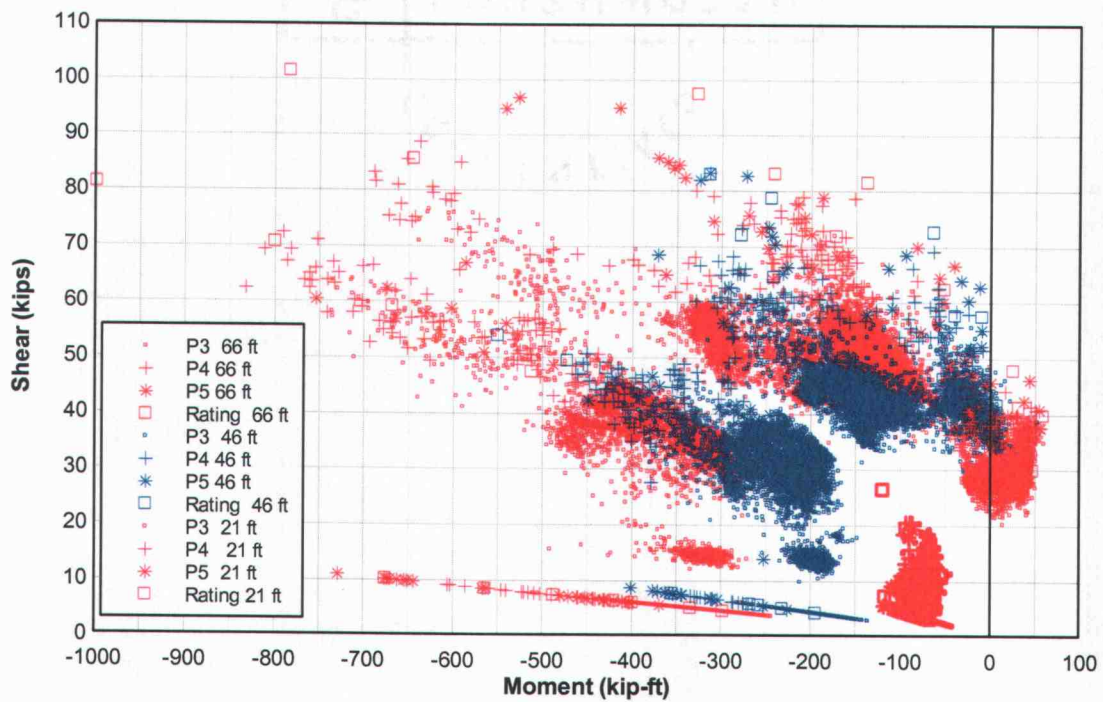


Fig. C14 - Summary of the maximum shear vs corresponding moment and the maximum moment vs corresponding shear for two-span continuous bridges with 70 ft, 50 ft, and 25 ft spans all evaluated 4 ft from the first continuous support in span one.

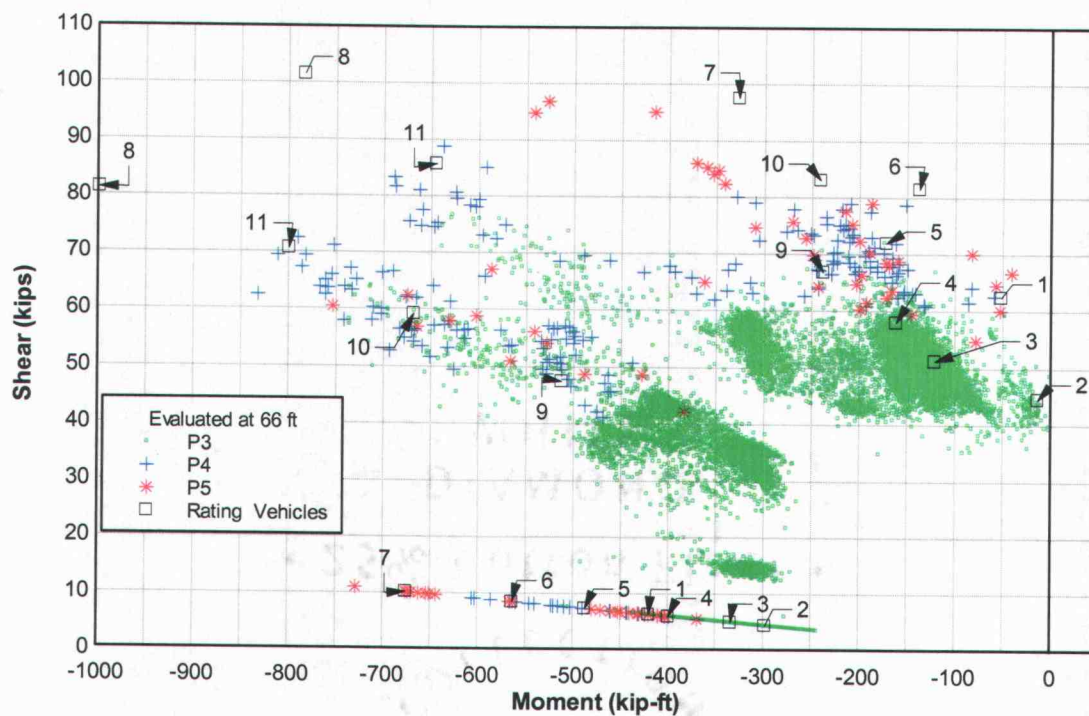


Fig. C15 - Maximum shear vs corresponding moment and the maximum moment vs corresponding shear load effects produced by one year of Wilbur WIM vehicles classified as Permit Tables 3, 4 and 5 and the eleven rating vehicles for two (70 ft) -span continuous bridge evaluated at 66 ft from left support in span one.

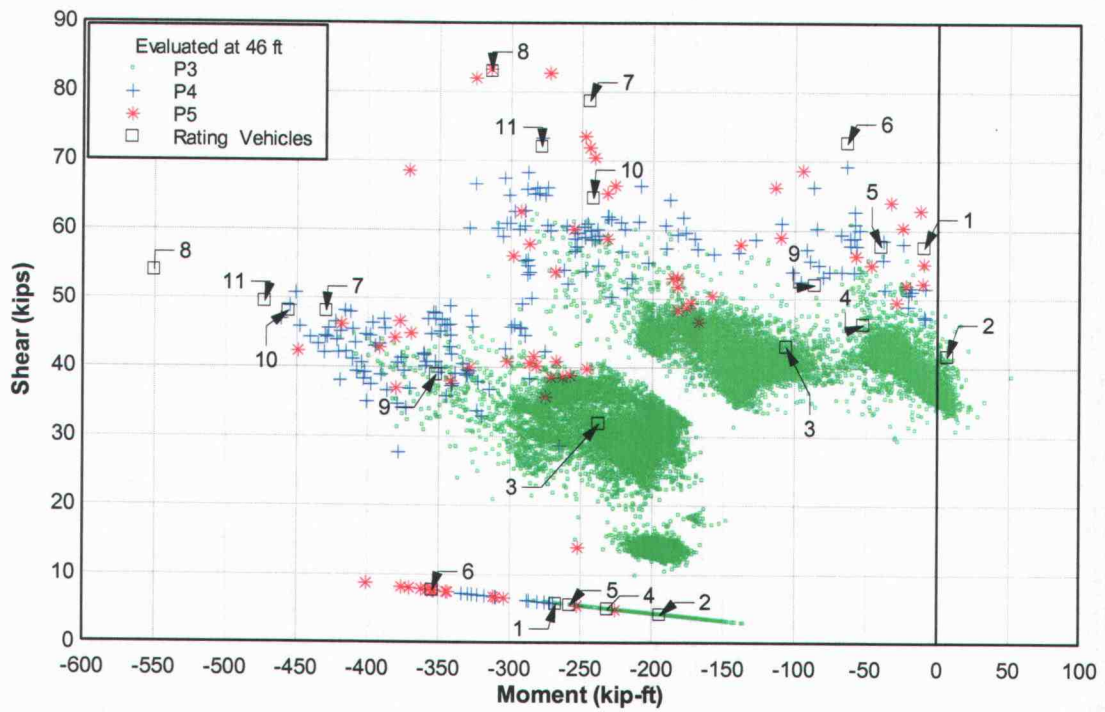


Fig. C16 - Maximum shear vs corresponding moment and the maximum moment vs corresponding shear load effects produced by one year of Wilbur WIM vehicles classified as Permit Tables 3, 4 and 5 and the eleven rating vehicles for two (50 ft) -span continuous bridge evaluated at 46 ft from left support in span one.

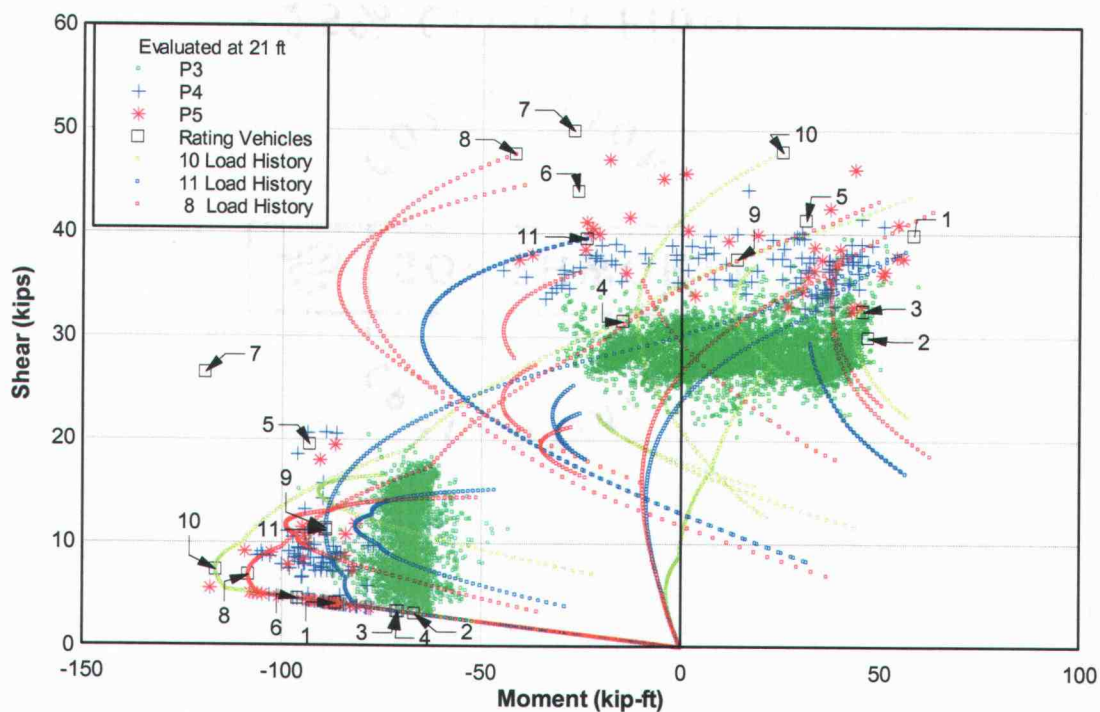


Fig. C17 - Maximum shear vs corresponding moment and the maximum moment vs corresponding shear load effects produced by one year of Wilbur WIM vehicles classified as Permit Tables 3, 4 and 5 and the eleven rating vehicles for two (25 ft) -span continuous bridge evaluated at 21 ft from left support in span one. Load histories of Rating Vehicles 10, 11 and 8.

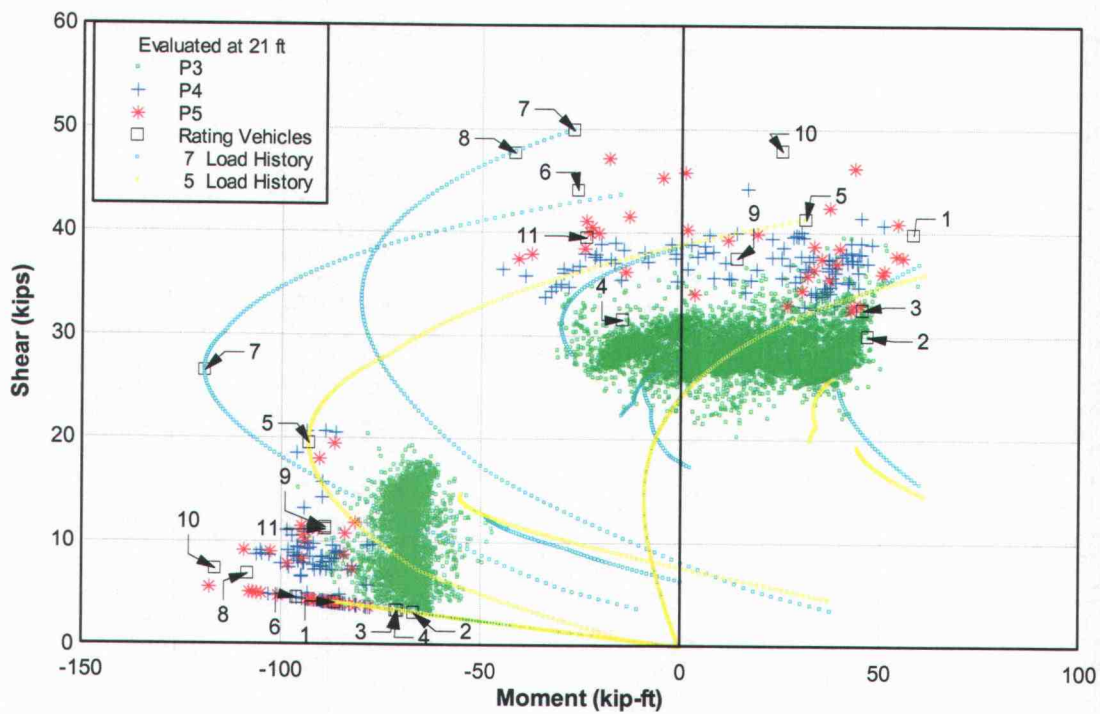


Fig. C18 - Maximum shear vs corresponding moment and the maximum moment vs corresponding shear load effects produced by one year of Wilbur WIM vehicles classified as Permit Tables 3, 4 and 5 and the eleven rating vehicles for two (25 ft) -span continuous bridge evaluated at 21 ft from left support in span one. Load histories of Rating Vehicles 7 and 5.

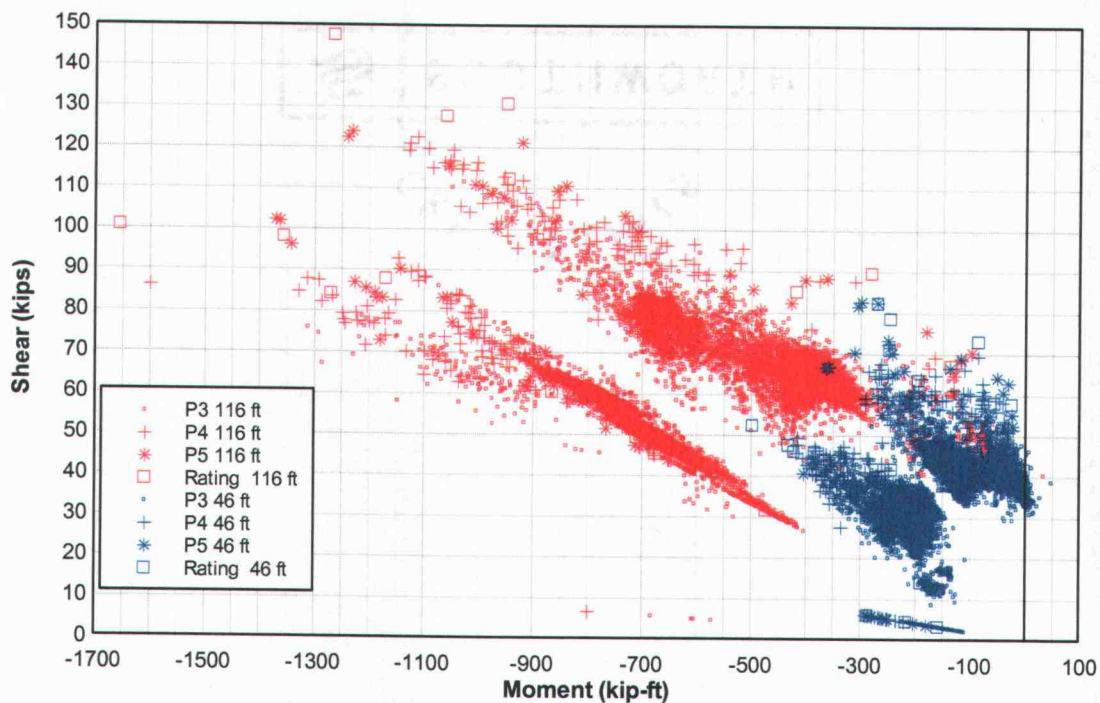


Fig. C19 - Summary of the maximum shear vs corresponding moment and the maximum moment vs corresponding shear for three-span continuous bridges with 120 ft and 50 ft spans both evaluated 4 ft from the first continuous support in span one.

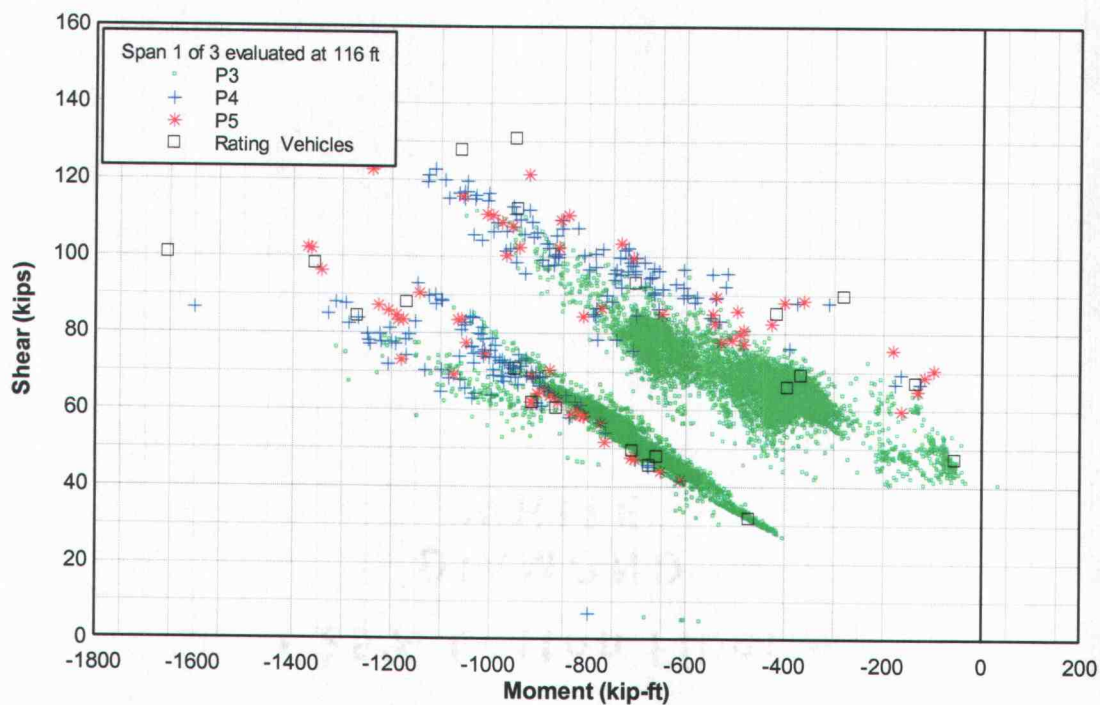


Fig. C20 - Maximum shear vs corresponding moment and the maximum moment vs corresponding shear load effects produced by one year of Wilbur WIM vehicles classified as Permit Tables 3, 4 and 5 and the eleven rating vehicles for three (120 ft) -span continuous bridge evaluated at 116 ft from left support in span one.

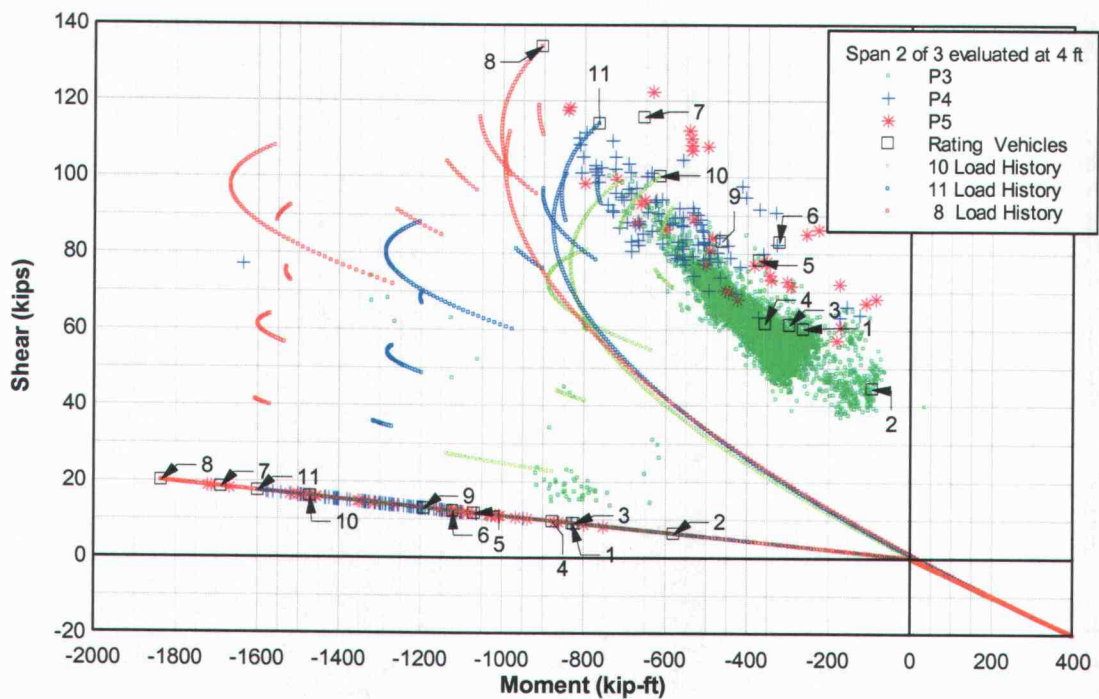


Fig. C21 - Maximum shear vs corresponding moment and the maximum moment vs corresponding shear load effects produced by one year of Wilbur WIM vehicles classified as Permit Tables 3, 4 and 5 and the eleven rating vehicles for three (120 ft) -span continuous bridge evaluated at 4 ft from left support in span two. Load Histories for Rating Vehicles 10, 11 and 8.

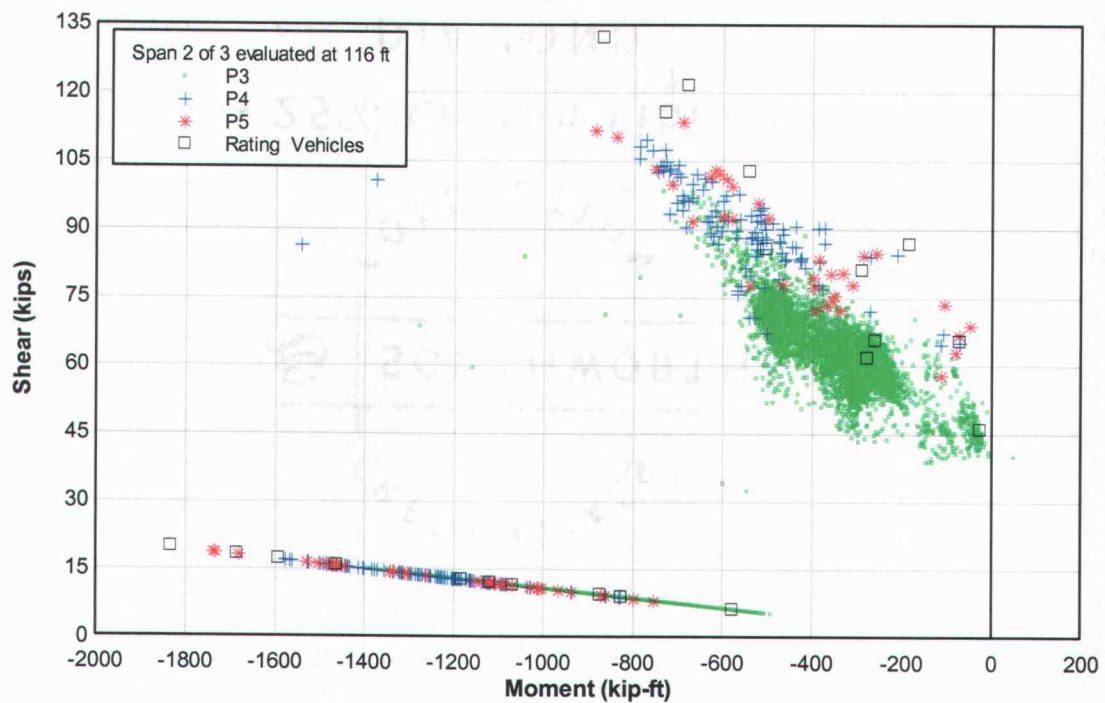


Fig. C22 - Maximum shear vs corresponding moment and the maximum moment vs corresponding shear load effects produced by one year of Wilbur WIM vehicles classified as Permit Tables 3, 4 and 5 and the eleven rating vehicles for three (120 ft) -span continuous bridge evaluated at 116 ft from left support in span two.

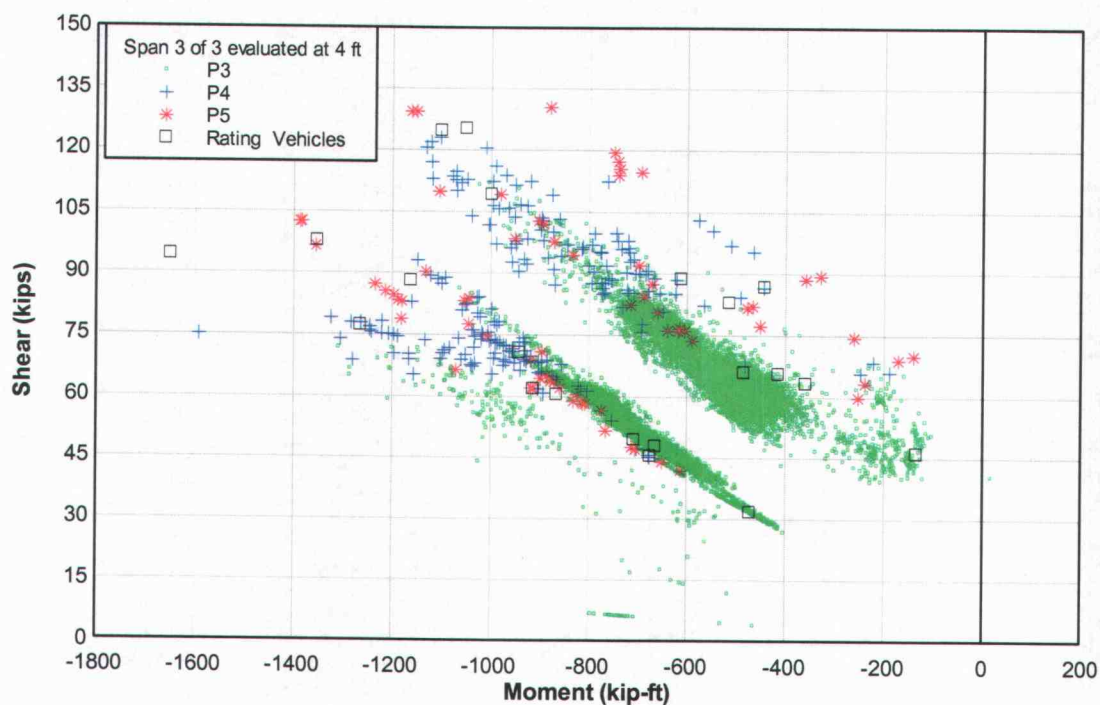


Fig. C23 - Maximum shear vs corresponding moment and the maximum moment vs corresponding shear load effects produced by one year of Wilbur WIM vehicles classified as Permit Tables 3, 4 and 5 and the eleven rating vehicles for three (120 ft) -span continuous bridge evaluated at 4 ft from left support in span three.

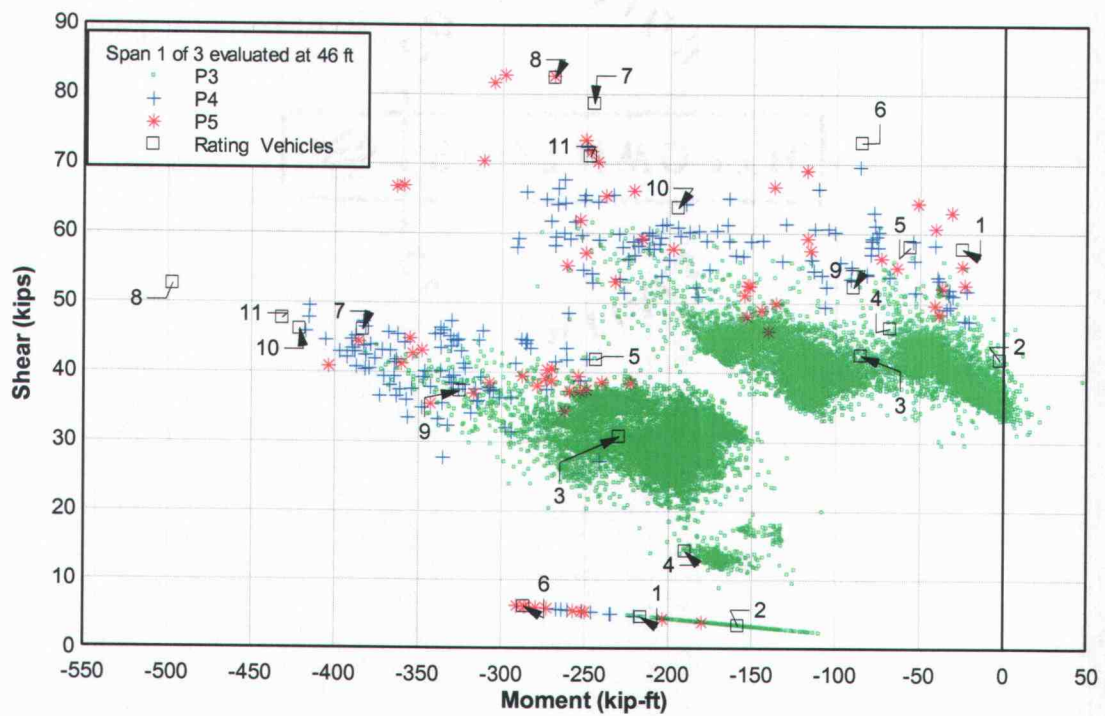


Fig. C24 - Maximum shear vs corresponding moment and the maximum moment vs corresponding shear load effects produced by one year of Wilbur WIM vehicles classified as Permit Tables 3, 4 and 5 and the eleven rating vehicles for three (50 ft) -span continuous bridge evaluated at 46 ft from left support in span one.

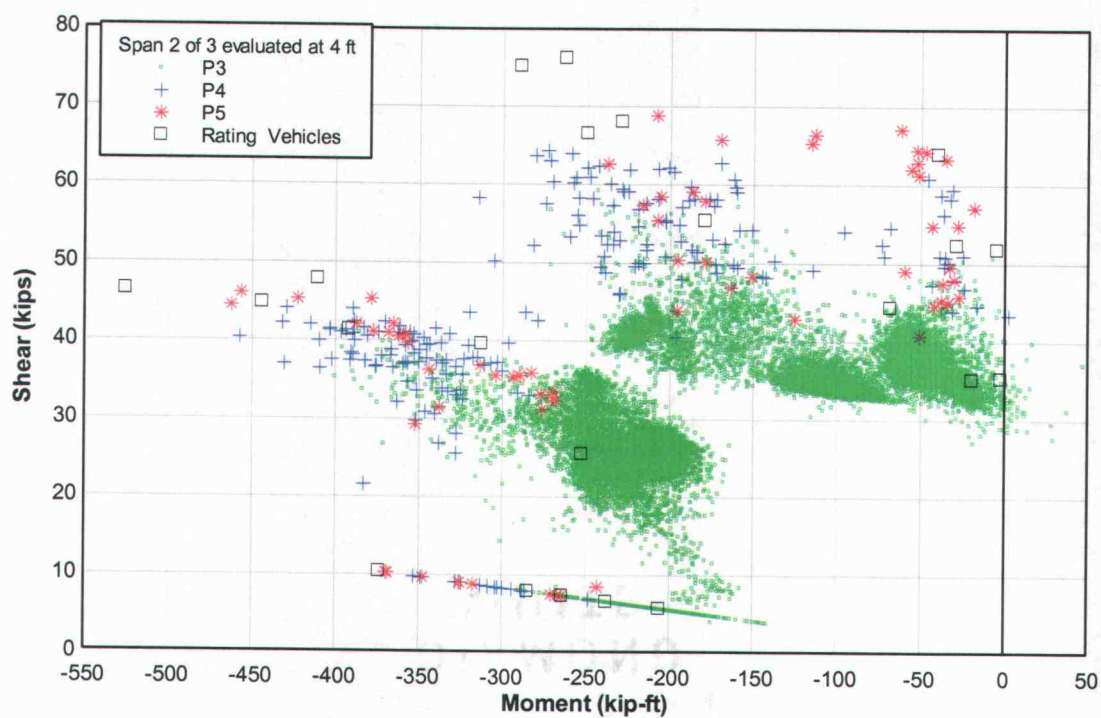


Fig. C25 - Maximum shear vs corresponding moment and the maximum moment vs corresponding shear load effects produced by one year of Wilbur WIM vehicles classified as Permit Tables 3, 4 and 5 and the eleven rating vehicles for three (50 ft) -span continuous bridge evaluated at 4 ft from left support in span two.

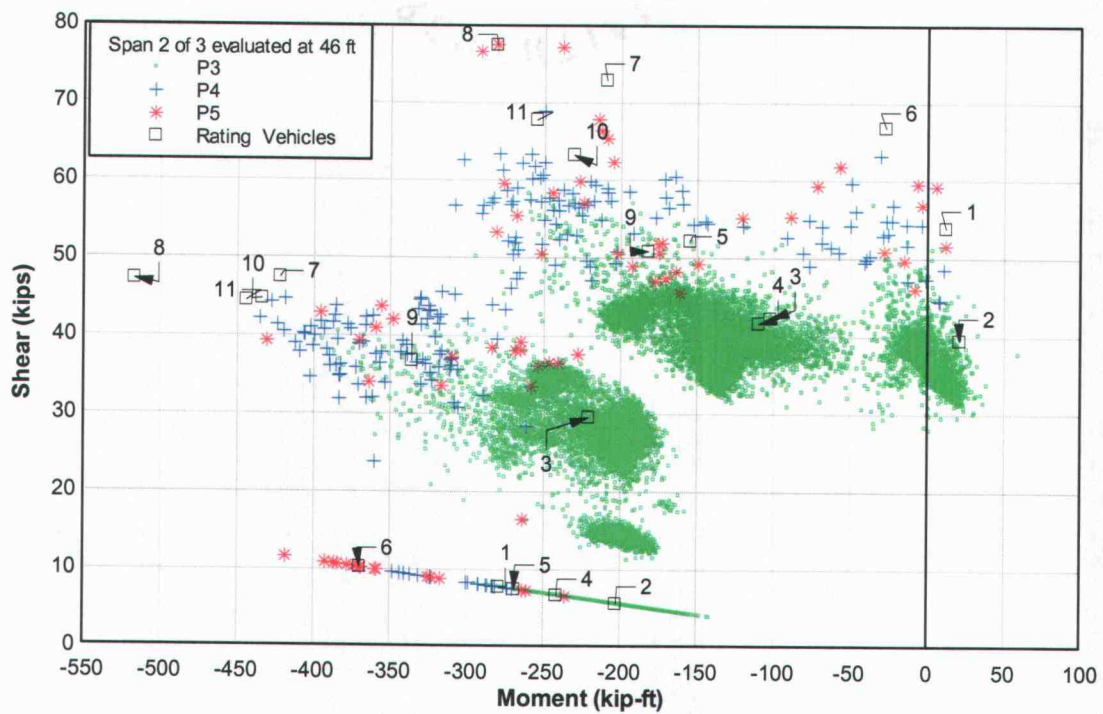


Fig. C26 - Maximum shear vs corresponding moment and the maximum moment vs corresponding shear load effects produced by one year of Wilbur WIM vehicles classified as Permit Tables 3, 4 and 5 and the eleven rating vehicles for three (50 ft) -span continuous bridge evaluated at 46 ft from left support in span two.

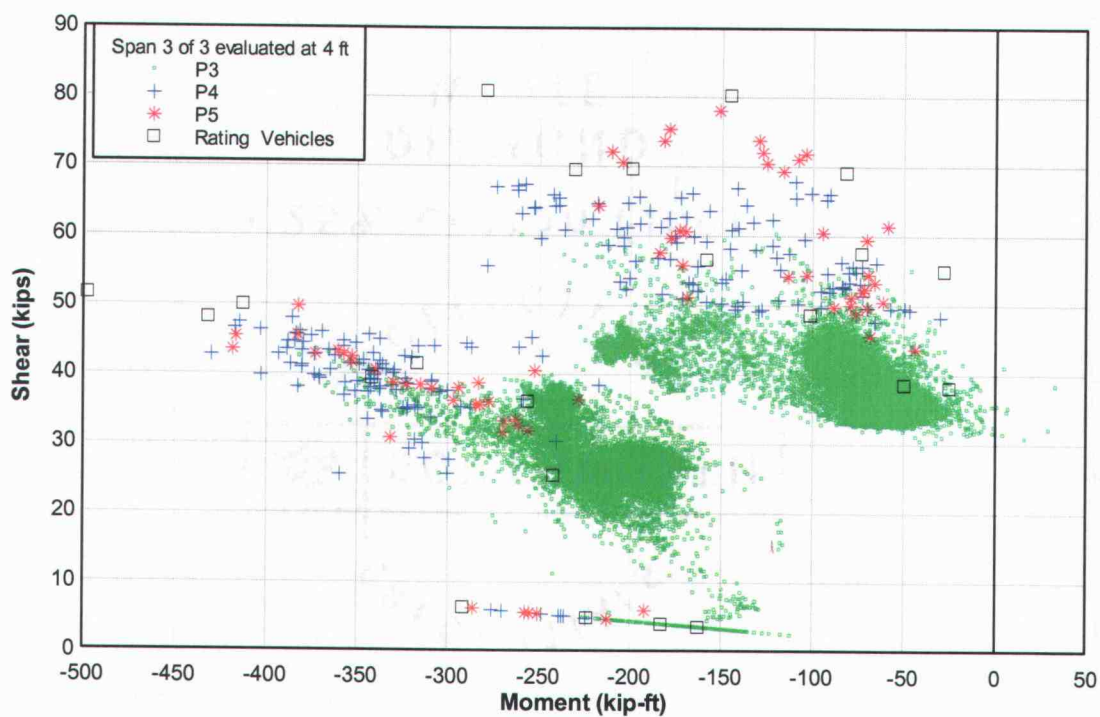


Fig. C27 - Maximum shear vs corresponding moment and the maximum moment vs corresponding shear load effects produced by one year of Wilbur WIM vehicles classified as Permit Tables 3, 4 and 5 and the eleven rating vehicles for three (50 ft) -span continuous bridge evaluated at 4 ft from left support in span three.

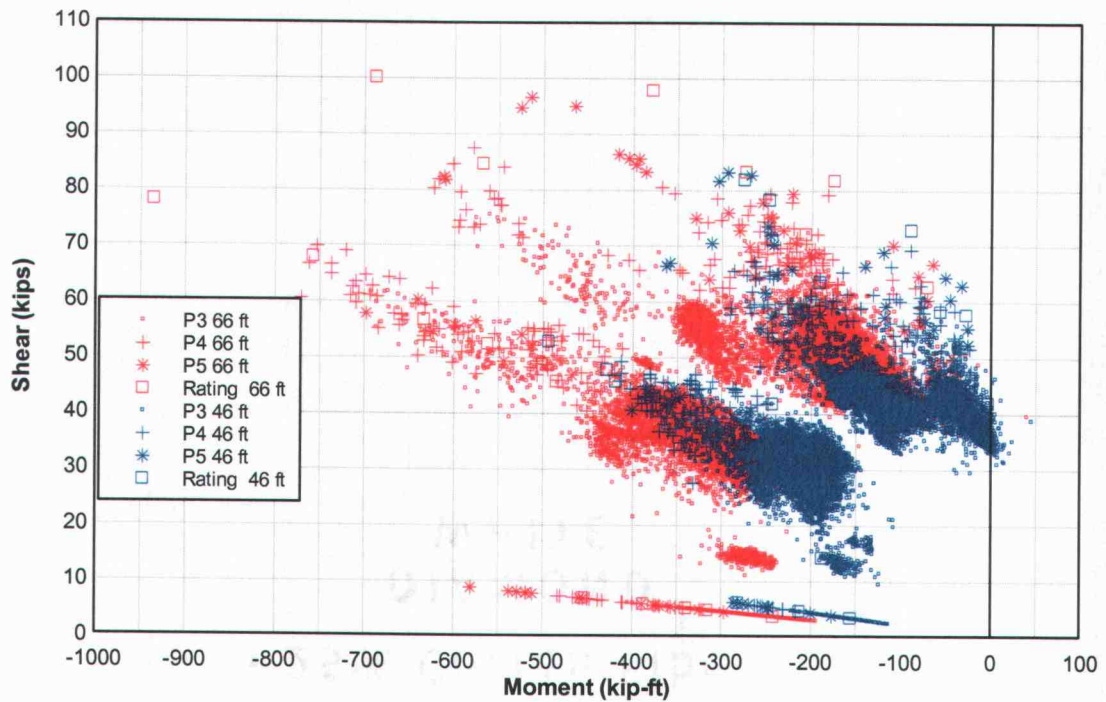


Fig. C28 - Summary of the maximum shear vs corresponding moment and the maximum moment vs corresponding shear for four-span continuous bridges with 70 ft and 50 ft spans both evaluated 4 ft from the first continuous support in span one.

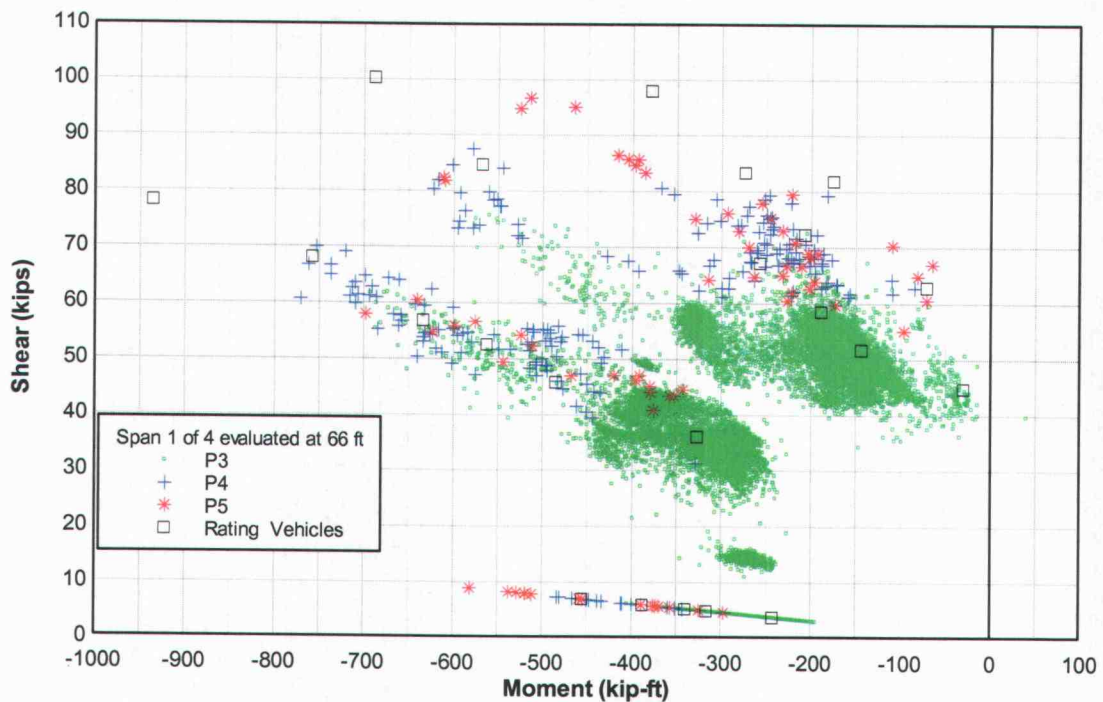


Fig. C29 - Maximum shear vs corresponding moment and the maximum moment vs corresponding shear load effects produced by one year of Wilbur WIM vehicles classified as Permit Tables 3, 4 and 5 and the eleven rating vehicles for four (70 ft) -span continuous bridge evaluated at 66 ft from left support in span one.

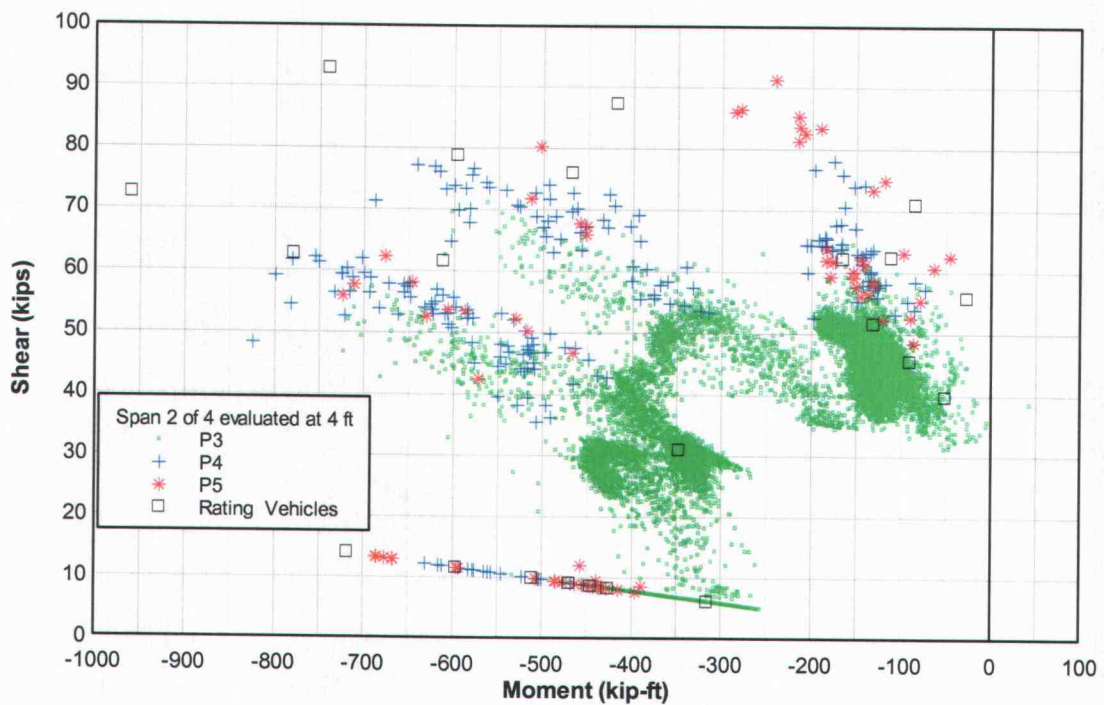


Fig. C30 - Maximum shear vs corresponding moment and the maximum moment vs corresponding shear load effects produced by one year of Wilbur WIM vehicles classified as Permit Tables 3, 4 and 5 and the eleven rating vehicles for four (70 ft) -span continuous bridge evaluated at 4 ft from left support in span two.

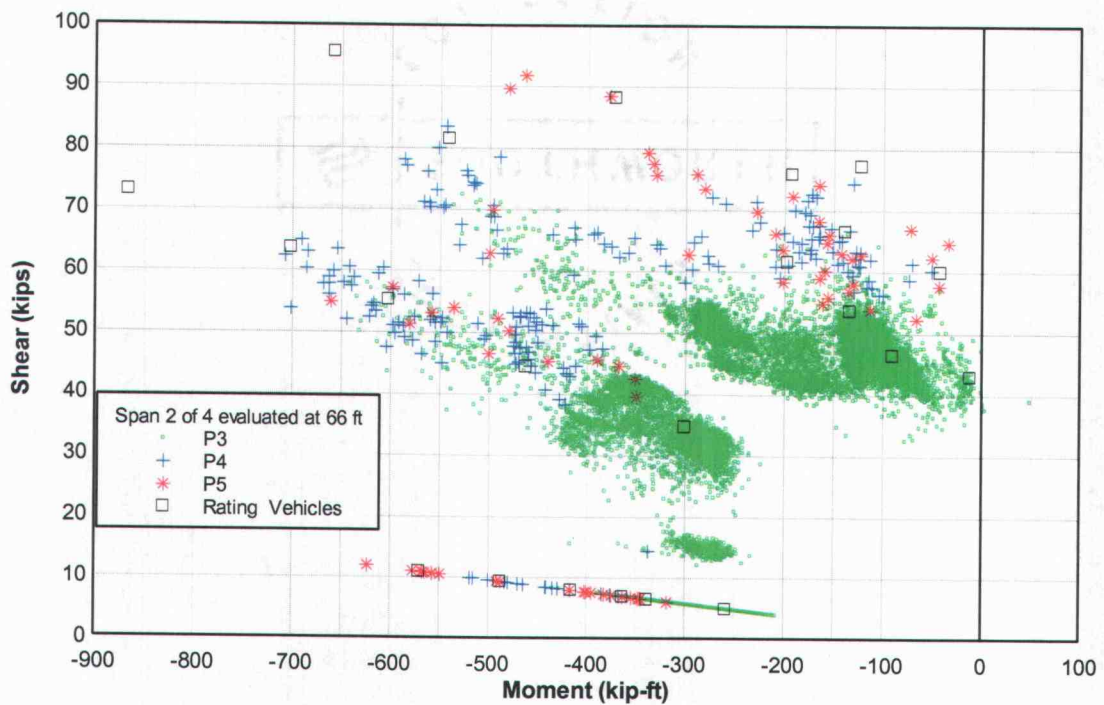


Fig. C31 - Maximum shear vs corresponding moment and the maximum moment vs corresponding shear load effects produced by one year of Wilbur WIM vehicles classified as Permit Tables 3, 4 and 5 and the eleven rating vehicles for four (70 ft) -span continuous bridge evaluated at 66 ft from left support in span two.

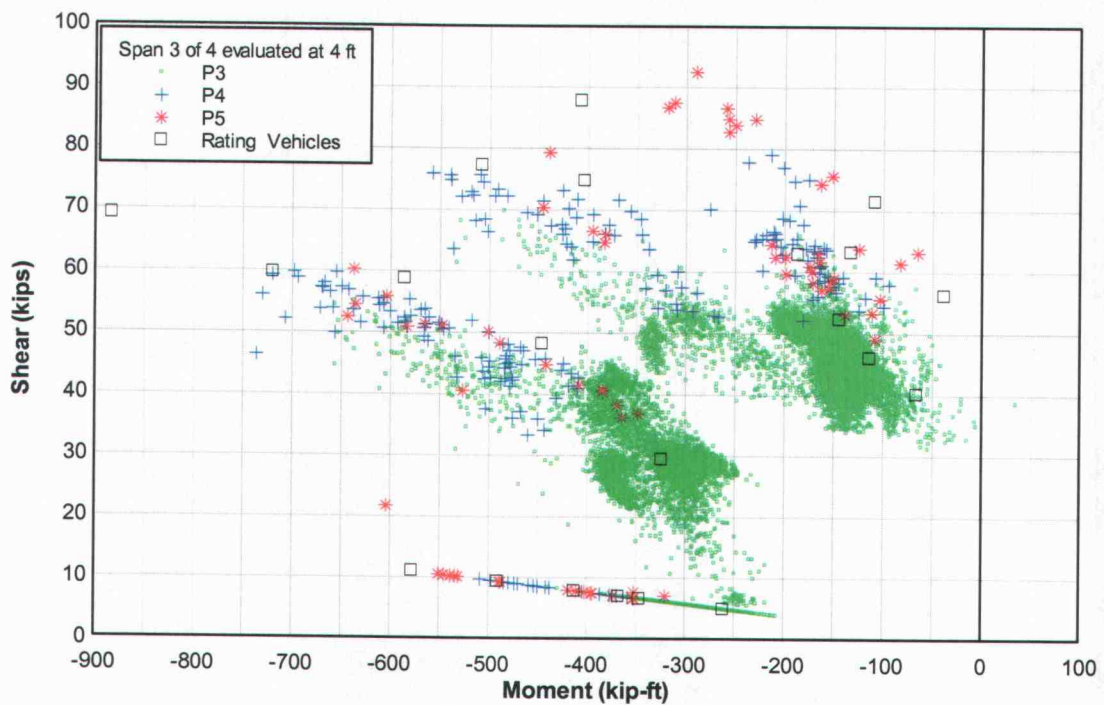


Fig. C32 - Maximum shear vs corresponding moment and the maximum moment vs corresponding shear load effects produced by one year of Wilbur WIM vehicles classified as Permit Tables 3, 4 and 5 and the eleven rating vehicles for four (70 ft) -span continuous bridge evaluated at 4 ft from left support in span three.

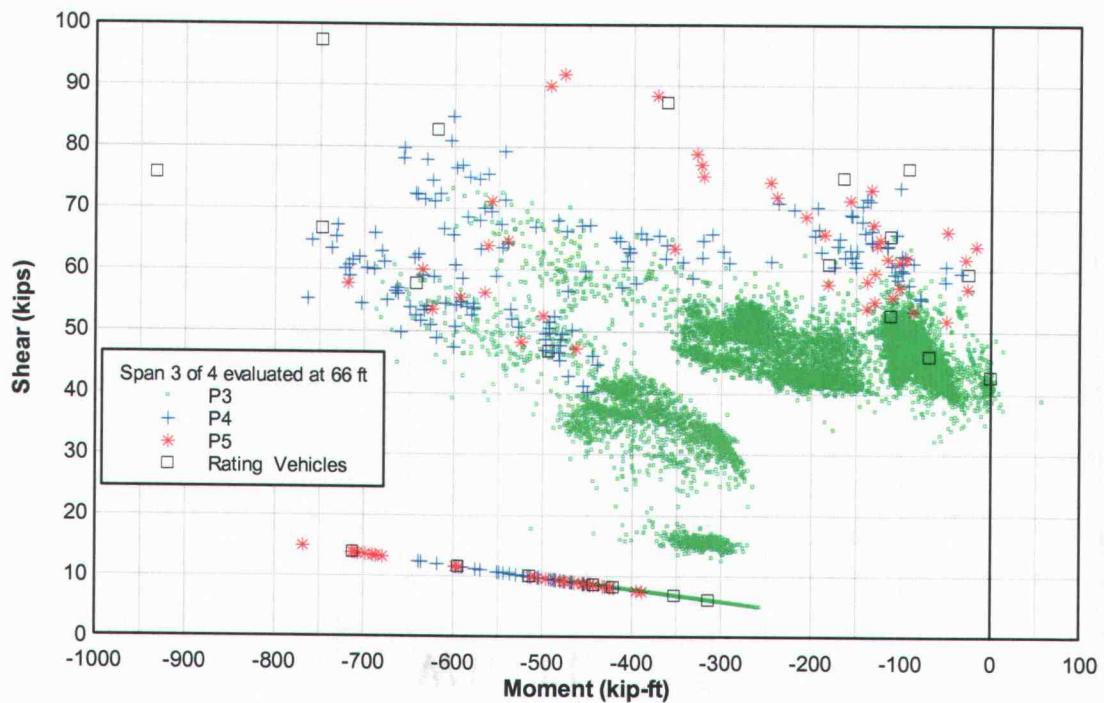


Fig. C33 - Maximum shear vs corresponding moment and the maximum moment vs corresponding shear load effects produced by one year of Wilbur WIM vehicles classified as Permit Tables 3, 4 and 5 and the eleven rating vehicles for four (70 ft) -span continuous bridge evaluated at 66 ft from left support in span three.

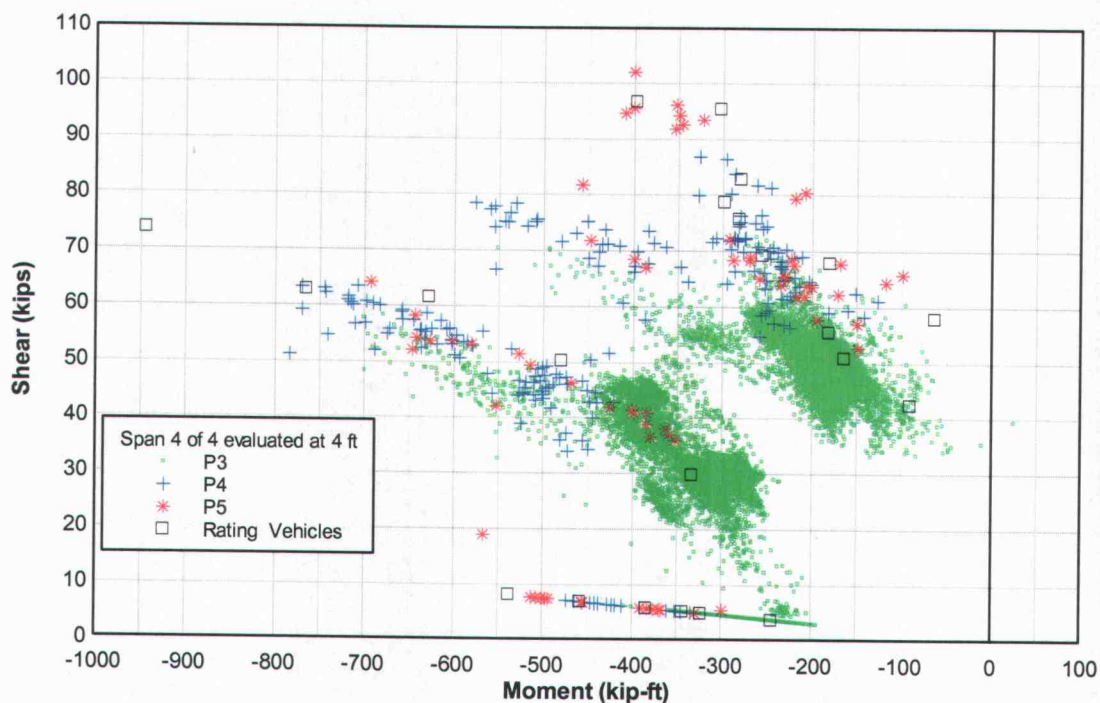


Fig. C34 - Maximum shear vs corresponding moment and the maximum moment vs corresponding shear load effects produced by one year of Wilbur WIM vehicles classified as Permit Tables 3, 4 and 5 and the eleven rating vehicles for four (70 ft) -span continuous bridge evaluated at 4 ft from left support in span four.

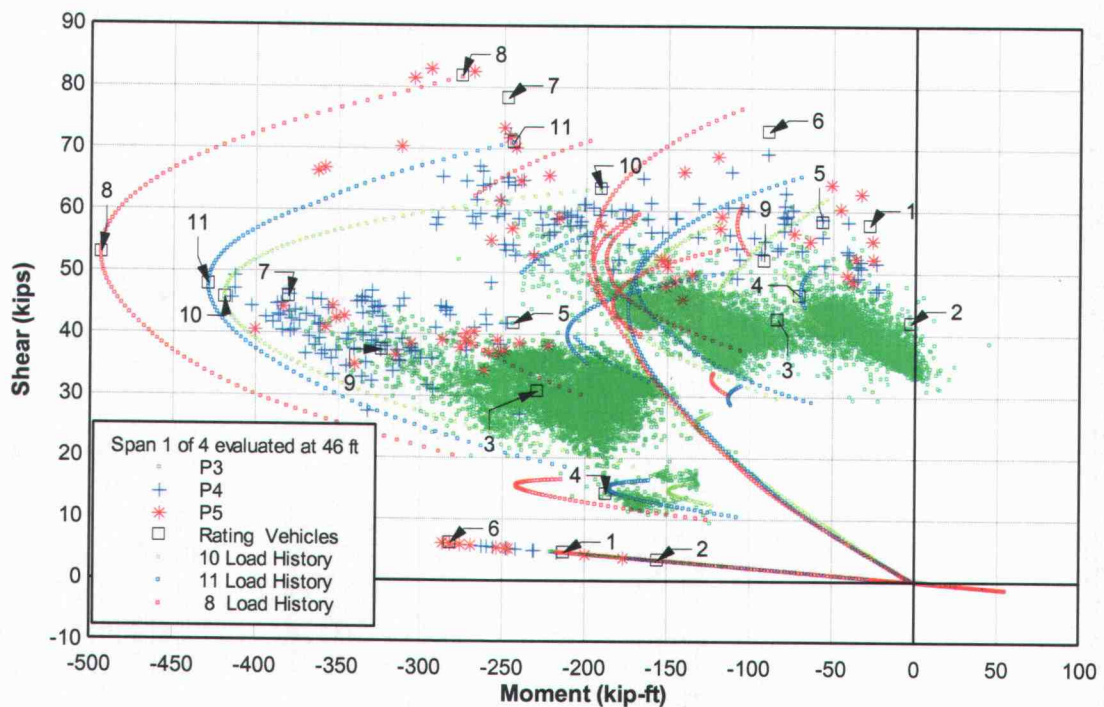


Fig. C35 - Maximum shear vs corresponding moment and the maximum moment vs corresponding shear load effects produced by one year of Wilbur WIM vehicles classified as Permit Tables 3, 4 and 5 and the eleven rating vehicles for four (50 ft) -span continuous bridge evaluated at 46 ft from left support in span one. Load Histories for Rating Vehicles 10, 11 and 8.

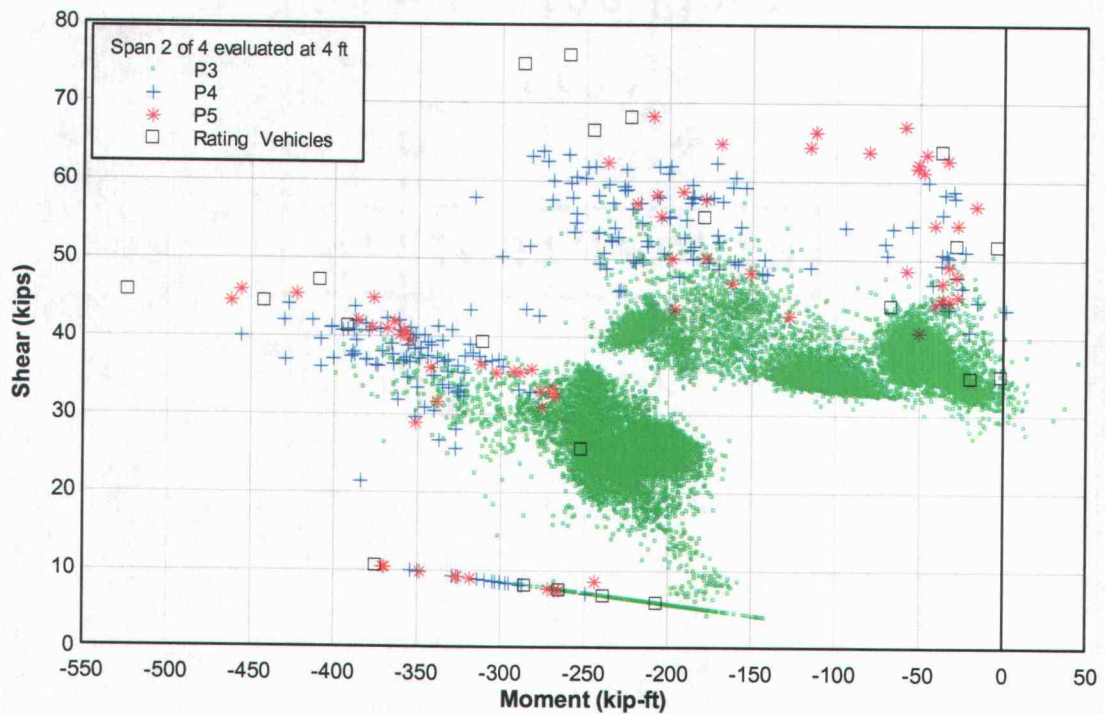


Fig. C36 - Maximum shear vs corresponding moment and the maximum moment vs corresponding shear load effects produced by one year of Wilbur WIM vehicles classified as Permit Tables 3, 4 and 5 and the eleven rating vehicles for four (50 ft) -span continuous bridge evaluated at 4 ft from left support in span two.

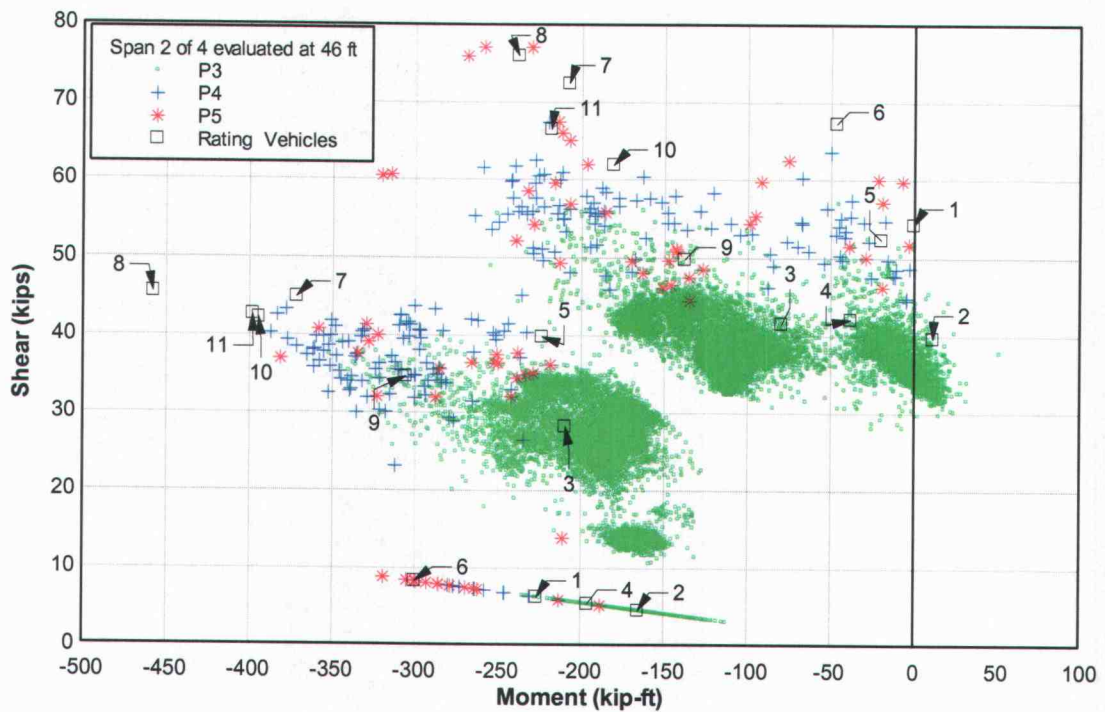


Fig. C37 - Maximum shear vs corresponding moment and the maximum moment vs corresponding shear load effects produced by one year of Wilbur WIM vehicles classified as Permit Tables 3, 4 and 5 and the eleven rating vehicles for four (50 ft) -span continuous bridge evaluated at 46 ft from left support in span two.

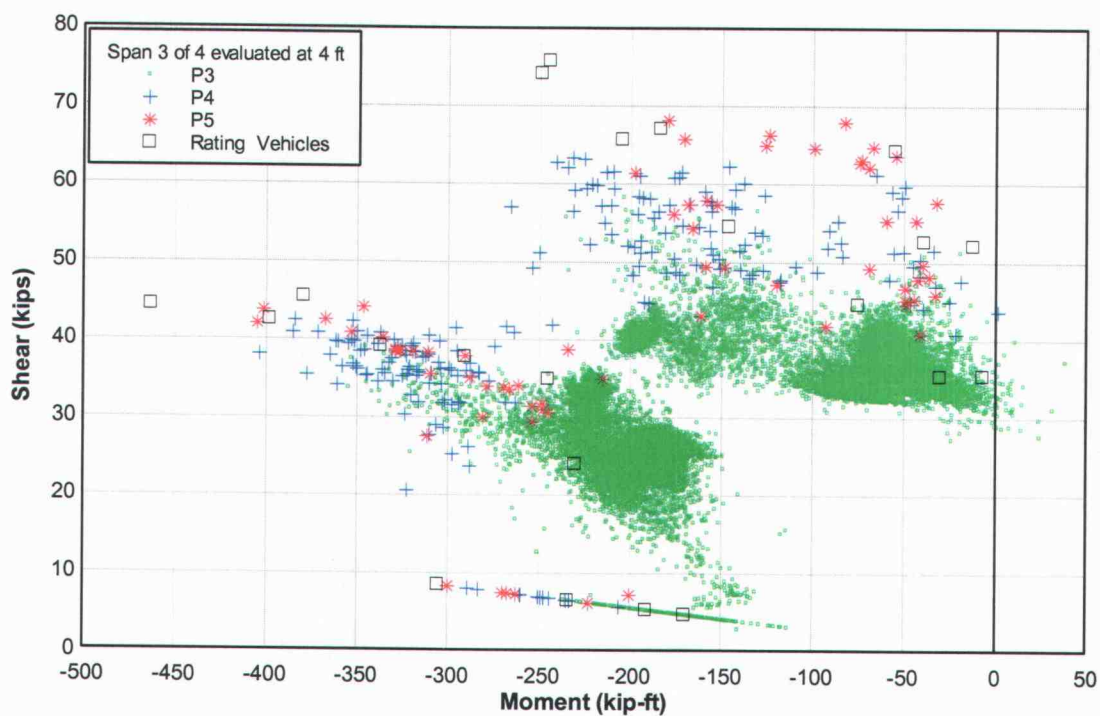


Fig. C38 - Maximum shear vs corresponding moment and the maximum moment vs corresponding shear load effects produced by one year of Wilbur WIM vehicles classified as Permit Tables 3, 4 and 5 and the eleven rating vehicles for four (50 ft) -span continuous bridge evaluated at 4 ft from left support in span three.

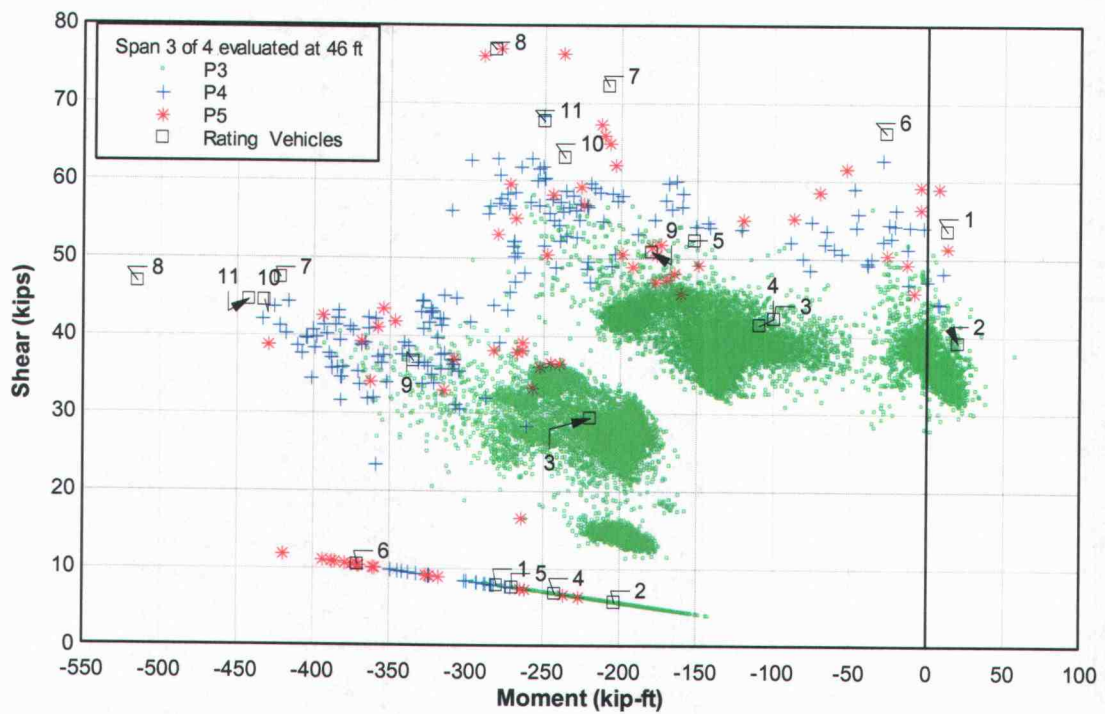


Fig. C39 - Maximum shear vs corresponding moment and the maximum moment vs corresponding shear load effects produced by one year of Wilbur WIM vehicles classified as Permit Tables 3, 4 and 5 and the eleven rating vehicles for four (50 ft) -span continuous bridge evaluated at 46 ft from left support in span three.

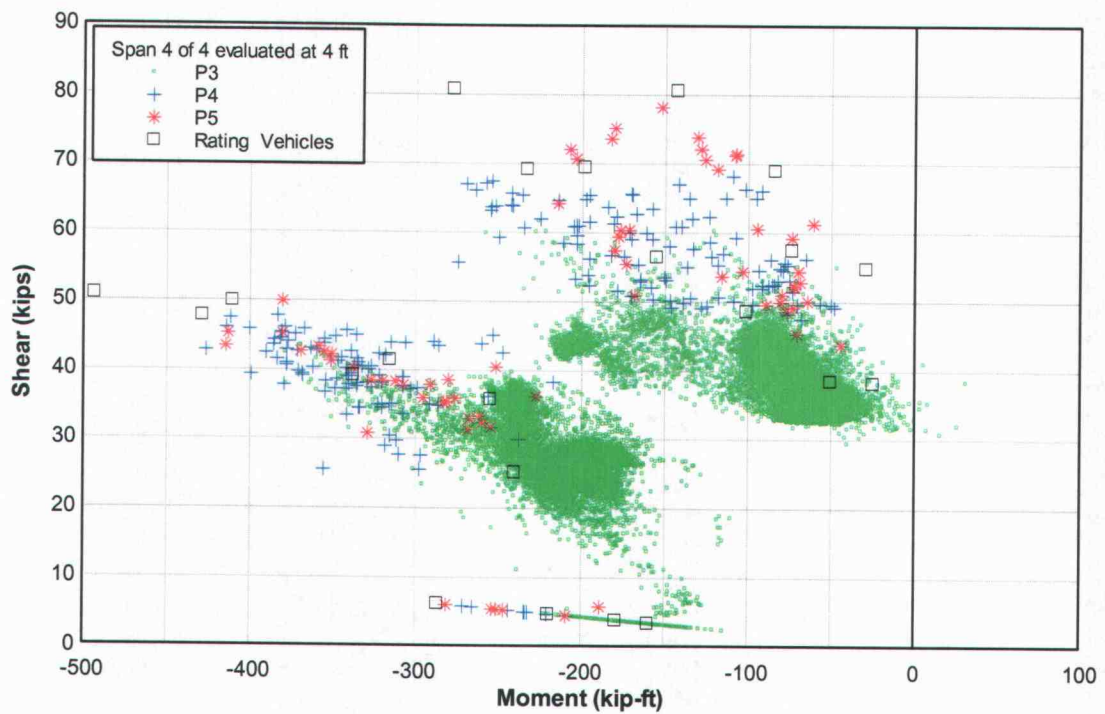


Fig. C40 - Maximum shear vs corresponding moment and the maximum moment vs corresponding shear load effects produced by one year of Wilbur WIM vehicles classified as Permit Tables 3, 4 and 5 and the eleven rating vehicles for four (50 ft) -span continuous bridge evaluated at 4 ft from left support in span four.

APPENDIX D
McKENZIE RIVER BRIDGE

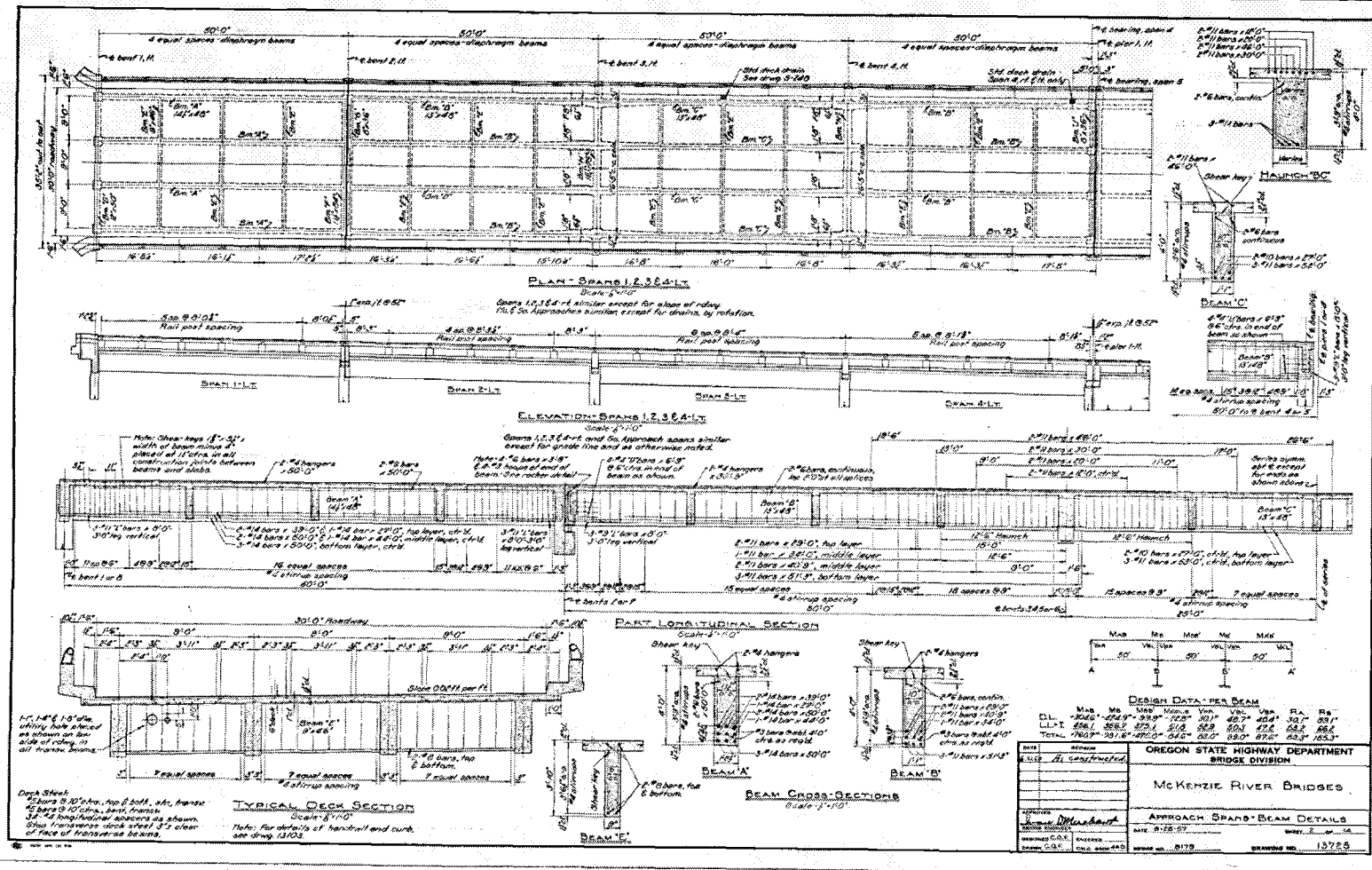
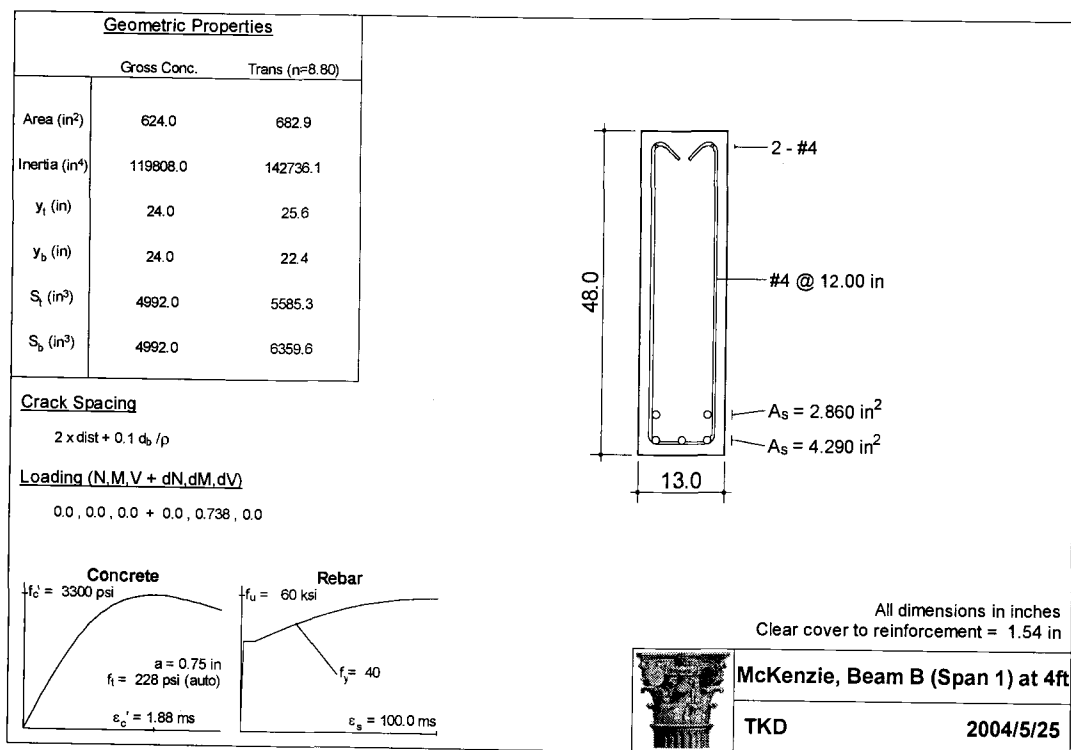
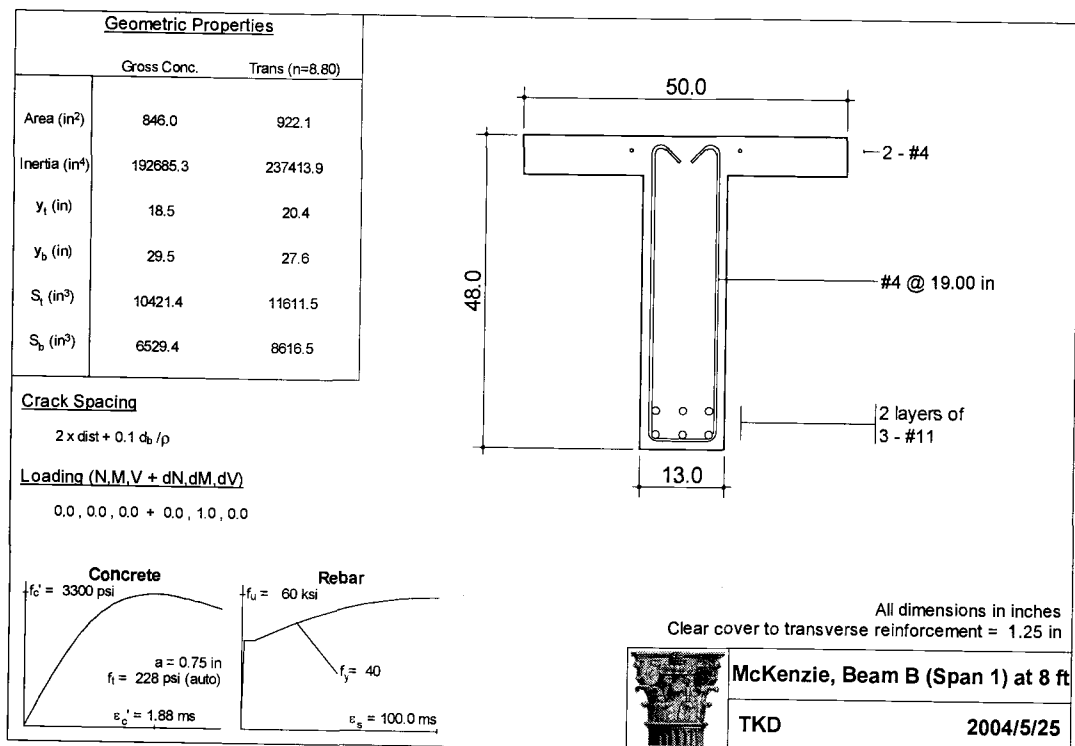
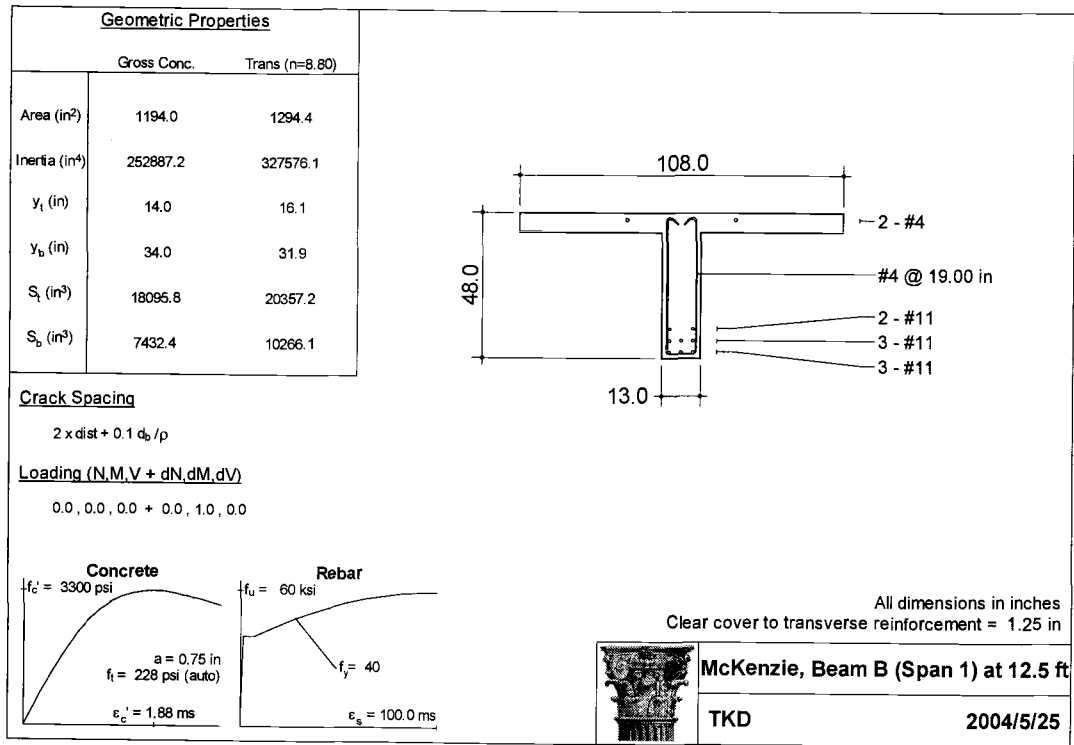
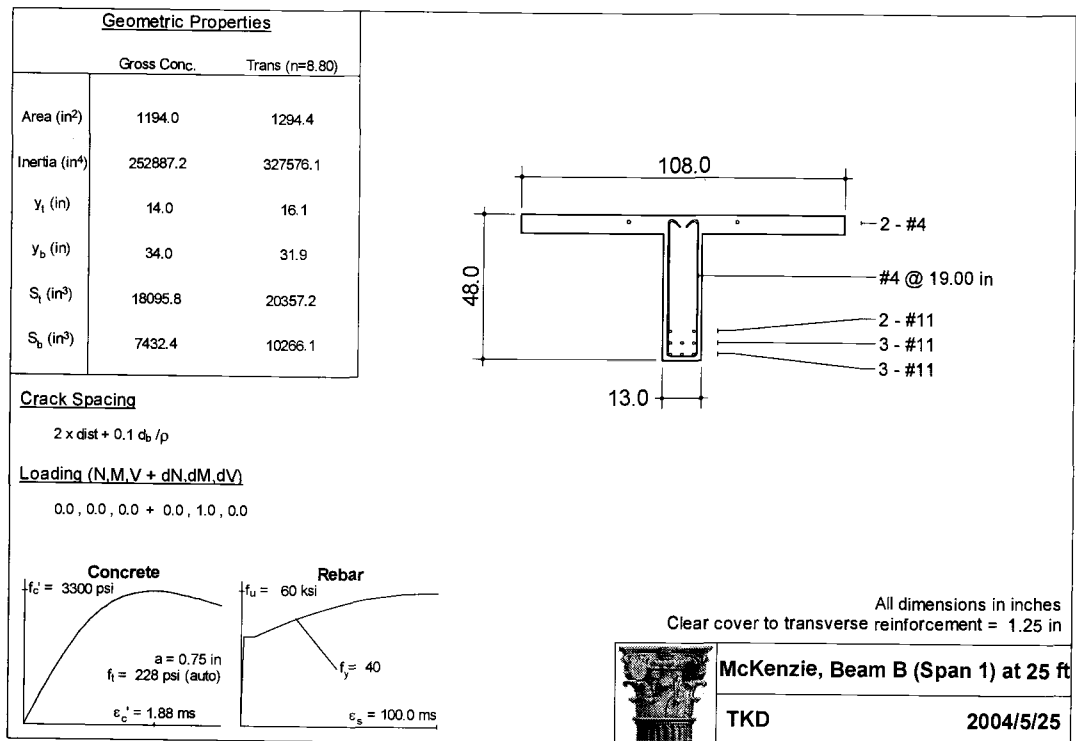
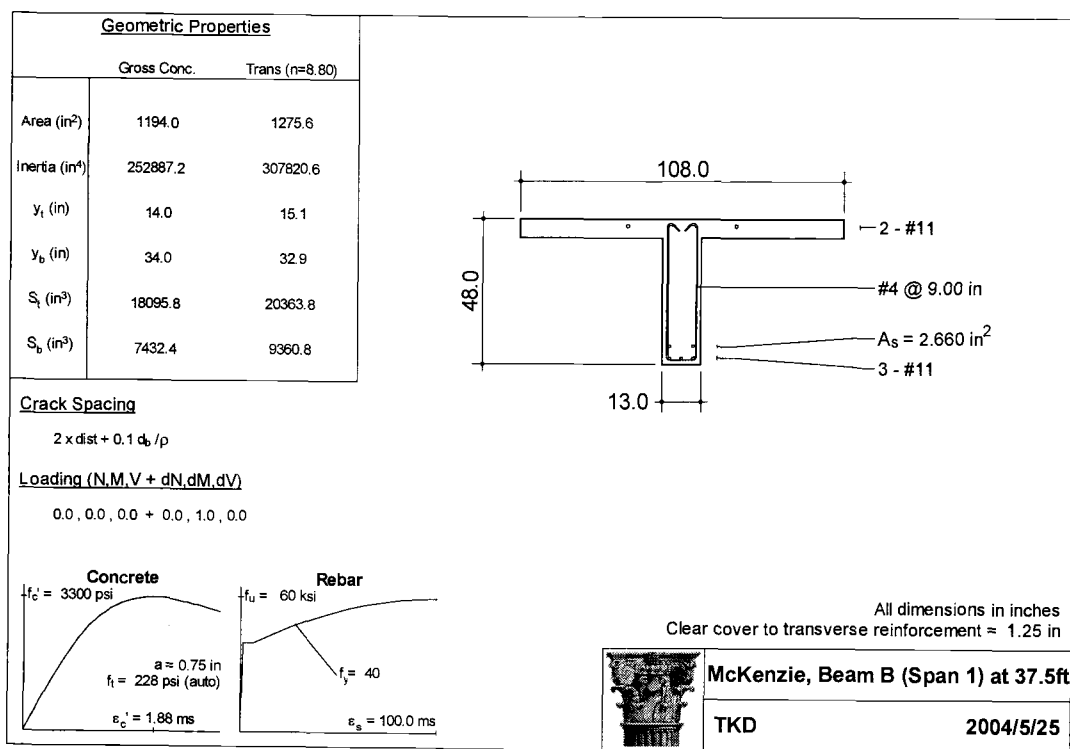
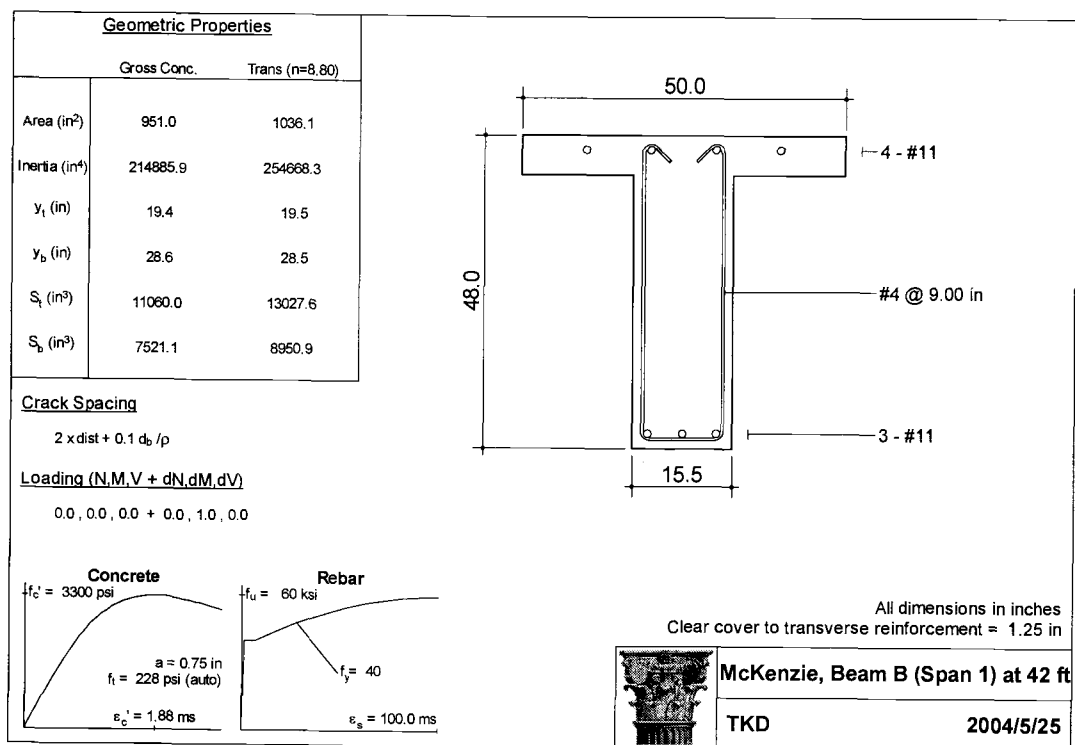
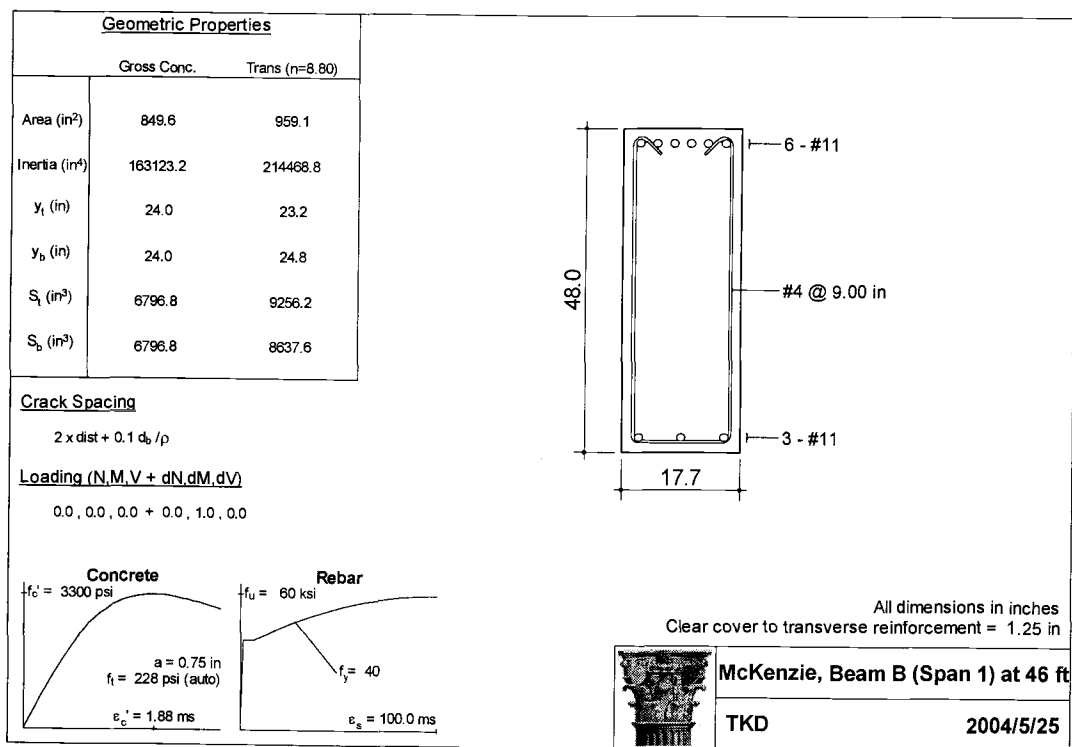
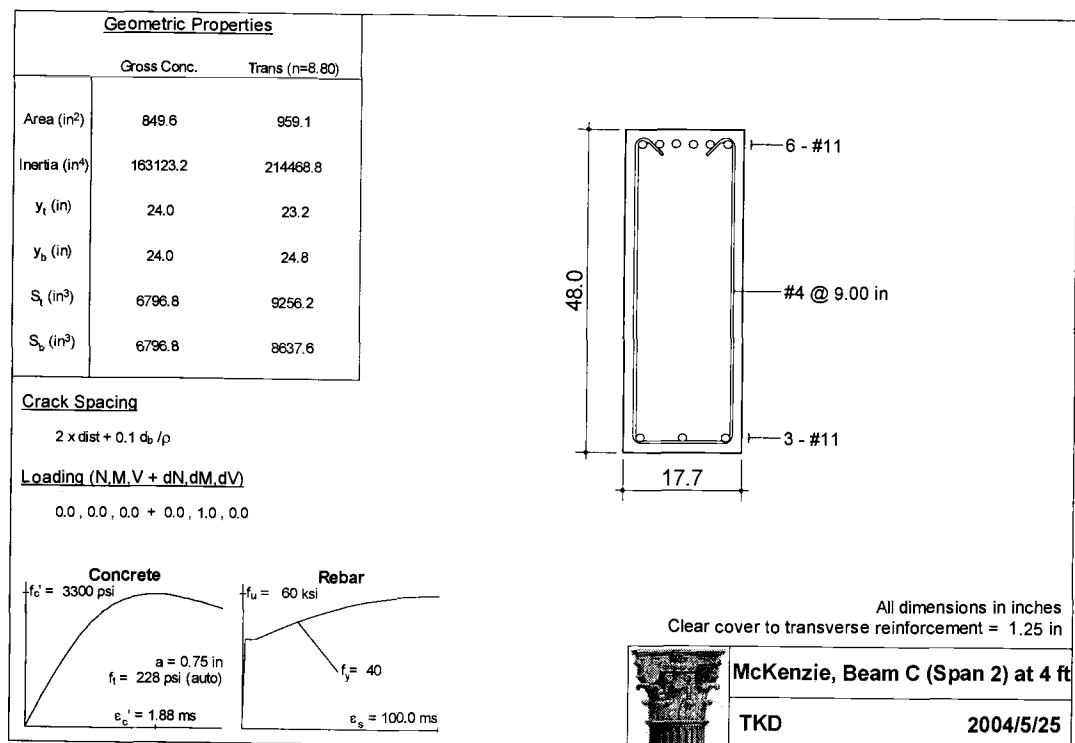


Fig. D1 - McKenzie River Bridge detailed drawing.

Fig. D2 – McKenzie R. Bridge; Span 1 at 4 ft. (*RESPONSE 2000™*)Fig. D3 – McKenzie R. Bridge; Span 1 at 8 ft. (*RESPONSE 2000™*)

Fig. D4 – McKenzie R. Bridge; Span 1 at 12.5 ft. (*RESPONSE 2000TM*)Fig. D5 – McKenzie R. Bridge; Span 1 at 25 ft. (*RESPONSE 2000TM*)

Fig. D6 – McKenzie R. Bridge; Span 1 at 37.5 ft. (*RESPONSE 2000TM*)Fig. D7 – McKenzie R. Bridge; Span 1 at 42 ft. (*RESPONSE 2000TM*)

Fig. D8 – McKenzie R. Bridge; Span 1 at 46 ft. (*RESPONSE 2000TM*)Fig. D9 – McKenzie R. Bridge; Span 2 at 4 ft. (*RESPONSE 2000TM*)

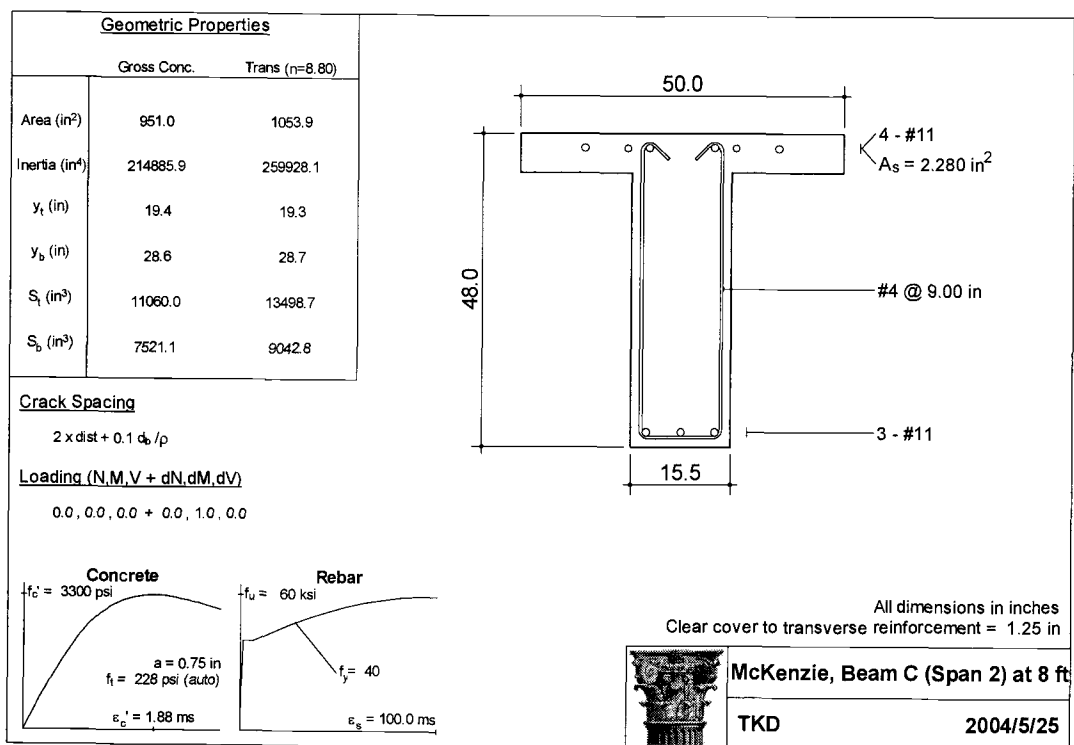


Fig. D10 – McKenzie R. Bridge; Span 2 at 8 ft. (RESPONSE 2000™)

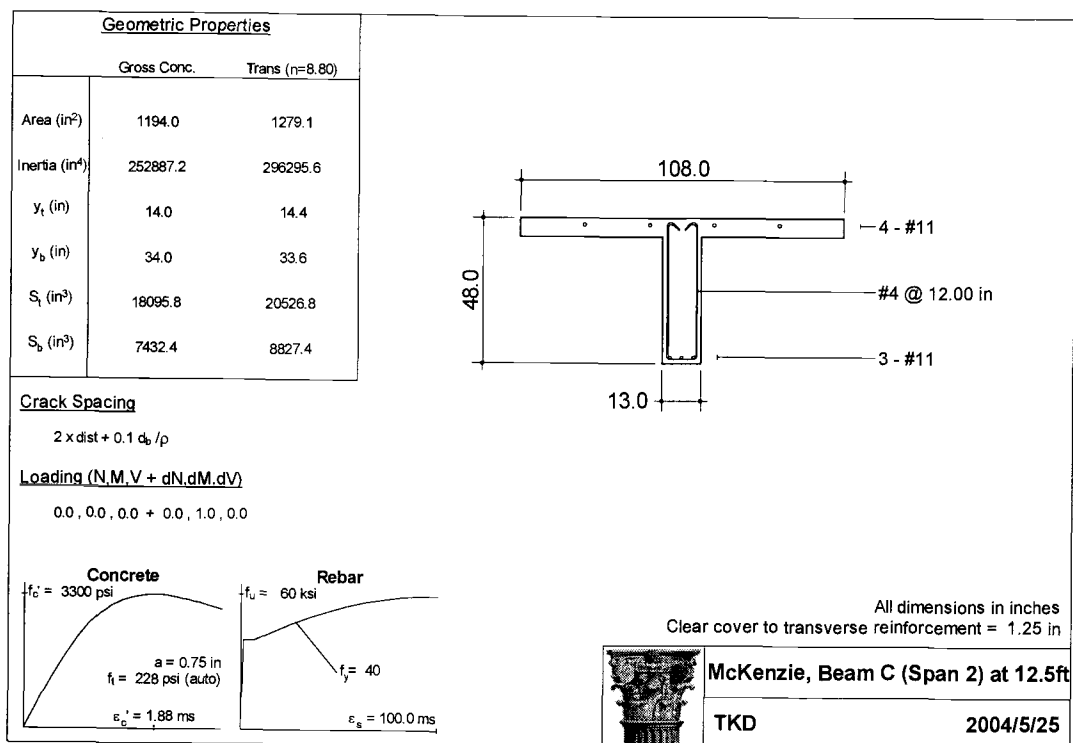


Fig. D11 – McKenzie R. Bridge; Span 2 at 12.5 ft. (RESPONSE 2000™)

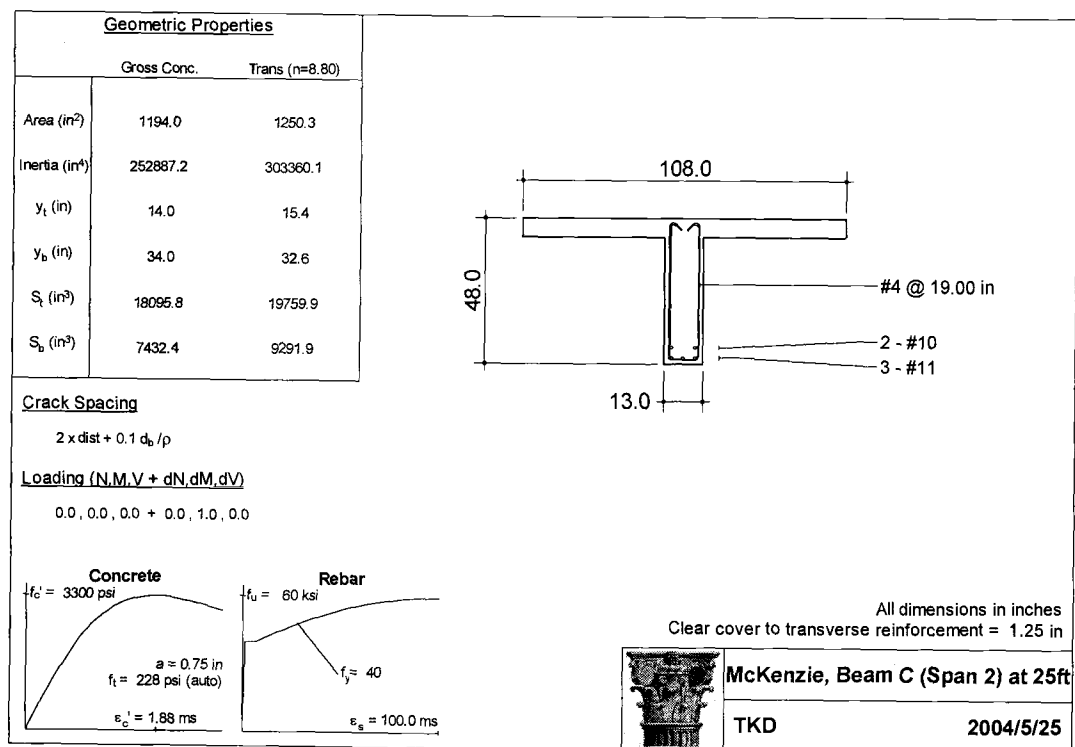


Fig. D12 – McKenzie R. Bridge; Span 2 at 25 ft. (*RESPONSE 2000TM*)

The bridge is symmetrical about this point.